

Suspension Melt Crystallization in Tubular and Scraped Surface Heat Exchangers

DISSERTATION

zur Erlangung des akademischen Grades
Doktor-Ingenieur (Dr.-Ing.)

vorgelegt der

Mathematisch-Naturwissenschaftlich-Technischen Fakultät
(Ingenieurwissenschaftlicher Bereich)
der Martin-Luther-Universität Halle-Wittenberg

von Herrn Dipl.-Ing. Tero Tähti
geb. am 18.08.1972 in Hämeenlinna, Finnland

Dekan der Fakultät: Professor Dr.-Ing. Holm Altenbach
Gutachter:

1. Professor Dr.-Ing. Joachim Ulrich
2. Professor Dr. Jörg Kreßler
3. Dr. Marjatta Louhi-Kultanen

Die Arbeit wurde am 19.10.2004 verteidigt.

urn:nbn:de:gbv:3-000007337

[<http://nbn-resolving.de/urn/resolver.pl?urn=nbn%3Ade%3Agbv%3A3-000007337>]

Acknowledgement

The work presented in this book has been constructed during my work as scientific researcher at the Institut für Verfahrenstechnik, Martin-Luther-Universität Halle-Wittenberg, Germany.

I would like to express my very special thanks to Professor Dr.-Ing. habil. Joachim Ulrich, my supervisor at the Martin-Luther-Universität. I am grateful for the opportunity to work with him in his field of expertise: melt crystallization. In addition to the professional advising, his encouragement and support have played an essential part in accomplishing the results leading to completion of this work.

I also thank Professor Dr. rer. nat. habil. Jörg Kreßler for taking the task to be a referee for this work.

Dr. Marjatta Louhi-Kultanen from Lappeenranta University of Technology, Finland, I do not only thank for being a referee for my work, but also for being an excellent scientific colleague and for the support I have received during my whole scientific career.

I would like to appoint my sincere thanks also to Professor Dr.-Ing. habil. Lutz Brendler and Dr.-Ing. Dieter Möhring for scientific guidance and invaluable and inspiring discussions over wide range of scientific and technical topics.

I am grateful to the guidance and support I have received during my cooperation with Niro Process Technology B.V., the Netherlands. The view to the background of industrial process engineering has provided me with valuable insight, helping me to assess my work in a different light. My special thanks go to Dr.-Ing. Reinhard Scholz, Mr. Bart Schreurs and Mr. René-Jeroen Verschuur.

I thank all my colleagues at the Martin-Luther-Universität Halle-Wittenberg for creating a friendly working climate and for being such a young and dynamic team. I also thank all my students for the support in the experimental work.

My very special gratitude is addressed to my loved wife Jun Jun, who has supported and fostered me during the years, and without whom the completing of this work would have been much much more difficult.

Tero Tähti

Halle (Saale), 20.10.2004

TABLE OF CONTENTS

1.	Introduction	1
2.	Suspension Melt Crystallization	3
2.1	Effect of Crystallization Kinetics on Suspension Melt Crystallization	4
2.1.1	Nucleation	5
2.1.2	Crystal growth	6
2.1.3	Secondary growth phenomena	8
2.1.4	Population balance	9
2.2	Suspension Melt Crystallization Processes	10
2.3	Solid-Liquid Separation in Suspension Melt Crystallization	14
2.4	Scraper Surface Heat Exchangers	15
2.4.1	Heat transfer properties of scraped surface crystallizers	16
2.5	Freeze Concentration	22
2.6	Summary of Existing Suspension Melt Crystallization Research	23
3.	Crystalline Deposits in Heat Exchangers	25
3.1	Effect of Flow Conditions	28
3.2	Effect of Crystalline Suspensions	30
3.3	Effect of Surface Structure of Heat Exchanger	32
3.4	Summary of Existing Research on Crystalline Deposits	33
4.	Experimental Work	35
4.1	Introduction to Experimental Work	35
4.2	Suspension Melt Crystallization in a Tubular Heat Exchanger	35
4.2.1	Experimental equipment	35
4.2.2	Used compounds	38
4.2.3	Suspension density measurements	39
4.2.4	Limiting surface temperature difference for incrustation	40
4.2.5	Heat transfer properties of the double-pipe heat exchanger	43
4.2.6	Particle size measurement	44

4.3	Experiments with Pilot Plant Equipment	46
4.3.1	Experimental equipment	46
4.3.2	Suspension density in the crystallizer loop	48
4.3.3	Crystal size and habit	50
4.3.4	Scraper speed of SSHE	51
4.3.5	Reduction in cooling efficiency due to heat production and losses to environment	52
4.4	Particle Characterisation from Laboratory Scale Suspension Melt Crystallization	56
4.4.1	Particle characteristics under scraping action	56
4.4.2	Particle characteristics under free growth in a suspension	62
4.4.3	Particle characteristics of ice crystals from stirred tank	67
4.5	Conditions for Formation of Crystalline Layers	69
4.5.1	Growth of pure components	71
4.5.2	Crystallization of fatty acid mixtures	74
5.	Discussion	76
5.1	Discussion to Crystallization in the Tubular Heat Exchanger	76
5.2	Discussion to Pilot Plant Equipment	80
5.3	Discussion on Laboratory Scale Suspension Melt Crystallization	86
5.3.1	Particle formation in laboratory scale SSHE	86
5.3.2	Crystal growth in suspension	88
5.3.3	Secondary growth of ice crystals	89
5.4	Discussion to Layer Growth Experiments	90
5.5	Conclusions and Outlook	93
5.5.1	Conclusions	93
5.5.2	Outlook	94
6.	Summary	95
7.	Zusammenfassung	97
8.	List of Symbols	99
9.	References	102

1. Introduction

Suspension crystallization processes offer a highly selective and energy-efficient method for separation of chemical mixtures. In the crystallization of organic melts heat transfer phenomena control the rate of crystal formation. The growth rate of crystals depends on the heat transfer coefficient, the heat of crystallization and the undercooling of the melt. The heat removal from the crystallization process is usually carried out using indirect heat exchangers, where heat is removed from the melt by a cooling medium through a separating heat exchanger wall. In such processes the problem of incrustations on heat exchanger surfaces by the crystallizing component results in additional resistance to heat transfer. The increased heat transfer resistance reduces the heat transfer rate, or necessitates a higher temperature driving force. Thereby, the energy-efficiency of the process is reduced and the costs for energy and cleaning are increased.

Another difficulty in suspension melt crystallization arises from the fact that the product from the crystallizer is a suspension consisting of the pure crystals and the impure liquid from which the crystals were grown. The final product purity depends on how well the solid-liquid separation can be achieved. In melt crystallization this is often difficult due to high viscosities, possible formation of soft deformable crystals and the sensitivity to temperature changes. High demands are set also by the aim of purification in melt crystallization processes, where the impurity concentration of the final product is often limited to a few ppm. This requires almost complete separation of crystals and mother liquor.

The difficulties with incrustations and the solid-liquid separation result in high construction requirements for suspension melt crystallizers. Suspension crystallization from melts is usually carried out in equipment with continuous mechanical cleaning of the heat exchange surface. Scraped surface heat exchangers are often used for this purpose. However, the relative complexity of such processes increases the investment costs and the need for maintenance.

Therefore, an optimization of the crystallizer construction has to be carried out in order to obtain a less complex equipment configuration. By reducing the number of moving parts the operating costs can be reduced. Together with the lower investment costs brought by the increased simplicity, the total costs of the crystallization process will be decreased. The characteristics of the crystals produced with such equipment also have to be investigated in order to estimate the influence of the simplification on the overall process efficiency.

The aim of this work is to investigate the possibility of simplifying the crystallization process. The crystal characteristics from suspension melt crystallization with and without scrapers were examined in order to optimize the process conditions. The improved control of the product crystal characteristics allows a more efficient application of the suspension melt crystallization processes in the industrial practice. The aim was also to investigate the incrustation mitigation in suspension melt crystallization with the aid of controlling the process conditions, e.g. the flow velocity of the suspension. Efficient deposit removal by adjusting the process conditions would allow simple standardized heat exchanger constructions to be used for crystallization, instead of the expensive and complex structures applied at present.

In this work the simplification of the crystallization process was investigated applying a tubular heat exchanger connected as a circulation loop, in which the crystals were given sufficient time to grow. In such equipment flow conditions at the heat exchanger surface can be controlled by the flow rate of the suspension. Relatively high forces for deposit removal can be obtained due to the high turbulence of the pipe flow. Whether the process can be applied to crystallization depends on the crystal production rate. In this work the combined crystallization, heat transfer and process functionality were investigated to evaluate the possibilities and limitations of such equipment.

The growth of the crystals in a circulation loop was investigated using industrial pilot-plant equipment. In this case heat exchange was achieved in a scraped surface crystallizer. The influence of the process parameters on the crystal characteristics and on the energy-efficiency of the equipment was examined.

The crystal characteristics from a laboratory scale scraped surface crystallizer are investigated. The effect of process parameters and the influence of the physical properties of the compound system are presented. The results are compared with data obtained from free growth in a suspension in order to discuss the difference the scraping action brings to the crystallization process.

The conditions at which crystalline layers form at cooled surfaces are studied. The structure of the layers formed is discussed and the forces necessary for breaking layers of different inner structure are demonstrated.

The results presented in this work will help to understand the crystal formation process and the phenomena at the cooled surface in crystallization processes better. This will provide a basis for the further development of suspension melt crystallization processes. The simplified crystallizer construction making use of a simple heat exchanger is presented. The results obtained for the deposit removal are applicable to incrustations in ordinary heat exchangers, especially where problems of deposition by freezing are encountered.

2. Suspension Melt Crystallization

Melt crystallization is a technique used for purification and separation of mixtures of chemicals and metals. The division between the more commonly used technique of solution crystallization and the melt crystallization cannot be precisely defined. However, the techniques used for these two cases can differ remarkably, which justifies the categorization. Commonly the fraction of the crystallizing component in melt crystallization is present in higher amount than all the other mixture components together. For example for ultra purification of benzene and naphthalene the feed concentrations can be as high as 99.5 wt.-% for benzene and 90.45 wt.-% for naphthalene [Mid69]. Actually, this point already brings with it the further aspects used to characterize melt crystallization: High viscosities and importance of heat transfer. When a mixture is brought to a temperature, at which most of the liquid is near its freezing point, the viscosity of such a mixture is high compared to solutions, where only small portion of the mixture is near its solidification temperature. Also, when the fraction of the crystallizing component is high the mass transfer of molecules to the growth sites is easy, and heat transfer will be the rate-determining factor. However, all the aspects mentioned above can be found in processes normally classified to the solution and high viscosity.

The advantages of melt crystallization are in the relatively low energy demand of the freezing process and in the high selectivity of crystallization [Ulr02]. The heats of fusion for majority of compounds with industrial importance are lower than the heats of vaporization by the term 0.2 - 0.5 [Win90]. The low energy demand can be demonstrated by the extreme example of water: The heat of vaporization is 2260 kJ/kg, whereas the heat of fusion is only 334 kJ/kg [Kir78]. However, in the most used industrial application of melt crystallization - batchwise crystallization on a cooled surface - the energy requirements of heating and cooling of the whole crystallizer equipment, as well as the heat transfer medium, has to be taken into account. Wintermantel and Wellinghoff [Win90] have stated that in such processes a multiple of the heat of crystallization is needed, which reduces the energy benefits of melt crystallization compared to distillation. It was also stated that future studies should be focused on continuous melt crystallization instead of batch processes. The high selectivity of the crystal lattice incorporation for eutectic systems allows separation of close boiling components, for example isomers. One important application in this field is the separation of p-xylene from its isomers with its production capacity exceeding ten million tons per year [Fis97]. The restriction of this selectivity to eutectic systems is a minor problem, knowing that 70% of the existing systems are eutectic [Mat91].

However, the high selectivity of the crystallization process depends strongly on how the crystallization is carried out. Melt crystallization can be carried out by a layer process, where the crystalline material to be separated forms on a cooled surface, or by crystallization from suspension. In this work the focus is given mainly to the suspension melt crystallization. By crystallization from a suspension high purities can be obtained in a single separation step due to a large surface area for mass transfer in comparison to layer crystallization processes. In suspension crystallization the surface area available for the same volume of crystals than in

layer crystallization is approximately two to three orders of magnitude higher. A further benefit of crystallization from suspension is the applicability for continuous operation. Due to the huge surface area compared to the layer processes, the separation is not affected by the kinetics of the crystallization step only. In suspension crystallization processes the following solid-liquid separation plays an important role on the final product purity. This is especially so for the melt crystallization, where the melt concentrated with impurities and high viscosity of the liquid phase make the separation even more difficult. For this reason special processes for solid-liquid separation have been developed for melt crystallization. The solid-liquid separation in suspension melt crystallization processes is very often carried out in wash or crystallization columns. A thorough study of the different melt crystallization processes have been published by Özogus [Özo92], Verdoes and Nienoord [Ver03b], Arkenbout [Ark95], Ulrich [Ulr02] and Ulrich and Glade [Ulr03].

Suspension melt crystallization is discussed in the next chapters as follows: In Chapter 2.1 the principles of suspension melt crystallization are discussed. The different processes of suspension melt crystallization have been discussed in Chapter 2.2. The solid-liquid separation in melt crystallization is presented in Chapter 2.3. A summary of the suspension melt crystallization processes is given in Chapter 2.4.

2.1 Effect of Crystallization Kinetics on Suspension Melt Crystallization

The kinetics in a crystallization process includes two factors: Nucleation and crystal growth. The prerequisite for both nucleation and growth are non-equilibrium conditions, at which a new solid phase will be formed as the system moves towards equilibrium. In industrial crystallization this means a liquid supersaturated by the crystallizing component. Because the supersaturation is in melt crystallization in almost every case created by reduction of temperature, the undercooling is usually used as a measure for the supersaturation. This also allows an easy tracking of the crystallization process in the phase diagram, usually presented by a temperature-concentration diagram. In every crystallization process different nucleation and growth mechanisms take place simultaneously. However, the dependence of nucleation

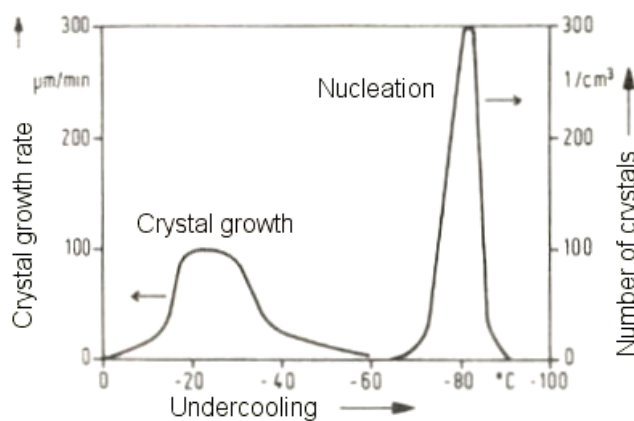


Figure 2.1.1 Effect of undercooling on crystal growth and nucleation [Rit85].

and growth processes on temperature and undercooling can be very different. This can be brought up with an example presented in Fig. 2.1.1 [Rit85]. From the figure it can be seen that for nucleation from a crystal free solution a certain limiting undercooling is necessary. This limiting undercooling is called the width of the metastable zone for primary nucleation, and it is

strongly dependent on heat exchange, fluid dynamics and the solution composition (concentration, presence of additives). By increasing undercooling the aggregation of the molecules becomes easier. This phenomenon is counter played by the increasing solution viscosity by decreasing temperature, which hinders the movement of molecules and makes their incorporation into an ordered crystal lattice more difficult. Thus the rate of nucleation has a maximum value at a certain temperature. Similarly goes crystal growth rate through a maximum. However, the regime for crystal growth lies in a totally different temperature region. It can also be seen, that for crystal growth there exists no limiting undercooling, which has to be overcome for the growth process to start.

The above mentioned behaviour of nucleation and crystal growth is the underlying principle for many suspension melt crystallization processes, and this will be pointed out by discussion of the processes, where the practical effect of these kinetic effects can be seen. In following a description of these two kinetic phenomena is given from the viewpoint of melt crystallization.

2.1.1 Nucleation

Nucleation can occur by a variety of processes. It is usually divided to homogeneous primary nucleation, heterogeneous primary nucleation and secondary nucleation. Secondary nucleation has its origins also in several different phenomena, which are usually taking place simultaneously. Nucleation by cavitation has also been presented as its own class of nucleation process [Jac65], being precisely speaking just one special type of homogeneous nucleation.

As mentioned before, nucleation is affected by various different parameters. In real industrial crystallization processes most of these parameters are not constant throughout the crystallization system. Therefore, theoretical equations to calculate the nucleation rate have hardly any use in industrial suspension melt crystallization processes. Indeed, the geometrical construction of the crystallizer has a significant influence on the nucleation rate.

In continuous crystallization processes the secondary nucleation is the dominating mechanism for the birth of new crystals [Ark95]. Usually this happens through collisions of crystals with each other and with agitator blades and crystallizer innings like walls and baffles. Especially, crystal suspensions transported through pumps are set under large mechanical impact, which greatly increases the rate of secondary nucleation. Therefore, secondary nucleation is often called contact nucleation. The magnitude of secondary nucleation due to mechanical effects depends on the crystal size (kinetic energy of collisions), the hardness of crystals, the agitation rate or the pump speed and the suspension density. The process of secondary nucleation due to collisions has been investigated e.g. by Ulrich [Ulr81] and Gerigk [Ger91], and recently by Gahn and Mersmann [Gah99], who have developed a model for the mechanical impact between crystal and impeller blade based on the crystal hardness. Secondary nucleation due to mechanical influence should not be mixed with crystal breakage to macroscopic crystal sizes. The breakage, even having a negative influence on the crystal size distribution, is usually a much smaller problem in industrial crystallization. This is

due to the remarkably higher energy of collisions needed to cause macroscopic breakage and the lesser amount of new crystal surface produced.

Excessive nucleation is in almost every crystallization process an unwanted phenomenon. However, in continuous crystallization processes secondary nucleation is necessary for the production crystals in order to balance the continuous flow of crystals out of the crystallizer in the product stream. In the design of industrial crystallizers it is an important task to find the optimal conditions for the desired production rate. A high driving force for crystallization results in a high nucleation rate. The higher the nucleation rate the smaller the average crystal size. On the other hand too low driving forces reduce the crystal growth rate resulting in high residence times necessary. Therefore, it is necessary to find the optimal process conditions (undercooling, suspension density, agitation rate, volume of crystallizer) for each type of process considering both the nucleation and crystal growth.

A review over research work done on secondary contact nucleation has been presented by Rousseau [Rou98].

2.1.2 *Crystal growth*

As mentioned in the introduction to Chapter 2, the surface area for phase change in suspension melt crystallization is approximately 10 million times larger than in layer crystallization processes. The result is that the same production rates can be achieved with drastically smaller growth rates in suspension crystallization processes. The linear growth rates in layer melt crystallization are typically between 10^{-6} and 10^{-4} m/s, while they are in the range 10^{-7} - 10^{-9} m/s for suspension melt crystallization [Ulr02]. This has an overwhelming effect on the separation potential of the crystallization step. The kinetics of a crystallization process influence directly the purity of the crystalline material produced. The effect of growth rate on the phase separation has been intensively investigated by König [Kön03]. In Fig. 2.1.2 is shown a phase diagram, and the apparent phase diagrams obtained by different growth rates. It can be seen that the higher the growth rate, the more the solid phase shows a solid-solution type behaviour and the apparent solidus line moves towards the liquidus line.

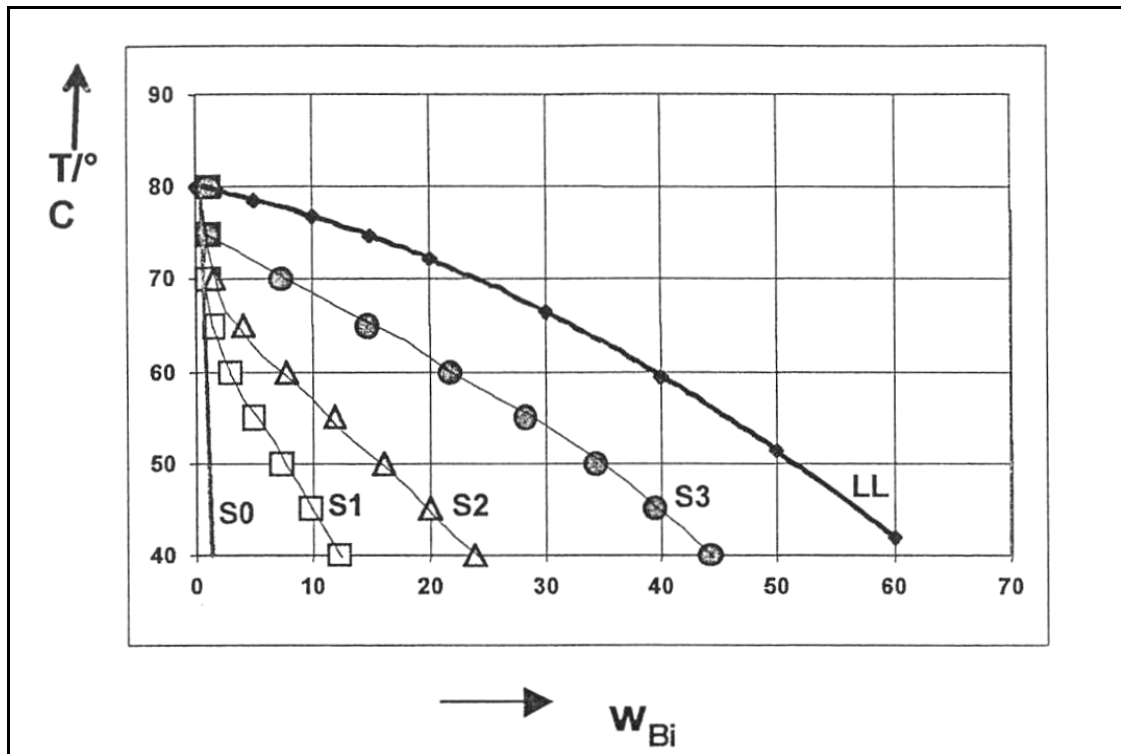


Figure 2.1.2 A part of phase diagram showing the effect of growth rate on the phase separation [Kön03]. LL = liquidus line, S0, S1, S2 and S3 are solidus lines obtained at growth rates G_0 , G_1 , G_2 and G_3 , respectively. $G_0 < G_1 < G_2 < G_3$.

The impurities inside crystals can be due to three different mechanisms: lattice substitution, entrapped impurities inside crystals and enclosed impurities in crystal agglomerates [Kön99]. By increasing crystal growth rate the time for the molecules to organize into the crystal lattice gets shorter and the increasing disorder at the phase boundary leaves more space for impurities. The amount of impurities in the crystalline product is usually described by the effective distribution coefficient [Win90] defined by equation:

$$k_{eff} = c_{2,Prod} / c_2 \quad (2.1.1)$$

For suspension melt crystallization combined with solid-liquid separation in a wash column the distribution coefficient can be as low as 0.02 to 0.002 [Ver03a].

While the crystal growth rate determines the rate at which growth units are organized into the crystal lattice, the other two factors having the greatest influence on the crystal purity – fluid dynamic and liquid viscosity - determine how effectively the impurity molecules are transported away from the vicinity of the crystal surface. The effect of both the crystal growth rate and the liquid viscosity can be demonstrated by Fig. 2.1.3 [Mac76]. Here the amount of inclusions in sugar crystals is shown at different growth rates and temperatures. It can be seen that the amount of inclusions is directly proportional to the growth rate, and that the amount of inclusion from solutions of higher temperature (lower viscosity) is smaller.

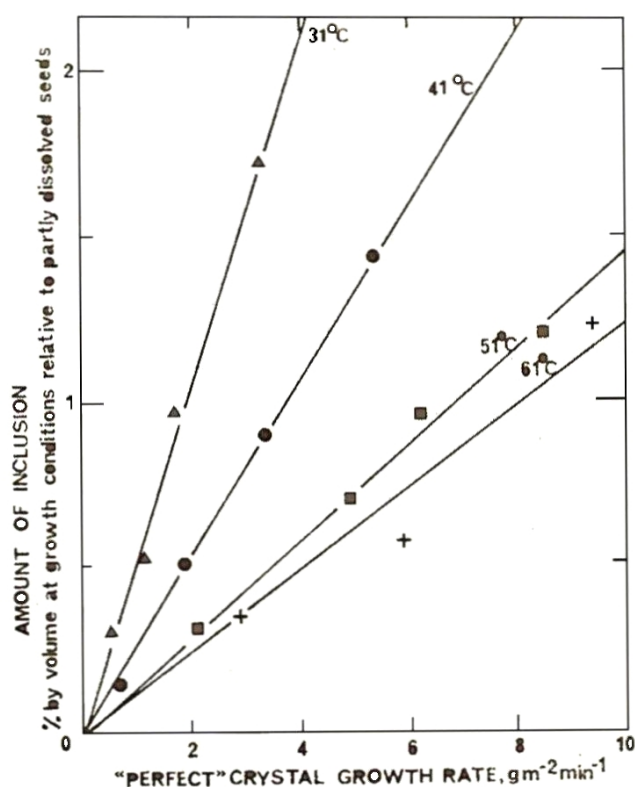


Figure 2.1.3 Impurity incorporation in sugar crystals at different process conditions [Mac76].

2.1.3 Secondary growth phenomena

Secondary growth phenomena include aggregation, agglomeration and ripening. These processes can be used in crystallization to increase the product crystal size beyond the limit achievable by the lattice growth process. The advantage of the secondary growth processes is that they usually can be carried out at conditions where nucleation is negligible. The secondary growth phenomena do not produce new crystalline material, but is aimed to change the size and shape characteristics of the crystal population.

While aggregation usually means crystals loosely grouped together, it is seldom used to give form to the final

crystalline product. Different to aggregation, agglomeration forms groups of crystals tightly bound to each other by growth bridges. By agglomeration it is possible to produce crystalline material with untypical crystal shapes (e.g. spherical) in order to reach better solid-liquid separation properties [Woo01]. Agglomeration of macroscopic crystals is caused by crystal collisions leading to attachment and formation of crystalline bridges between the particles. A so-called contact nucleus-bridges mechanism has been proposed [Dav91, Lin04]. This mechanism presumes that the crystals forming an agglomerate stay in contact long enough for the crystalline material to initiate growth at the contact location and form strong enough growth bridges between the crystals. The fact that the agglomeration can occur at very low undercoolings where the growth rate is very low suggests that in such cases some other phenomena might be responsible for the forming of agglomerates. One possible effect is that the surface melting temperature of crystalline material is known to be lower than the bulk melting temperature. When a crystal surface, which is in a more unstructured state as the bulk of a crystal, loses its contact with the solid-liquid interface, the melting temperature changes to refer to the bulk melting temperature of the material. This happens when two crystal surfaces come in contact with each other, and the higher degree of freedom of these two surfaces at the crystal-crystal interface will be lost [Tab91]. This interface gets a more crystalline state and the two crystals are attached onto each other. Surface effects on agglomeration of paracetamol have been recently investigated by Ålander *et al.* [Åla04].

The ripening is a phenomenon based on the fact that the equilibrium conditions for small crystals are different to those of the large ones. When the crystal size is not very small (less than one micron), the ripening process is typically a very slow process. However, the ripening process has also been applied successfully in industrial applications. Among others, Huige [Hui72] has shown that large nearly spherical crystals can be produced in a ripening tank from population of small crystals. In his work the feed crystal size of approximately 20 μm could be increased tenfold to average sizes of about 250 μm using residence times of 1 to 4 hours. The process applied by Huige, however, included most probably an unintentional removal of fines from the ripening tank, which in its part helped to increase the average crystal size.

The difference in the equilibrium conditions between crystals of different size is based on the Gibbs-Thompson effect. The relationship between particle size and solubility for a non-electrolyte can be given by equation:

$$\ln \left[\frac{c(r)}{c^*} \right] = \frac{2M\gamma}{RT\rho r} \quad (2.1.1)$$

Another method of increasing the size of ice crystals has been presented by Kobayashi *et al.* [Kob96]. The authors have used agglomeration to increase the ice crystal size in order to improve the solid-liquid separation. The ice crystals were found to agglomerate during two hours when the initial supercooling was low (less than 0.2 K). At high undercoolings (1.25 K) ice crystals failed to agglomerate. It was found out that minimum of 6 % to the volume of seed crystals must be added to the system for the ice crystals to agglomerate properly. The size or size distribution of the seed crystals themselves did not affect the agglomeration behaviour. This shows that the seeds are effecting as growth surface for depletion of undercooling, thus controlling the undercooling value, and initiating the crystallization process. Rising the impurity concentration (glucose) to 20% deteriorated the method of producing agglomerated ice crystals whatever the conditions. The agglomeration succeeded in 10% solution.

2.1.4 Population balance

For continuous crystallization processes the kinetics of nucleation and crystal growth are usually determined using the population balance technique developed by Randolph and Larson [Ran88]. The population balance is developed for steady-state conditions assuming perfect mixing, uniform shape of crystals, no classification at withdrawal and negligible breakage (MSMPR crystallizer). Differentiation of the population balance equation from zero size nuclei assuming the ΔL law applies gives the equation:

$$n = n^0 \exp(-L/G t_R) \quad (2.1.3)$$

The nucleation rate is the formation of zero size clusters per time and volume and is given by the equation:

$$B^0 = n^0 G \quad (2.1.4)$$

When the population density, n , is plotted in semilog coordinates against the crystal size ($\ln(n)$ against L) a straight line is obtained. The intercept is found at $\ln(n^0)$ and the slope of the line is $-1/G\tau$. Using this information the nucleation and the crystal growth rate can be determined. The mass concentration in a given size range can be given by the equation:

$$dm = \rho k_v L^3 n dL \quad (2.1.5)$$

Knowing that the weight fraction of a size class $dW = dm/M_T$, the population density can be defined from the mass based size distribution by the equation:

$$n = \frac{M_T dW}{\rho k_v L^3 dL} \quad (2.1.6)$$

The parameters on the right hand side of the equation 2.1.6 can be experimentally determined. The equation 2.1.3 can be linearized to the form

$$\ln n = \ln n^0 - \frac{L}{G t_R} \quad (2.1.7)$$

The plot of the calculated values of $\ln n$ against the crystal size has the slope $-1/(G t_R)$ and the intercept $\ln n^0$. Using these data the growth rate can be calculated from the slope and the nucleation rate using equation 2.1.4.

2.2 Suspension Melt Crystallization Processes

The first suspension melt crystallization process combining crystal formation in a scraped surface heat exchanger (SSHE) and a wash column was the so-called Phillips column developed already 1945 by Arnold [Arn45]. The process serves as a model for many later suspension melt crystallization processes. The crystals are created in an SSHE, from where the small crystals and crystal nuclei are led to a separation column. During their way the crystals grow further in the undercooled melt. In the separation column the crystals sink by gravity. At the bottom of the column the crystals are melted, part of the molten crystals is taken as the product and part is pumped up the column. The portion pumped back up to the column counter-currently to the sinking crystals serves as the washing liquid removing impure melt from the crystal surfaces. A further development of the Phillips column is the Phillips pressure column [Sch50], where the crystal slurry is transported by means of a piston.

The piston consists a filter, through which the mother liquor is separated from the crystals. The two forms of the Phillips column are shown in Fig. 2.2.1.

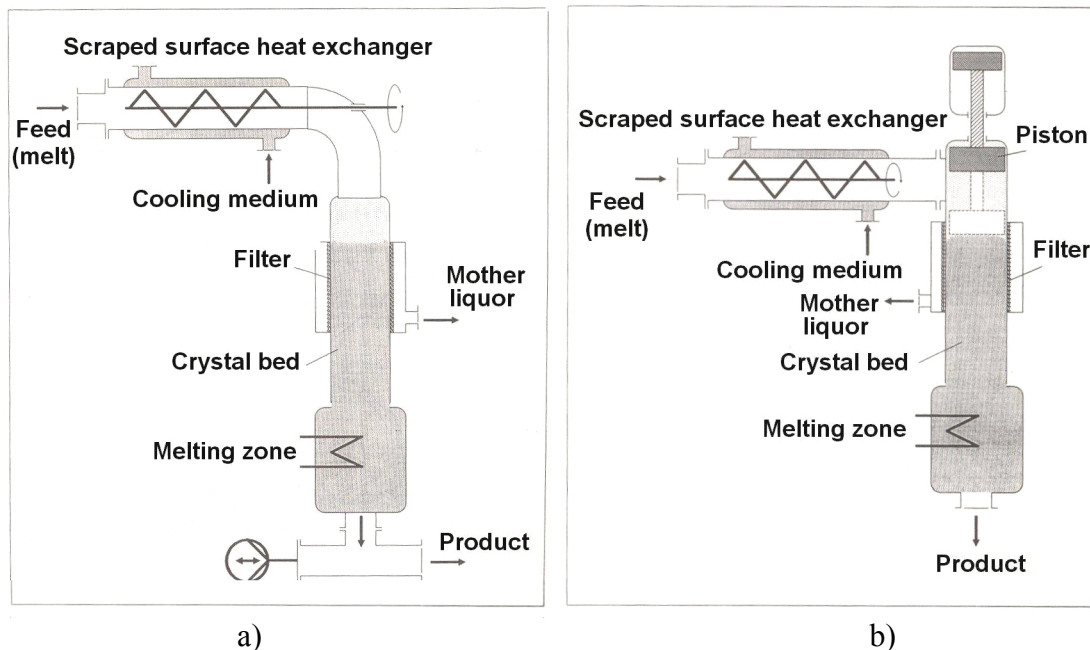


Figure 2.2.1 a) Phillips column [Arn45], b) Phillips pressure column [Sch50] for crystallization and counter-current washing.

A modification of the Phillips process is the Brennan-Koppers counter-current column, where the crystal suspension is fed into the column at the bottom [Bre80]. In this way the crystals pushed up by the stream form a dense bed, which improves the fluid dynamic at the solid-liquid interface, thus improving the washing. The crystal bed in the top of the column is removed to a heat exchanger for melting by a rotating scraper disc. This process, together with the Phillips pressure column, can be seen as a predecessor for the Niro wash column [Sch02] discussed later in this chapter.

Usually it is not enough to use only an SSHE as a crystallizer unit. The crystal characteristics can often be influenced positively if the mixing conditions and undercooling are milder than in the SSHE, where conditions for nucleation are favourable. For these purposes the SSHE is combined with a growth tank. In such a process the melt can be pumped through an SSHE, after which adequate residence time for crystal growth is provided in the growth tank. Another possibility is to circulate the crystal slurry continuously through an external heat exchanger. Such a crystallizer is called a forced-circulation crystallizer, and they are very often used in solution crystallization of inorganic salts. The two types of processes taking use of the growth tank, SSHE combined with a growth tank and the forced-circulation crystallizer, are presented in Fig. 2.2.2.

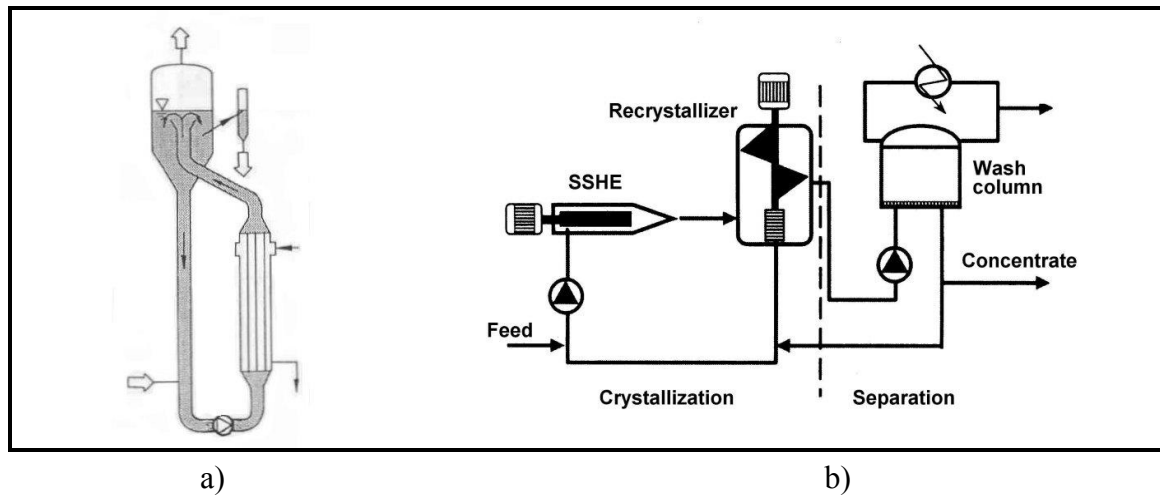


Figure 2.2.2 Crystallization processes making use of an external heat exchanger: a) forced-circulation crystallizer [Mer95], b) the Niro-process [Sch03a].

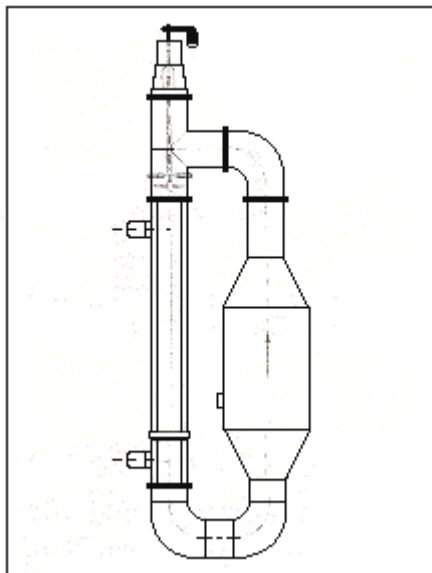


Figure 2.2.3 Ring crystallizer [Wöh91].

A further development of the forced-circulation crystallizer used in continuous crystallization of inorganic salts is the ring crystallizer presented in Fig. 2.2.3. A suspension is pumped in a loop by a propeller pump, at which a minimal mechanical stress to the crystals can be guaranteed. The heat exchange is carried out in a tube and shell heat exchanger, while on the other side of the loop an expansion can be installed to increase the residence time of the crystals. This process has been applied for the purification of bisphenol A, where a production rate of $50 \text{ kg/m}^3\text{h}$ has been reported [Wöh91]. It can be seen from the extremely low production rate, that the temperature difference over the heat exchanger wall must be very low. Therefore, modifications of this type of a process to achieve higher crystallizer efficiency should be

investigated. For example, the pilot plant unit of Niro Process Technology equipped with a scraped surface heat exchanger reaches production rates of approximately $190 \text{ kg/m}^3\text{h}$. This process is also studied as a part of the present work.

A highly sophisticated crystallizer construction, where an agitated vessel is equipped with a cooling jacket, a scraper, a draft tube and a settling zone is provided by Tsukishima Kikai Co. Ltd. (TSK) [Mor86]. While incrustations on the heat exchange surface are prevented by the scraper, agitation is achieved by the rotating draft tube with internal and external impellers. This crystallizer construction serves as the basis for the TSK-CCCC (Counter Current Cooling Crystallization) process shown in Fig. 2.2.4 [Tak84]. The process consists of three crystallizers in a cascade. The feed enters at the first stage crystallizer and the crystals are transported between the crystallizers through hydrocyclones counter currently to the melt flowing by gravity downwards the cascade. The crystallizers at stages 2 and 3 are used to

increase the recovery of the process. In such a way adequately large crystals can be grown for the separation in the gravity wash column. In addition, the crystals in the last tank before the solid-liquid separation are suspended in the melt with the lowest impurity content, which has a positive influence on the final product quality. The disadvantages of the TSK 4C are the long residence time, which reduces the production capacity per unit volume, and the high investment cost due to constructional complexity.

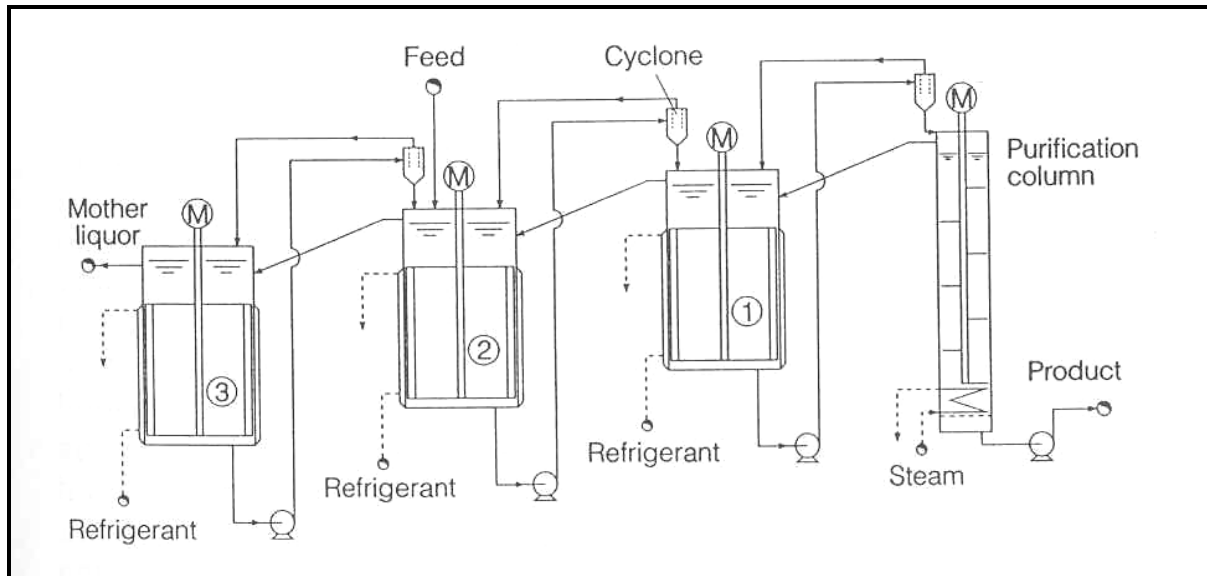


Figure 2.2.4 TSK-CCCC suspension melt crystallization process [Tak84].

Another type of crystallizer with an internal scraped heat exchanger is the cooling disc crystallizer of GMF Gouda presented in Fig. 2.2.5 [deM84]. In this type of a crystallizer the cooling is provided by large discs, which are placed in a declined trough forming a series of compartments. The discs are kept clean of crystals by wipers and the crystal slurry is transported co-currently to the melt through the compartments. The speciality of the cooling disc crystallizer is that the equipment is successfully used for both solution and melt crystallization applications.

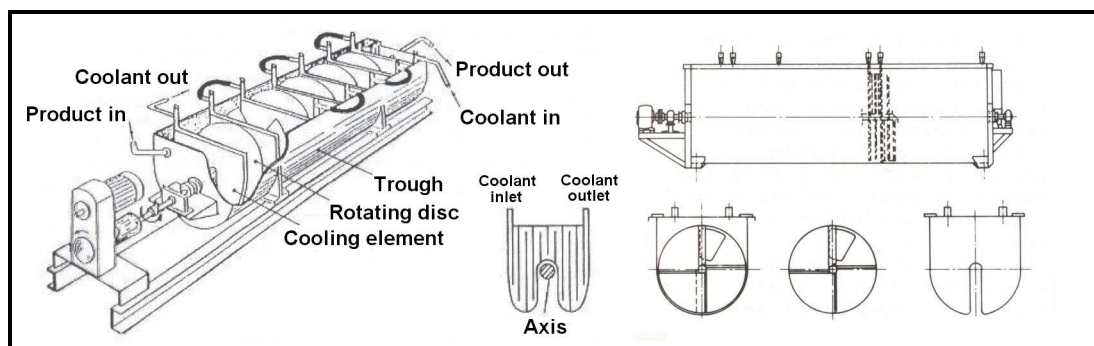


Figure 2.2.5 GMF Gouda cooling disc crystallizer [deM84].

Looking at the application for suspension melt crystallization relevant in industrial practise one point can be clearly pointed out: No process involving indirect cooling is carried out without some kind of cleaning of the heat exchange surface. This is usually done with

scrapers or wipers (as in the cooling disc crystallizer). Also special techniques are often applied for the solid-liquid separation step. These two aspects set high demands on the equipment construction, thus make the crystallization equipment complex and expensive. For future development of suspension melt crystallization as a lucrative separation technology these two aspects should be further investigated.

2.3 Solid-Liquid Separation in Suspension Melt Crystallization

As mentioned before, the solid-liquid separation is in all suspension crystallization processes of utmost importance for the final product purity. Wash columns have already been presented where they have been an essential part of the crystallization process. Most of the solid-liquid separation in industrial suspension melt crystallization is still carried out with centrifuges. However, in melt crystallization applications practical problems can arise from the need of a precise control of the temperature during washing [Ver03]. Wash columns offer a method of highly efficient separation with precise temperature control. The most important applications making use of the wash column technique are described here: The Niro process, the TNO wash column and the Kureha crystal purifier.

In a wash column the crystals are flowing counter-current to a stream of pure liquid, which replaces the impurities at the crystal surfaces. This liquid can be whether a saturated solution of the crystallizing component, or melt. In melt crystallization and freeze concentration the crystals are fed into a wash column at the other end of the column, and melted in the other. Part of the pure melt thus formed flows in opposite direction to the crystals and gradually replaces the impure melt carried along with the crystals from the crystallization process. In melt crystallization and in freeze concentration the product is collected in a molten form, whereas in solution crystallization processes the crystals remain solid.

The Niro wash column has been originally developed for the separation of ice crystals from concentrated solutions, thus to be used for freeze concentration. In this field the process is applied for concentrating food stuffs and for purification of waste water streams. Later applications for purifying organic chemicals have been developed. The process is based on mechanical transport of the crystal suspension using a piston driven wash column like the Phillips pulsation column. In the case of ice crystals the flow of the crystal bed is upwards in the column, in the case of separation of organics the direction of bed movement can be changed. The impure mother liquor is removed through a filter at the bottom of the column and a dense crystal bed forms. The crystals are scraped at the top of the column to a heat exchanger for melting like in the Brennan-Koppers process. Part of the melted product is pumped back into the wash column as wash liquid. The pure wash liquid replaces the impure mother liquor still attached on the crystals and crystallizes at the crystal surfaces. Thereby, no pure product is lost as impure wash liquid. A sharp wash front builds up in the column at the point where all the wash liquid has crystallized. The principle of the Niro wash column is presented in Fig. 2.3.1 a) [Sch03a].

In the TNO wash column the transportation of the crystal suspension is carried out by hydraulic pressure of the feed. The filters that were in the Niro process placed at the bottom of the column are in the TNO column placed as filter tubes inside the column. The bed level in the column is controlled by the filtrate recycle determining the hydraulic pressure at the top of the column. Pure crystals at the bottom of the column are transported to a melter by a scraper and part of the molten crystals is led up the column as the washing liquid. A wash front develops at the point where the all washing liquid has crystallized on the crystal surfaces, similar to the mechanical wash column. The layout of the TNO-column is presented in Fig. 2.3.1 b).

In the Kureha crystal purifier an almost solid crystal mass is fed to the column at its bottom. The crystals are transported upwards by means of a twin-screw conveyor. As in the other wash columns the crystals are melted at the top and the reflux runs down the column washing crystal surfaces. The discontinuous design of the conveyor blades prevent the crystals from turning with the screw and squeeze the impure melt downwards with the washing liquid. The column is not completely filled with liquid, but only the crystal surfaces are rinsed. A temperature gradient forms over the column length between the equilibrium temperatures of the pure product and the impure feed. The separation takes place by combined washing and sweating. Known industrial applications of the Kureha purifier are purification of p-dichlorobenzene, naphthalene and 3,5-dichloroaniline. The Kureha crystal purifier is presented in Fig. 2.3.1 c) [Ark95].

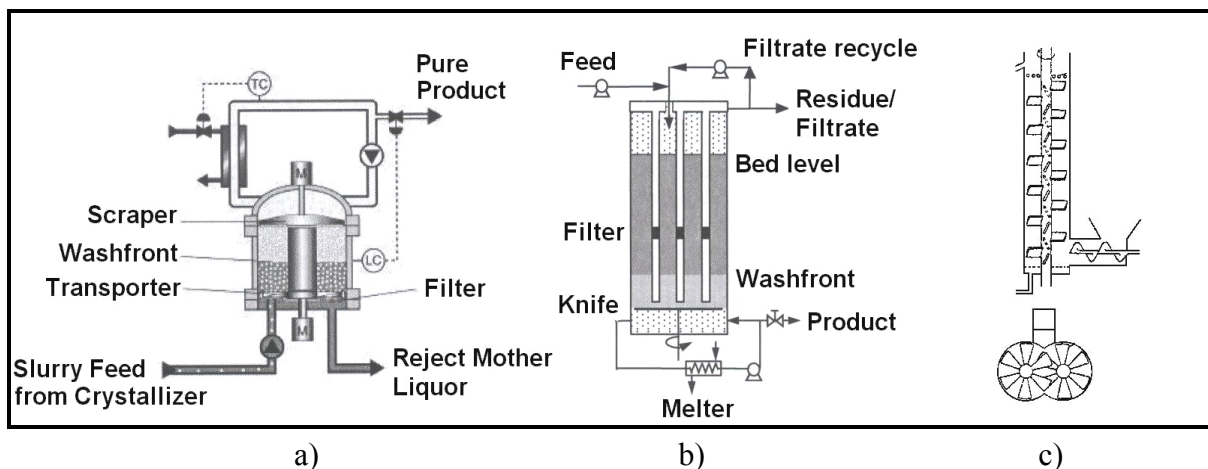


Figure 2.3.1 Processes applying wash column technology in melt crystallization: a) the Niro Purifier [Sch03a], b) the TNO wash column [Ver03b], c) the Kureha crystal purifier [Ark95].

2.4 Scraped Surface Heat Exchangers

Because of their importance for melt crystallization processes and for the investigations presented in the experimental part in Chapters 4.3 and 4.4, scraped surface crystallizers are described here in their own chapter. Special attention is given to the correlations describing the dependence of the heat exchange efficiency on the process conditions.

A scraped surface crystallizer is a double-pipe heat exchanger in which a shaft with scraper blades is mounted at the central axis of the inner pipe. As the shaft rotates the heat transfer surface is cleaned periodically by the scraping action. The scraper blades can be spring-loaded for better contact with the heat transfer surface, they can be pressed against the surface by the centrifugal force of the rotating shaft, or they can be set at a fixed distance from the heat exchange surface. Thus, the scraped surface crystallizer can be designed so that the crystallization takes place in the heat exchange surface or in the solution close to the surface. The most suitable SSHE construction is governed by the properties of the mixture to be crystallized and the specifications for the product out of the SSHE. Scraped surface crystallizers are used in petrochemical industry for production of waxes and fats, and for production of viscous materials such as lard, margarine and ice cream. Another application is the concentration of foodstuffs such as fruit juices, vinegar, tea and coffee by freeze concentration [Mul01]. The crystals produced by scraped surface crystallizers are usually very small, since nucleation and crystal breakage caused by the scraper action can be excessive. Indeed, the advantage of SSHEs that high undercoolings are applicable at the heat exchange surface due to scraping action result in high nucleation rates at the heat exchange surface. For that reason the scraped surface crystallizers are often used solely for production of seed crystals for further growth zone of another equipment. Examples are the uses as a crystal forming equipment in Phillips and TNO columns as well as in a Brodie purifier [Mol74]. A particular advantage of the scraped surface crystallizer is that the liquid hold-up is very low. However, when a crystal growth zone is combined with the SSHE, the total volume of the system must of course be taken as the crystallizer volume. In such cases the liquid hold-up is comparable to common crystallization processes applying agitated vessels.

2.4.1 Heat transfer properties of scraped surface crystallizers

It was first reported by Huggins [Hug31] that with viscous liquids remarkable improvements in heat exchange coefficients can be achieved using scrapers. With low viscosity liquids the change in the heat transfer coefficient was less pronounced. The heat transfer coefficients achieved in scraped surface heat exchangers, where crystallization takes place at the wall, have been reported to be approximately 200 –1000 W/m²K. When crystallization takes place in the solution near the wall the range of the heat transfer coefficients has been reported to be 1000-2000 W/m²K [Mul01]. If the scraped surface crystallizer is used solely for heat transfer purposes heat transfer coefficients up to 4000 W/m²K can be achieved. These data must be gathered from equipment with spring loaded scrapers pressed against the heat exchange surface, because of good agreement with the heat exchange coefficients from such equipment presented by de Goede [deG89].

The heat exchange properties of scraped surface crystallizers were first quantitatively researched by Houlton [Hou44]. He used a laboratory scale votator type heat exchanger applying product flow rates of 150-800 kg/h, cooling medium flow rates of 650-3700 kg/h and rotation frequencies of 5-31.7 s⁻¹. The overall heat transfer coefficients achieved were 3000-6400 W/m²K. Skelland [Ske58] was the first one to investigate the inner heat transfer

coefficient of a scraped surface crystallizer. Based on his experimental measurements he developed a correlation for the Nusselt number, given by equation:

$$Nu = 4.9 \left(\frac{D_i v \rho}{\mu} \right)^{0.57} Pr^{0.47} \left(\frac{D_i N}{v} \right)^{0.17} \left(\frac{D_i}{l} \right)^{0.37} \quad (2.4.1)$$

After the work of Skelland first Latinen [Lat59], followed by several authors [Har59, Nik65, Bra64, Kon71], developed a theoretical solution for the inner heat exchange coefficient based on the temperature distribution in a one side infinite body. In these models it is assumed that the liquid cools on a surface layer by molecular heat transfer, until it is mixed to the bulk liquid by the succeeding rotation of the scraper. The correlation thus observed is given by the equation:

$$Nu = (2/\sqrt{\pi})(Re Pr Z)^{1/2} \quad (2.4.2)$$

Harriott [Har59] has reported that the correlation works satisfactorily for low and middle viscous liquids. For high viscous liquids the correlation gives up to 50% too high values due to the inefficient mixing of the surface layer for the highly viscous systems. Skelland *et al.* [Ske62] investigated the inner heat exchange coefficient for high and low viscosity liquids. They varied the axial Reynold's number, rotational frequency, votator diameter, the number of scrabers and the Prandtl number and achieved a correlation given by the equation:

$$Nu = C Pr^e Re_{ax} (D_i N/v)^{0.62} (D_v/D_i)^{0.55} Z^{0.53} \quad (2.4.3)$$

where $C = 0.014$ and $e = 0.96$ for high viscosity liquids and
 $C = 0.039$ and $e = 0.70$ for low viscosity liquids.

Investigations on the heat exchange properties of scraped surface crystallizers during cooling and crystallization of water and ice have been first reported by Dinglinger [Din63]. For cooling conditions he obtained a correlation given by equation:

$$Nu = 0.487 Re^{0.652} Pr^{1/3} \quad (2.4.4)$$

For the crystallization conditions the heat exchange could be described by equation:

$$Nu = 14.1 \cdot 10^{-6} Re^{0.83} Pr^{3.32 - 0.332 \ln Pr} \cdot (\theta_{in}^*/\theta_{out}^*)^{1.76} - 0.22 \ln(\theta_{in}^*/\theta_{out}^*) \quad (2.4.5)$$

where θ_{in}^* and θ_{out}^* are the dimensionless temperatures at the inlet and at the outlet, respectively. The dimensionless temperature was here defined by equation:

$$\theta^* = \frac{\theta_e - \theta}{\theta_e - \bar{\theta}_{cm}} \quad (2.4.6)$$

Kulatschinski [Kul65] investigated heat exchange in a helical scraped surface heat exchanger and achieved a correlation given by equation:

$$Nu = 21.67 Re^{0.44} Pr^{0.33} (\mu/\mu_w)^{0.14} [(D_i - D_v)/D_i]^{0.35} \quad (2.4.7)$$

Sykora and Navratil [Syk66] investigated heat exchange by heating of highly viscous oils and sugar syrups at different rotational frequencies and different numbers of scrapers. The result was a correlation given by the equation:

$$Nu = 0.478 Re^{0.48} Re_{ax}^{-0.01} Pr^{0.40} Z^{0.24} \quad (2.4.8)$$

It can be seen that the influence of the number of scrapers is given by $Z^{0.24}$, not by $Z^{0.5}$ as was suggested by the theoretical model of Latinen [Lat59]. Trommelen [Tro67] evaluated the results of Skelland *et al.* [Ske62] anew together with own measurements. He introduced a correction factor to the theoretical solution of Latinen, thus taking into account the process conditions. The results of Trommelen can well be described by equation:

$$Nu = Nu_{th} \left[1 - 2.78 (Pe_{ax} + 200)^{-0.18} \right] \quad (2.4.9)$$

The experimental results could be better interpreted by equation 2.4.9 than by equation 2.4.3 given by Skelland *et al.* Nikolajew [Nik67] has given a correlation for a scraped surface heat exchanger with two scrapers given by equation:

$$Nu = 0.00475 \left(\frac{D_i v \rho}{\mu} \right)^{0.89} \left(\frac{N D_s}{v} \right)^{0.66} \left(\frac{Pr}{Pr_w} \right)^{0.25} Pr^{0.58} \quad (2.4.10)$$

A correlation for a votator type scraped surface heat exchanger with two scrapers was given by Ghosal *et al.* [Gho67] in the form of equation:

$$Nu = 0.123 \left(\frac{N D_i}{v} \right)^{0.89} Re_{ax}^{0.79} Pr^{0.6} \quad (2.4.11)$$

Sykora *et al.* [Syk68] published results for the laminar region up to $Re = 44$ and the transition region in the form of equations:

$$Nu = 0.80 Re^{0.35} Pr^{0.37} Z^{0.25} \quad (Re < 44) \quad (2.4.12a)$$

$$Nu = 2.00 Re^{0.48} Pr^{0.24} Z^{0.15} \quad (Re > 44) \quad (2.4.12b)$$

From these equations it can also be seen that the exponent for the number of scrapers is smaller than that given by the theoretical solution (equation 2.4.2).

Penney and Bell [Pen69] found out in their investigations that the distance between the heat exchanger wall and the rotating blade had no influence on the heat transfer coefficient when the Reynolds number was over 700. For Reynolds numbers over 400 they suggest an equation:

$$Nu = 0.123 Re^{0.78} Pr^{1/3} \left(\mu / \mu_w \right)^{0.18} \quad (2.4.13)$$

The exponents for the Prandtl number and the viscosity relation were obtained from an equation:

$$Nu = 0.308 Re^{0.68} Pr^{1/3} \left(\mu / \mu_w \right)^{0.18} \quad (2.4.14)$$

presented by Uhl [Uhl66], who had constructed it from the data from the experiments of Houlten and Skelland. In his investigations Weisser [Wei72] found the following correlations for the Nusselt number in a scraped surface crystallizer during cooling and freezing:

$$Nu = 1.5 Re^{0.47} Pr^{0.33} Z^{0.27} \quad \text{for cooling} \quad (2.4.15a)$$

$$Nu = 1.41 Re^{0.5} Pr^{0.45} Z^{0.5} \quad \text{for freezing} \quad (2.4.15b)$$

Miyashita *et al.* [Miy97] have studied heat transfer in a votator type scraped surface heat exchanger by an electrochemical method. The authors obtained a correlation for the Nusselt number by analogy between heat and mass transfer, presented by the equation:

$$Nu = 1.53 Re^{0.51} Pr^{0.33} \left(D_i / D_e \right)^{0.44} \quad (2.4.16)$$

It was shown in the work of Miyashita *et al.* that the mass flow rate had only a negligible effect on the mass (heat) transfer coefficient due to the dominating influence of the votator rotational velocity. The conclusion that the parameters for mass and heat transfer are exactly the same seems, however, to be too easy. For example, Wenzlau *et al.* [Wen82] suggested the following equation as a correlation for mass and heat transfer in a scraped surface heat exchanger:

$$Nu \text{ (or } Sh) = a Re^{b1} Pr \text{ (or } Sc)^{b2} \left(1 - m_T / m_{T,max} \right)^{b3} \quad (2.4.17)$$

The parameters for Reynolds numbers under 900 are for heat transfer $a=0.053$, $b_1=0.53$, $b_2=1.3$, $b_3=1.35$, and for mass transfer $a=1.62$, $b_1=0.45$, $b_2=0.85$, $b_3=2.2$. For Reynolds numbers higher than 900 the parameters are $a=0.00475$, $b_1=1$, $b_2=1.1$, $b_3=1.6$ for heat transfer and $a=0.0322$, $b_1=0.65$, $b_2=1.15$, $b_3=2.25$ for mass transfer. Thus, the parameters get different values for heat and mass transfer.

De Goede has studied crystallization in scraped surface heat exchangers with the Exxon paraxylene plant. De Goede stated that latent heat is negligible compared to the transferred sensitive heat. In the work of de Goede and de Jong [deG89] the heat transfer coefficients were measured as a function of the coolant temperature. The heat transfer coefficient decreased by decreasing coolant temperature. The reduction in the heat exchange coefficient was due to the increasing thickness of the incrustation layer caused by higher undercooling values. The values varied from 150 to 1500 W/m²K at temperatures between -50 to -25°C surface temperature. From this the authors calculated the thickness of the incrustation layer. A conclusion was made from the experimental results that scraping does not remove the layer completely, but only removes growth irregularities from the wall.

It has been reported [deG88] that in the Exxon-process for production of p-xylene the heat flux in the scraped surface crystallizer amounts 8 kW/m², the heat transfer coefficient lying in the range 1000-2000 W/m²K. The temperature difference between the wall of the heat exchanger and the bulk suspension has been reported to be 4-8 K. De Goede has stated that the crystal size distribution can be affected by controlling the wall temperature, which is directly responsible for the nucleation rate in the heat exchanger. Because the recovery of the process is fixed and depends on the heat flux and on the bulk temperature in the crystallizer, the wall temperature can only be affected by the heat transfer coefficient.

Therefore, it was suggested [deG88] that the scraped surface heat exchanger should be run in conditions where the incrustation is still negligible. If the wall temperature is lowered further the forming crystalline layer will hinder heat transfer despite the scraping action. De Goede [deG93] has modelled the heat transfer in a scraped surface heat exchanger by the Gnielinski [Gni75] equation:

$$Nu_{tube} = \frac{\xi/8 (Re_{ax} - 1000) Pr}{1 + 12.7 (\xi/8)^{0.5} (Pr^{2/3} - 1)} \left[1 + \left(\frac{D_h}{l} \right)^{2/3} \right] \left(\frac{Pr}{Pr_w} \right)^{0.11} \quad (2.4.18)$$

The equation 2.4.18 has been developed for flow in tubes, where

$$\xi = (1.82 \log Re_{ax} - 1.64)^2 \quad (2.4.19)$$

For a flow through an annular space for heat transfer to the outer tube the Nusselt number for pipe flow has to be corrected by

$$Nu = Nu_{tube} \left[1 - 0.14 (D_v/D_i)^{0.6} \right] \quad (2.4.20)$$

as suggested by Petrukov and Roisen [Pet64], the inner cylinder is assumed to be fully isolated. The scraper blades are taken into account by including the wetting of the blades in the hydraulic diameter, which is 4 times the cross-sectional area divided by the wetted perimeter.

Nucleation on scraped metal surface was studied by Liu and Garside [Liu99]. They showed the dependence of heterogeneous and homogeneous nucleation on the surface undercooling. No data was presented on the heat transfer or heat transfer coefficients. An intensive literature study on scraped surface crystallizers has been done by Patience *et al.* [Pat01]. The authors, however, do not discuss the parameters of heat transfer in such equipment. A recent work of Vaessen [Vae03] presents an excellent investigation on scraped eutectic crystallizers, including studies on scraped surface crystallizer. In his crystallizer construction both the inner wall of the outer cylinder as the outer wall of the inner cylinder were cooled and scraped. This was done to increase the cooled surface. The scrapers were made of teflon. Scaling on the heat transfer surfaces by ice was observed in all experiments. The rotational velocities used in the work of Vaessen were only up to 1 rev/s, which is not enough to avoid crystallization of ice on the cooled surfaces. For the outer cylinder wall he presented a correlation for the Nusselt number by equation

$$Nu = 16.2 Re^{0.27} Pr^{0.30} \quad (2.4.21)$$

for non-crystallizing conditions. No correlation was presented for crystallizing conditions. It was reported that at crystallizing conditions the heat transfer coefficient diminishes by increasing solids content. Impurities in the ice slurry were found to be due to the adhering impure liquid, which could be removed by washing, thus the crystals produced were pure.

The heat exchanger correlations presented in Chapter 2.4.1 are presented in Table 2.1 with the applications and constructions at which they were determined.

Table 2.1 Application of heat exchange correlations for scraped surface heat exchangers. The numbering of the equations refers to the correlations in Chapter 2.4.

Equation	heat exchange	crystallization	water/ice	chemicals	food stuffs	used compounds	construction
1						water, glycerin, mineral oils	votator
2						purely theoretical	votator
3						water, glycerin and their mixtures	votator
4						water	rigid knives
5							rigid knives
7						water, Rahm	helical
8						viscous oils, sugar syrups	votator
9						glycerin solutions	votator
10						water	
11						molasses, glycerin, their mixtures with water, water	votator
12						no data	
13						no data	blade mixer
14						data taken from work presented in Eq. 1	votator
15a						water, water-sugar solutions, water-glycerin solutions	votator
15b						water, water-sugar solutions, water-glycerin solutions	votator
16						ferri-/ferrocyanide solution in water	votator
17						60/40 wt.-% p-nitroacetophenon/p-nitroethylbenzol	votator
18-20						p-xylene	spring loaded blades
21						aqueous KNO ₃ - HNO ₃	scrapers in inner and outer cylinders

2.5 Freeze Concentration

A crystallization process where water is crystallized out of an aqueous solution is called freeze concentration. Freeze concentration has been performed by both layer and suspension growth modes, but suspension crystallization processes are the more used methods. Aqueous solutions form mainly eutectic systems, so ice can be crystallized in a very pure form. After the separation of the ice crystals from the mother liquor a more concentrated aqueous solution and pure water are obtained.

Freeze concentration is mainly used in food industry for concentrating of aqueous foodstuffs and in chemical industry for purification of wastewater containing highly toxic components. The applications in food industry include concentration of coffee, juices, beer, milk, alcoholic beverage and vinegar [Mul01, Nir98]. The applications for wastewater treatment are usually combined with an incinerator. The removal of water can cause significant savings to the investment and energy costs of the incinerator, due to the smaller amount and higher caloric value of the feed [Nir00]. In addition, the pure water produced can be reused in the plant. Based on this, attempts have been made to use freeze concentration for reduction of fresh water usage in pulp and paper mills to achieve so called closed operation. However, up to now this has not been successfully realized in the industrial praxis [Lon98]. The reasons for this are worth mentioning, as they are interesting for the work done on crystallization in a tubular heat exchanger. In industrial pulp and paper mills the feed properties can significantly change on day-to-day basis, which changes the thermodynamic properties of the solution. These changes are small compared to the temperature differences required for crystal formation. However, this caused frequent plugging and scaling in undesired locations where the crystallization should have not taken place. It was reported that problems with ice formation in the pipes was encountered at every change in pipe size or direction, even at surface irregularities at straight pipes. Another problem reported was inefficient washing. The freeze concentration process was designed and realized by the Louisiana-Pacific BCTMP Mill [Roy90]. By the description of the problems it is probable that the freeze concentration process should work well also in the presented application when the scaling problems are overcome by better planning of the piping, and when an industrially proved freeze concentration process with efficient and reliable solid-liquid separation would be employed. Other fields of application suggested for freeze concentration include desalination of seawater [Bar82], concentration of vaccines and protein and polypeptide solutions [Nir98], however, no industrial applications have been reported.

The method most commonly used to concentrate aqueous solutions is still evaporation. However, by freeze concentration it is possible to preserve volatile or temperature sensitive components in the solution, e.g. flavors and vitamins in foodstuffs. By freeze concentration it is also possible to avoid problems with gaseous handling and corrosion present in evaporation systems and achieve reduction in emissions and transport, packaging and storage costs. Evaporation is also more energy intensive. It has been reported that freeze concentration can be an economical alternative in the pulp industry if the price of electricity is low compared to the price of oil [Lou96].

The ice crystal shape from freeze concentration has been reported by many authors to be disc like [Ara54, Hal65, Hui72, Lin66]. However, Huige [Hui72] has also shown in his work that ice crystals can get a spherical shape during a ripening process, where melting of small crystals provides a heat sink for the growth of larger ones. In this case the lower the undercooling during the ripening process, the more emphasized is the sphericity of the ice crystals.

Freeze concentration for purification of wastewater from an industrial distillery has been carried out applying the method of ice crystal agglomeration presented in Chapter 2.1.3 [Shi98]. However, sufficient purification was not achieved by one crystallization and solid-liquid separation step. Further purification was carried out by layer crystallization of ice, which remarkably reduces the energy efficiency of the total process.

2.6 Summary of Existing Suspension Melt Crystallization Research

In the theoretical part for suspension melt crystallization basic kinetic considerations concerning suspension melt crystallization are discussed in Chapter 2.1. In Chapter 2.2 the most important industrial applications of suspension melt crystallization and crystallizer constructions comparable to the current study are described. The solid-liquid separation processes making use of the wash column technology are presented in Chapter 2.3 due to the relevance to the experimental work with a pilot plant presented in Chapter 4.3. Scraped surface heat exchangers are handled in Chapter 2.4 together with the semi empirical correlations for their heat transfer calculations. Aspects of freeze concentration relevant to the applications described in the experimental part are discussed in Chapter 2.5.

The equipment of suspension melt crystallization is prone to incrustations. However, relatively few studies have investigated the possibilities to prevent incrustations by process conditions. The reason is that most suspension melt crystallization equipment use scraped surface heat exchange elements with mechanical removal of incrustations, or agitated vessels. In agitated vessels the removal forces on the heat exchange surfaces are not easily adjusted sufficiently high by the flow conditions and the heat exchange surface area is restricted. Therefore, in this work a new equipment construction making use of an ordinary heat exchanger for crystallization is investigated. At the industrial pilot-plant experiments have been carried out to investigate the growth conditions at a circulation loop, instead of in an agitated vessel.

Another aspect missing in studies on industrial melt crystallization is the lack of data over the crystal size distributions. Especially this is the case for the scraped surface crystallizers, where in-line measurements are complex due to the scraping action. A truly reliable method for deduction of size and shape is in many practical cases possibly only by tedious image analysis. This has been done in the current work for the crystals produced by the various equipment used, as well as for the crystals produced in a scraped surface crystallizer right after their formation at the cooled wall.

With the research carried out in this work the phenomena at the cooled surface in crystallization processes and the crystal formation process will be better understood, which gives a basis for the further development of the suspension melt crystallization processes.

3. Crystalline Deposits in Heat Exchangers

According to the mechanism responsible for the deposit generation, fouling of heat exchange surfaces has been classified into crystallization fouling, particulate fouling, chemical reaction fouling, corrosion fouling and biological fouling.

- *Crystallization fouling* is the deposition of a solid layer on a heat transfer surface by a phase change process. In aqueous systems crystallization fouling mainly results from the presence of dissolved inorganic salts in the flowing solution, which become supersaturated under the process conditions (*precipitation fouling*). Typical scaling problems in such cases are calcium carbonate, calcium sulphate and silica deposits. In oil pipelines and in dewaxing processes crystallization fouling can occur by solidification of higher melting fractions of the organic mixture (*freezing or solidification fouling*).
- *Particulate fouling* is the accumulation of particles suspended in a fluid onto a heat exchange surface. Suspended particles can be crystals, ambient pollutants (sand, silt, clay), upstream corrosion products or products of chemical reactions occurring within the fluid.
- *Chemical reaction fouling* involves deposits that are formed as the results of chemical reactions at the heat transfer surface. The heat exchanger surface material does not react itself, although it may act as a catalyst. This kind of fouling is a common problem in chemical process industries, oil refineries and dairy plants.
- *Corrosion fouling* occurs when the heat exchanger material reacts with the fluid to form corrosion products on the heat transfer surface.
- *Biological fouling* is the development and deposition of organic films consisting of micro-organisms and their products (microbial fouling) and the attachment and growth of macro organisms, such as barnacles or mussels (macrobial fouling).

Generally, several fouling mechanisms occur at the same time, nearly always being mutually reinforcing. One notable exception is particle deposition occurring together with crystallization, which weakens an otherwise tenacious scale [Bot95]. Although the sedimentation of particles (thus particulate fouling) very often is the origin of hard crystalline deposits forming in crystallizer vessels, the focus in this work is given to crystallization fouling on a clean surface, which is the common fouling problem encountered in melt crystallization systems.

Crystallization fouling is called freezing fouling in the literature. This might be because one of the most practical examples – freezing of water pipes at winter – is a typical case of this type of deposit formation process. Other examples are blockage of chemical process lines or oil pipes and the freezing of liquid metals and glass, when poured through channels and nozzles [Wei97]. The progress of freezing fouling is presented in Fig. 3.1. An initiation period

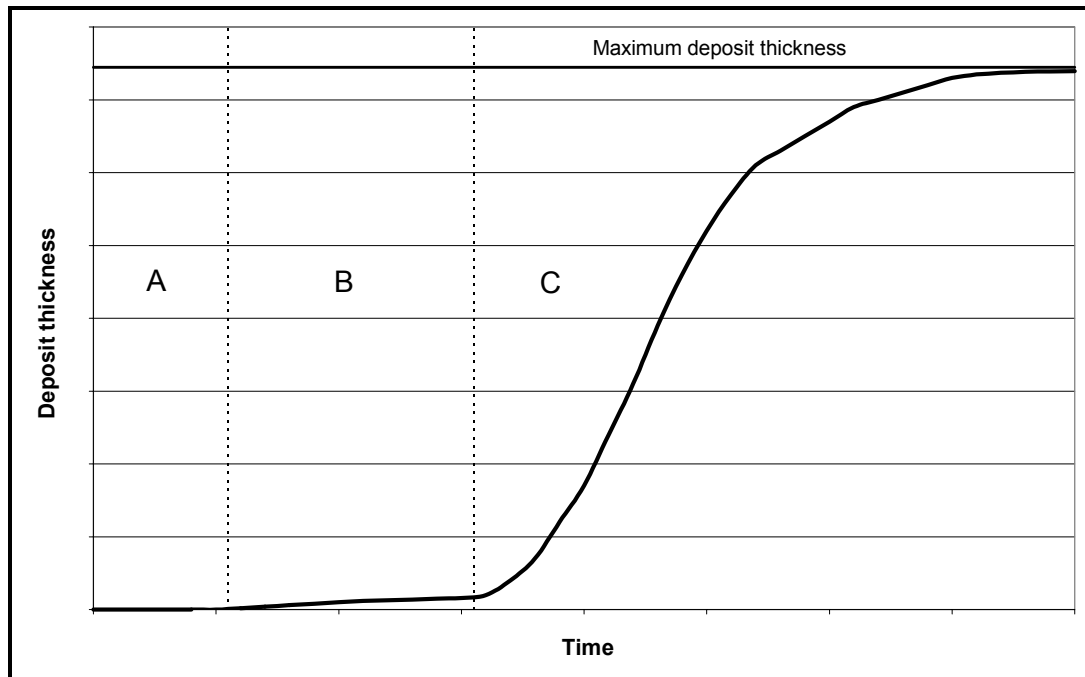


Figure 3.1 Development of a crystalline deposit in freezing fouling. A: induction period, B: surface nucleation period, C: growth of the deposit layer.

(A) is needed for the surface nucleation (similar to crystallization processes described in Chapter 2.1). After the surface nucleation a period (B) can be observed, during which the surface is covered with the crystalline deposit. Depending on the temperature difference on the surface and the properties of the crystallizing component, this period can be infinitely short, or total coverage may not be achievable at all. The growth of the deposit layer thickness (C) follows. In fouling mitigation it is often the aim to prolong the induction period as long as possible. The induction period can be extended according to Mersmann [Mer95] by:

- low heat flux and small temperature difference at the wall
- optimal flow velocity of crystal suspension
- smooth or coated pipes
- ultrasonic vibration on pipes
- presence of additives (fouling inhibitors)

The resistance to heat transfer due to the deposit layer is described by the fouling resistance, defined by

$$R_f = \frac{x_d}{k_d} = \frac{1}{h_f} - \frac{1}{h} \quad (3.1)$$

The nucleation on the heat exchanger surface can lead to surface roughening, which leads to increasing turbulence and higher heat transfer coefficient on the surface. In this case the fouling resistance can get negative values. However, when the deposit thickness increases heat transfer from the surface is hindered. The driving force for crystallization fouling is the

temperature difference (undercooling) on the solid-liquid phase boundary. For a flat plate the temperature on the phase boundary can be calculated by assuming that the system is at pseudo-steady state by the equation:

$$(T_s - T_a) \left[\frac{1}{h_o} + \frac{x}{k_w} + R_f \right]^{-1} = [(T_b - T_s)h_i + \dot{N} \Delta H_f] \quad (3.2)$$

For a pipe flow this equation must be transformed to the following form:

$$(T_s - T_a) \left[\frac{1}{h_o} \frac{D_i}{D_o} + \frac{x}{k_w} \frac{D_i}{D_{\log}} + R_f \right]^{-1} = [(T_b - T_s)h_i + \dot{N} \Delta H_f] \quad (3.3)$$

It can be seen from equations 3.2 and 3.3 that by increasing fouling resistance the temperature difference between the deposit surface and the bulk solution becomes smaller. When the driving force for the deposit formation (crystallization) becomes smaller, the growth rate of the deposit gradually decreases. Finally, the limiting deposit thickness is reached, at which the heat transfer is hindered by the deposit by such extent that no driving force exists. Theoretically this limiting thickness is approached only asymptotically. In a practical case of a pipe flow the whole pipe can of course be blocked before the limiting thickness is achieved. For a given system this process can be influenced by two main factors: The surface temperature, T_s , and the flow conditions influencing the heat transfer coefficient on the phase boundary, h_o . For many technical applications the formation of a frozen crust must be allowed, because of constructive limitations or additional costs needed for preventing the crystallization fouling. In such cases it is important to investigate the freeze shut of the system in order to prevent damage to process equipment by the increasing pressure drop [Wei97].

In addition to the pure heat exchange approach, it is important to understand that there are simultaneously a deposit growth phenomenon and a deposit removal phenomenon taking place in the system. How strong is the deposit removal effect depends on the one hand on the forces in the flow, and on the other hand on the cohesion forces in the deposit layer and adhesion forces of the deposit to the heat exchange surface. The forces in the flow can be affected by the flow conditions, and in crystallization processes additionally by the suspension density of crystals in the flowing stream. The adhesion forces between the deposit and the heat exchange surface are influenced by the surface temperature difference and the surface properties. For the deposit removal rate has been presented an equation [För99]

$$\dot{m}_r = C_R \left(\frac{\mu g}{\rho} \right)^{1/3} \frac{\rho_f}{\sigma_f} \tau \quad (3.4)$$

where C_R is a constant, μ is the viscosity of the solution, g the acceleration by gravity and ρ and ρ_f the densities of the solution and the deposit, respectively. The shear strength of the deposit is given by σ_f and τ is the shear stress. This equation has been developed for the case

of a removal from the surface of a fully developed deposit. However, it can as well be applied to the induction period, where no fully developed deposit layer exists, or for the case where the whole deposit thickness is removed from the surface. In these cases the shear strength of the deposit, σ_f , should be replaced by the adhesion forces between the deposit and the surface.

3.1 Effect of Flow Conditions

It has been proved that when the flow velocity increases in the laminar region the deposit thickness increases due to better heat exchange conditions on the surface. However, when the flow velocity reaches the turbulent region and further increases, the deposit thickness decreases due to higher shear forces of the fluid stream. Thereby, the deposit thickness reaches a maximum value at a certain flow velocity.

In pipe flow it very often occurs that the deposit layer possesses a wavy profile, as presented in Fig. 3.1.1 [Hir85]. The reason for this are the changing flow conditions along the pipe length. It can be seen that the deposit can at some flow conditions melt and almost disappear. From Fig. 3.1.1 it can also be well observed how the flow conditions (Re_D) and the surface temperature difference (θ_c) are related to each other in the case of crystallization fouling. At higher Reynolds numbers (in this case higher flow velocity) larger surface temperature differences are necessary to produce a deposit layer of comparable thickness.

The limiting deposit layer thickness and the conditions for formation of wavy deposit layers have been well investigated (e.g. [Eps76]). However, the limiting flow conditions have been paid less interest to. The reason may be that in the cases where freezing fouling usually occurs the flow conditions may not be easily adjustable (long oil and water supply lines, flow of metals). However, in chemical process equipment, such as crystallization processes, the flows can be chosen more freely, which offers a possibility for mitigation of crystallization fouling. It has been reported that shear dispersion causes crystals in a suspension to migrate toward the opposite direction of the shear rate gradient [Gra91, Mon94]. That means that a flow has a tendency to hinder deposit formation. When Fig. 3.1 and Fig. 3.1.1 are compared it can be seen that the curves presented have similar form. However, Fig. 3.1 shows the deposit thickness vs. time and Fig. 3.1.1 vs. the pipe length. Anyway, it has been reported by Ribeiro *et al.* [Rib97] that, similar to the induction time in Fig. 3.1, an induction length is obtained in pipelines transporting crude oil at which no crystallization fouling occurs on the pipe surface. The authors have mentioned that up to this point the inner surface of the pipe has not yet reached the saturation temperature needed for crystallization to take place. However, this is not probable, because a sudden increase of the deposit thickness at the point of formation is observed, which suggests that a certain undercooling already exists at this point.

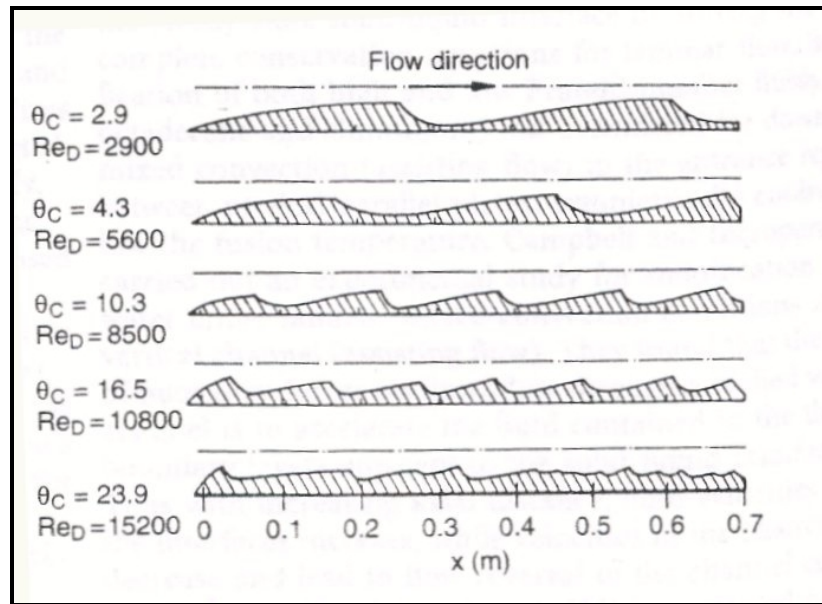


Figure 3.1.1 Steady-state wavy ice layers in a pipe flow [Hir85].

Bohnet [Boh85] has developed an equation for the time needed to reach the asymptotic maximum fouling layer thickness by crystallization fouling. The equation can be written:

$$\ln \frac{R_f}{R_f^*} = K_p v^2 t \quad (3.1.1)$$

where K_p is constant including the physical parameters of the liquid and the crystalline deposit. From this formula it can be concluded that by crystallization the layer thickness can be affected by the flow velocity of the cooled stream. However, the flow velocity appears also in the equations for mass transfer and heat transfer, and an absolute value cannot be calculated without knowing these effects. Anyway, the heat transfer is known to play in melt crystallization processes much more important role than the mass transfer. Thereby, the increment of heat transfer by increasing flow velocity influences the process of fouling mitigation far more positively than can be effected negatively by boosted mass transfer rate. It was reported by Bott [Bot95] that the asymptotic fouling resistance due to wax deposits from a kerosene stream was inversely proportional to the square of the Reynolds number.

The way in which the flow velocity affects the fouling process has been demonstrated in the work of Yang *et al.* [Yan02]. The authors investigated the induction time at different conditions for the case of CaCO_3 . Higher flow velocities at a fixed heat flux decreased the wall temperature through more effective heat exchange on the surface. Thereby, CaCO_3 being a salt with inverse solubility, was the driving force for crystallization reduced and the induction time prolonged. The opposite was observed when the heat exchange surface temperature was kept constant – increasing flow velocity caused the induction time to get shorter. The reason is that, the driving force being the same, the mass transfer of ions was increased by the increasing turbulence, which affected the growth of the surface deposits positively. In addition to the heat and mass transfer effects the removal phenomena was investigated. For this purpose the flow was periodically switched between flow rates of 1.39

and 1.62 m/s every five minutes. It was found out that when the higher flow rates were periodically used from the beginning on, the induction time was longer and the deposit grew slower. However, when the same treatment was used to a grown deposit layer the deposit growth was faster than without the periodical change of the flow velocity. The authors did not try to explain this phenomenon, but it should be clear that the adhesive and cohesive forces of the deposit play an important role on such a process. In this case the adhesive forces between the heat exchange surface and the deposit are weaker than the cohesive forces in a developed layer of the hard ionic crystals. When at lower flow rates merely changes in heat and mass transfer processes were observed, the removal was first noticeable at the flow rate of 1.62 m/s for the period of nucleation and spread over the surface. On the other hand, this flow velocity again merely enhanced the heat and mass transfer processes applied to a fully grown layer. From this can be concluded that every type of connecting force (adhesive/cohesive) has its limiting flow velocity (shear force by the flow), at which the removal forces grow in importance higher than the positive influence to the deposit growth by the improved heat and mass transfer.

A reported way of fouling mitigation by adjusting the flow conditions is pulsation of the process stream flow, which increases the shear stress on the heat exchange surface [För99]. If the pulsation period is sufficiently short (e.g. 10 s) the shear forces are sufficient to remove formed crystallites from the heat exchange surface. When the length of the oscillation period is increased the amount of crystals and a longer residence time on the surface result in better attachment of the deposited material and necessitate a higher shear stress for deposit removal.

3.2 Effect of Crystalline Suspensions

Söhnel *et al.* [Söh96] have investigated the influence of the crystal suspension on the incrustation behaviour of sodium perborate. The authors showed that an incrustation forming on a clean surface took place in two steps: formation of a complete layer and further linear growth of the layer thickness. In a case where the surface was covered initially with a crystalline layer only the linear growth was observed from beginning of the experiment. With the substance studied the authors concluded that the mechanism of initiation of incrustation was attachment of crystals to the surface, which was concluded from the influence of the suspension density. From the experimental results it could also be seen that despite that the initiation period for higher suspension densities through eased attachment is shorter, the further growth is faster in the case of lower suspension density. This is due to the higher attrition force of the higher suspension density. This was also partly proven by the observation that on the calm side of the baffle the crystalline layer, even thinner than on the flow side, always covered the whole surface, whereas on the flow side the shear forces never allowed the whole surface to be covered. The mechanism in this case is not exactly crystallization fouling, but sedimentation with further growth of the attached crystals. However, the results show that a suspension provides a higher shear force for removal of the deposit layers.

The higher shear force of the flow at higher suspension densities is the result of increased apparent viscosity of the flowing fluid by suspended solids. It has been found that suspensions of high solids concentration show yield dilatant rheological behaviour [Wag77, Cha77, Hof74]. The same behaviour was observed by Hafaiedh [Haf88], who has also shown the effect of increasing solids concentration presented in Fig. 3.2.1. Dilatant rheological behaviour means that the shear stress increases exponentially when the shear rate (flow velocity) increases, by equation

$$\tau = \tau_y + K \dot{\gamma}^n \quad n > 1 \quad (3.2.1)$$

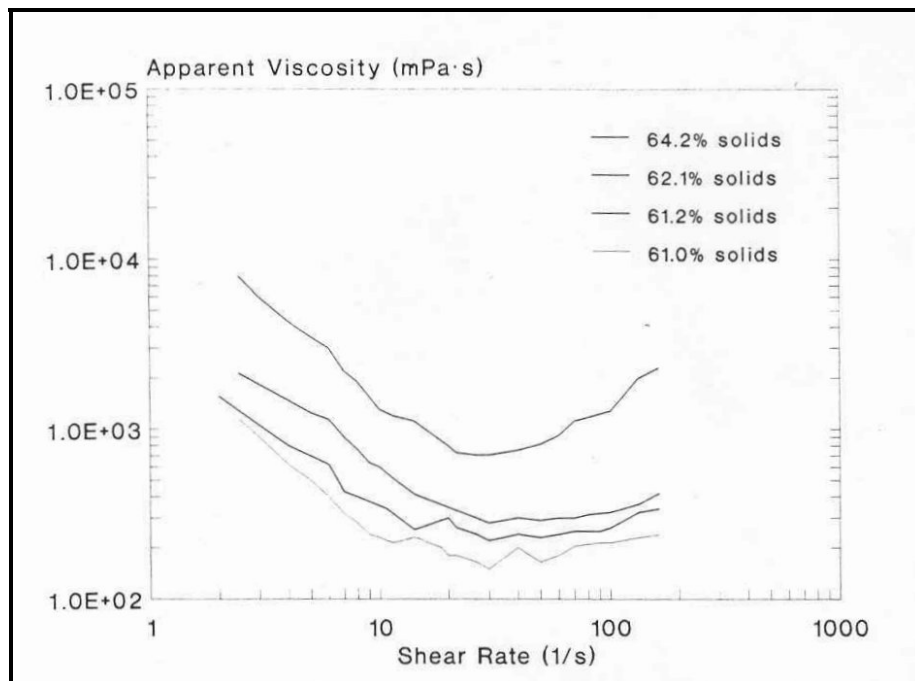


Figure 3.2.1 Effect of solids concentration on the apparent dynamic viscosity of a suspension [Haf88].

The result of a dilatant behaviour of a suspension is that an increment in the flow velocity brings a larger increment in the shear stress than for a Newtonian fluid (typical for a clear liquid), and that by higher solids content the shear stress also is higher. From Fig. 3.2.1 it can be seen that the apparent viscosity has a minimum accompanied with a slow rise in the case of yield dilatant rheology. In addition to shear stress, the viscosity also affects the processes of heat and mass transfer. The higher viscosity affects these processes negatively, which increases the surface temperature difference. It can be seen that running a suspension process at a low shear rate (low flow velocity) can lead to problems with deposit formation due to the high viscosity.

Solids present in a system can also act as catalysts for nucleation, as shown by Vendel and Rasmuson [Ven97]. The authors found out that the contact between a surface and a crystal can induce contact nuclei, which attach on the surface. However, secondary nuclei are always created in a supersaturated crystal suspension. Whether the nuclei attach and grow further on

the surface depends also on the surface characteristics. Vendel and Rasmuson also investigated the effect of surface characteristics and the results of their work are discussed in Chapter 3.3.

Deposit removal by particle abrasion was studied by Mori *et al.* [Mor96]. It was proven that particle abrasion increases the heat transfer coefficient on the surface. After the asymptotic fouling resistance was reached the heat transfer coefficient could be returned to 95% of the initial value by addition of glass beads. However, when the value was corrected for the real removal process taking into account the improvement in the heat exchange coefficient, the fouling resistance of the deposit (*ipso facto* the thickness) was decreased by 43%. It was stated by the authors that using glass beads the heat transfer coefficient approached a constant value when the suspension density of beads was over 50 kg/m^3 . It was noticed that higher flow rates did not result in more effective deposit removal. On the opposite, the deposit was even harder to remove. This was explained by saying that the fluid velocity has an influence on the fouling layer bond strength.

3.3 Effect of Surface Structure of Heat Exchanger

The effect of the surface structure of the heat exchanger can be divided to two factors: the geometrical configuration of the heat exchanger and the properties of the heat exchanger surface. While the geometrical construction brings its effect through its influence on the flow patterns, the surface properties influence the adhesive forces between the surface and the deposit.

The adhesive forces can be divided into mechanical interactions and molecular interactions, such as Lifshitz-van der Waals forces, Lewis acid base forces and double layer forces [Boh03]. The attachment forces between particles and a surface have been recently investigated by Sonnenberg and Schmidt [Son04], who modelled the attachment forces for various particle shapes based on the van der Waals forces between the particle and the surface.

In her experiments Schuldei [Sch00] found out that glass and stainless steel produced different results concerning the fouling of the heat exchange surface by crystallization. She found out that in metal surface the crystallization formed evenly on the surface. On the other hand, on the glass surface the incrustations started from a joint position and grew from that position on until the pipe was totally blocked. In a glass pipe the volume flow was influenced by an incrustation sooner at higher Reynolds numbers of the stream and also the pipe was sooner blocked when higher Reynolds numbers were applied. In a metal pipe the situation was different: As in a glass pipe the growth of an incrustation started earlier when the Reynolds number was higher, but the time needed for the blockage of the pipe was decreased. Also the time, which the equipment could operate without disruption, was shorter for the metal pipe, which is explained by the higher surface roughness of the metal pipe and higher heat conductivity of the wall material. The heat flux through metal and glass walls are different. From that follows that the temperature at the inner surface of the metal wall is by cooling lower, which makes the growth easier and faster. Therefore, the pipe will be blocked

sooner. The way in which a pipe most efficiently could be blocked by ice was studied by Keary and Bowen [Kea98]. They state that the pipe diameter has influence on the freezing behaviour through different turbulence conditions.

The influence of different surface materials on crystallization of organic chemicals has been investigated by Haasner [Haa02]. He showed that the effect of the surface material also depended on the compound system to be crystallized. The decisive factor for the ease of formation of crystalline layers on a cooled surface was found to be the interfacial tension between the melt and the cooled surface. The forces influencing the attachment of solid matter of a surface can be described with the help of the interfacial tensions with the equation [Isr85]:

$$W_{csl} = \gamma_{cl} + \gamma_{sl} - \gamma_{cs} \quad (3.3.1)$$

W_{csl} represents the work needed to remove a crystal from the surface and to create the corresponding crystal-liquid and surface-liquid interfaces.

Vendel and Rasmuson [Ven97] have investigated the influence of the surface material on the attachment of crystals. They found that organic crystals tend to attach on teflon surfaces, but crystals formed on a steel surface tend to detach from the surface. It was also found that the adhesion onto the surface was governed by the same physical properties as the catalytic activity of the crystal-surface interface on primary nucleation. These results are in good agreement with the results presented by Haasner [Haa02] for the influence of teflon surfaces. As the conclusion was stated that increasing the affinity of the crystallizing substance to the solid surface promotes catalyzed primary nucleation, collision initiation and adhesion of the deposit on the surface.

Nucleation can be avoided using special types of surface materials or by additives (like polyamides). In the case of special surface materials the negative aspects are high price and low heat transfer coefficients. The additives may influence the process negatively by influencing the product quality or by accumulation in the process streams [Cor01].

Bansal *et al.* [Ban01] compared crystallization fouling properties in plate-and-frame and double-pipe heat exchangers. They stated that the fouling on the heat exchange surface depended strongly on the shear rates prevailing in the different apparatuses. High shear rates were beneficial in avoiding crystallization fouling. Fouling inhibition could in their work be more efficiently achieved in the plate heat exchanger, where the surface profile enhanced high local shear rates.

3.4 Summary of Existing Research on Crystallization Fouling

In the theoretical part considering crystallization fouling on heat exchanger surfaces the basics of fouling phenomena and their influence on the heat transfer are presented. The mechanisms by which crystalline incrustations are initiated and by which the deposit growth proceeds have been discussed. In Chapter 3.1 the focus was given to the effect of flow conditions on

incrustation. In Chapter 3.2 has been presented the work on the influence of crystal suspensions on the fouling of the heat exchange surfaces. In Chapter 3.3 the structure of the heat exchange surface, especially the properties of the surface material, were discussed.

The fouling phenomena are manifold and a large amount of research has been carried out in this field. The research has, however, concentrated on the fouling mechanisms taking place in heat exchangers without phase change. The work on crystallization fouling has focused mainly on incrustations caused by inorganic salts. The freezing fouling phenomena are usually discussed in context of solidification of pipelines without any intentional heat exchange or phase change process.

The lack of research on incrustations in melt crystallization processes probably has its reason in the severity of the problem. It is commonly thought that deposit formation on cooled surfaces in melt crystallization is inevitable, and cannot be mitigated simply by adjusting the process conditions. However, the same laws of physics are behind the deposit formation in melt crystallization processes, as in any kind of crystallization fouling.

This work serves to investigate the possibilities of incrustation mitigation in suspension melt crystallization processes making use of the process conditions. The influence of the forces acting on the heat exchange surface are experimentally proved. Also the conditions, at which crystalline deposits form on a cooled surface, and the influence of these conditions on the layer structure, are investigated. With the research carried out in this work on the fouling phenomena the deposit formation and the deposit removal processes, and how they are influenced by the process conditions will be better understood. This gives the physical background for application of novel constructions for suspension melt crystallization processes.

4. Experimental Work

4.1 Introduction to Experimental Work

Here is presented the work carried out on melt crystallization in the laboratory and the pilot plant equipment. The experimental work is divided into four parts. The emphasis is on suspension melt crystallization processes. In addition, a chapter is dedicated to growth of crystalline layers. Chapter 4.2 deals with suspension melt crystallization in a tubular heat exchanger. In Chapter 4.3 the principles investigated in the previous chapter are applied to a pilot plant of industrial scale. Crystal growth and nucleation are more closely observed in Chapter 4.4. Finally, the investigations on the growth of crystalline layers are presented in Chapter 4.5.

4.2 Suspension Melt Crystallization in a Tubular Heat Exchanger

In order to simplify a suspension melt crystallization process, possibilities to apply a common heat exchanger construction as a crystallizer were investigated. Such processes have been applied in industry for solution crystallization processes. According to Scholz [Sch03b] precise conditions for reliable operation can be found. Melt crystallization presents an even greater challenge for such an application, due to the high concentration of the crystallizing component. This may cause unwanted incrustations to form on the heat exchange surfaces.

A usual way of handling the incrustations is their mechanical removal using scrapers or wipers, which periodically clean the heat exchange surface. However, the costs for construction and maintenance, as well as the sensitivity to mechanical defects, is for such equipment higher than for standard heat exchangers. Therefore, the possibilities to avoid incrustations by control of the flow conditions in the heat exchanger were investigated.

4.2.1 *Experimental equipment*

The experiments were carried out using a continuous suspension melt crystallization equipment presented in Fig. 4.2.1. A double-pipe heat exchanger made of glass was used as the heat exchange equipment. The characteristics of the experimental equipment are given in Table 4.2.1.

The double-pipe heat exchanger formed a continuous loop, in which nucleation and crystal growth took place. A membrane pump (P1) driven by compressed air was used to circulate the suspension inside the crystallizer loop. In order to simulate a continuous crystallization process a stream of suspension was led out of the crystallizer by the pump P2 through the valve V1 back to the feed tank. The crystals in the suspension melted away during their way to the feed tank and returned as fresh feed at temperature TI 8 to the crystallizer.

The temperatures TI 1-3 were measured in the crystallizing stream and the temperatures TI 4-7 in the cooling medium. The flow velocity of suspension in the crystallizer was measured by taking a sample at the valve V3.

In order to measure the suspension density in the crystallizer a sampling line (valve V2) was installed, through which a sample was taken to a filter. The temperature in the filter was controlled by two thermostats, which allowed a swift change in the temperature. The temperature switch was used to melt the crystal cake in order to prepare the filter for the next sample.

A cooling machine (Lauda H3000) was used to cool the crystallizer loop. A 50/50 wt.-% mixture of ethylene glycol and water was used as a cooling medium, which was circulated counter currently to the crystal suspension (C_{in} and C_{out} in Fig. 4.2.1). The cooling medium line was equipped with a switch that allowed the cooling medium to be circulated either in the heat exchanger or just through the thermostat itself. This made it possible that the cooling medium could be cooled down to the final temperature, while the temperature in the heat exchanger remained at the ambient temperature. The temperature in the heat exchanger could be suddenly changed to a lower level (crash cooling) by switching the cooling medium stream to flow through the heat exchanger.

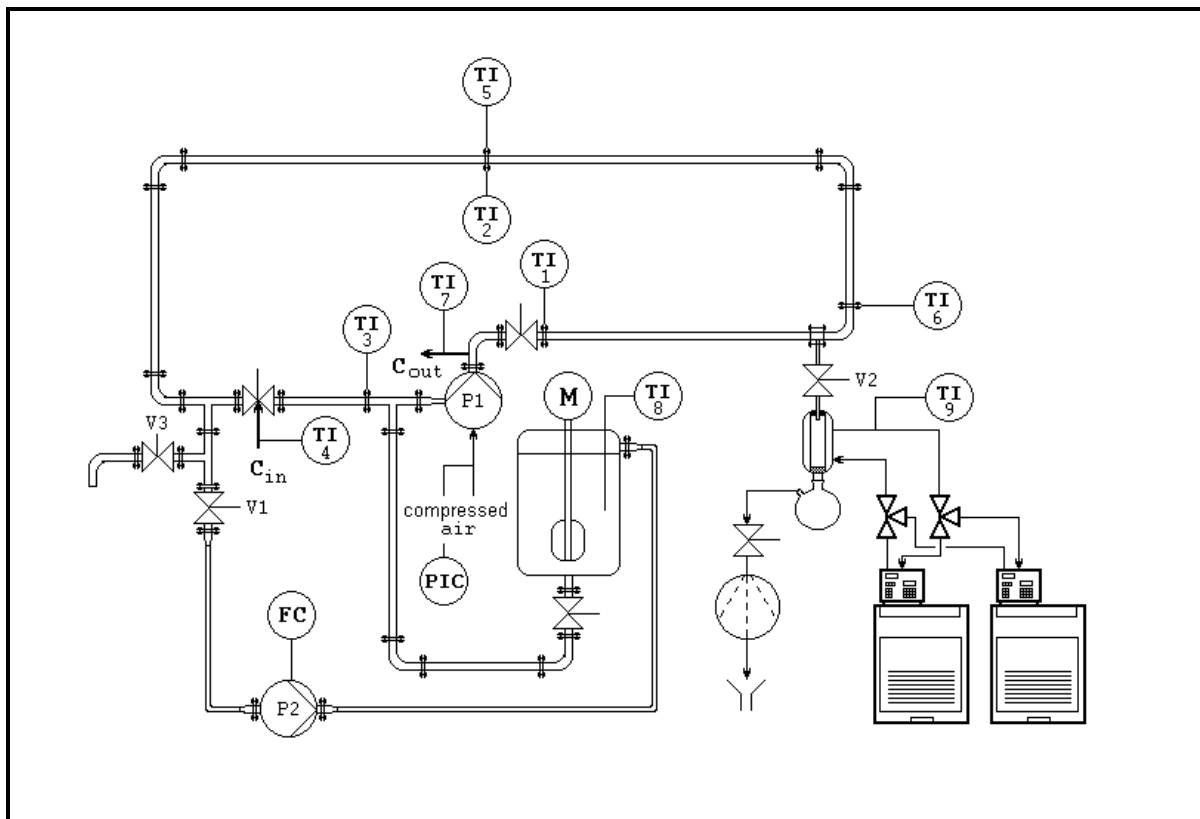


Figure 4.2.1 Experimental equipment for continuous suspension melt crystallization.

Table 4.2.1 Characteristics of the experimental equipment.

Heat exchange surface	0.26 m ²
Diameter (inner pipe)	15 mm
Equivalent diameter (outer pipe, annular gap)	17 mm
Crystallizer volume	1.8 dm ³
Flow velocity (crystal suspension)	1.00 – 2.17 m/s
Flow velocity (cooling medium)	1.10 m/s

Terminology used to define the temperature differences in the equipment is presented with the help of Figures 4.2.3 a) and is as follows:

Operational temperature: Temperature of the bulk stream of crystal suspension in the crystallizer. Fig. 4.2.3 a), T1.

Operational temperature difference: Temperature difference between the equilibrium temperature of the initial liquid mixture in the crystallizer and the actual operational temperature. Fig. 4.2.3 a), $\Delta T1$.

Metastable zone width: The difference between the crystallization temperature by cooling and the equilibrium temperature of the liquid mixture, shown by the temperature rise due to the released latent heat. Fig. 4.2.3 a), $\Delta T2$.

Undercooling: The temperature difference between the equilibrium temperature of the actual liquid fraction in the crystallizer and the operational temperature. Fig. 4.2.3 a), $\Delta T3$.

Bulk temperature difference: Temperature difference between the bulk streams of cooling medium and suspension. Fig. 4.2.3 a), $\Delta T4$.

Surface temperature difference: Temperature difference between the bulk stream of suspension and the inner wall of the heat exchanger. Fig. 4.2.3 a), $\Delta T5$.

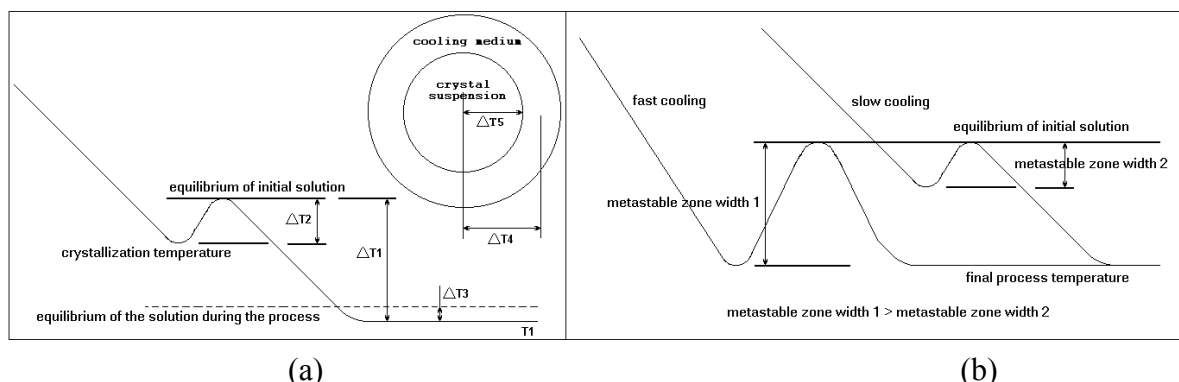


Figure 4.2.3 a) Definition of the temperature differences used in the work, b) comparison of the initial conditions for crystal formation at different cooling rates.

Fig. 4.2.3 b) presents the difference in the crystal formation process when different cooling rates are used. Here the terms fast and slow cooling describe simply that one cooling rate is faster than the other. In the case of the faster cooling rate the temperature proceeds to lower temperature before nucleation begins. Therefore, different initial undercoolings (metastable

zone widths) are caused by different driving forces for the heat transfer. If the metastable zone width at the start of the process is too large, problems may be caused by incrustation on the heat exchange surface. More on this phenomenon will be discussed in Chapter 4.3.

4.2.2 Used compounds

The crystallization process was investigated using mixtures of dimethyl sulfoxide (dmsO) and water. The compound system was chosen, because of the advantageous temperature range of the freezing temperatures and low toxicity. When the freezing point of the used mixture lies below the ambient temperature, as by the chosen system, blocking of the equipment can be avoided. If the freezing point of a compound system is above the ambient temperature problems with blockage occur frequently. This is especially the case at the junctions with a sudden reduction in the flow velocity. The concentration of the crystallizing component (dmsO) was varied during the experiments between 94-99 wt.-%. The concentration was controlled by analysing the water content by Karl-Fischer titration. The phase diagram for the compound system dmsO-water for the investigated concentration range is shown in Fig. 4.2.2. The equilibrium temperature was measured in laboratory microscopically. A linearization of the liquidus curve is shown as the calculated line in Fig. 4.2.2. The metastable zone width of dmsO-water was measured at two cooling rates: 7 K/h and 10 K/h. A deviation between the results using the two cooling rates was found only for the case of the pure dmsO. The physical properties of dmsO are given in Table 4.2.2.

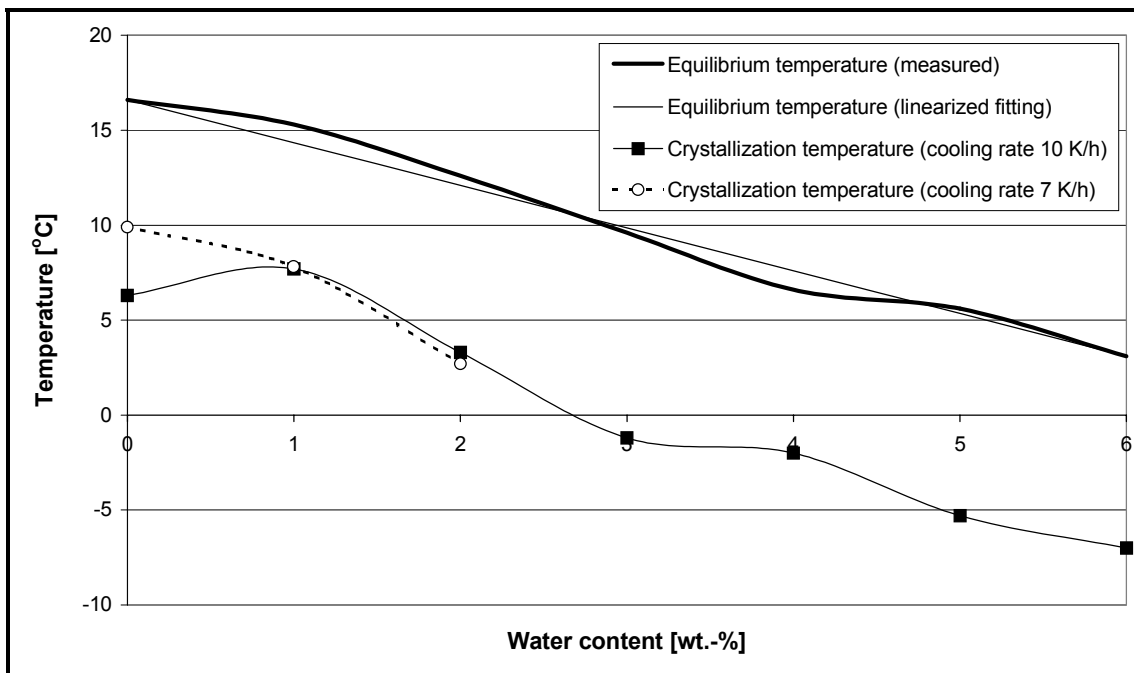


Figure 4.2.2 Part of the phase diagram of the compound system dmsO-water for the investigated concentration range.

Table 4.2.2 Physical properties of dimethyl sulfoxide (dmsO) at the pure substance melting point 18.5°C [Dau89].

Liquid density [kg/m ³]	Solid density [kg/m ³]	Viscosity [mPas]	Specific heat capacity of liquid [kJ/kgK]	Liquid thermal conductivity [W/mK]
1102	1230	2.42	1957	0.159

4.2.3 Suspension density measurements

The suspension density inside the crystallizer loop plays an important role in the crystallization process. It affects directly the productivity of the crystallization process [kg/h], and it also influences strongly the crystallization kinetics and the flow properties of suspension. Thereby, the tendency of forming of incrustations is also affected by the suspension density present in the crystallizer. The suspension density of crystals is in the investigated process affected by two factors: The operational temperature difference in the crystallizer and the residence time.

The suspension density was first measured without product out/inflow in order to prove whether it is possible to apply the proposed process in melt crystallization with high suspension densities. A sample was taken into a temperature controlled filter and the solid fraction present in the crystallizer was calculated from the mass balance. The amount of melt left in the filter cake was calculated from the mass balance by equation:

$$m_{RM} = \frac{x_{2,FC} m_{FC}}{x_{2,filtrate}} \quad (4.2.1)$$

assuming that the crystals are pure. The mass balance for the solid fraction then gives an equation:

$$F_S [\%] = \frac{m_{FC} - m_{RM}}{m_{tot}} \cdot 100\% \quad (4.2.2)$$

The measured solid fractions at different operational temperature differences are shown in Fig. 4.2.3. It was thought that high suspension densities might lead to unsatisfactory heat and mass transfer causing blockage and severe incrustation. However, it was found that the suspension density in the crystallizer is directly proportional to the operational undercooling and no blockage was observed during the operation even with the highest solid fractions. Actually, the solid fractions measured were limited by problems in sampling the high suspension densities, not by the function of the process itself. This can be seen as a scattering of the measured values at the highest solid fractions in Fig. 4.2.3.

It can be seen from Fig. 4.2.3 that an operational undercooling of about 0.5 K is necessary to obtain suspension into the crystallizer loop. This represents the metastable zone width of

primary nucleation for the investigated compound system at the applied operational conditions. It can also be seen that the water content at the examined concentration range shows no influence on the solid fraction measured. The reason is that the liquidus line of the phase diagram for the investigated range of concentrations can be considered linear, as can be seen from Fig. 4.2.2.

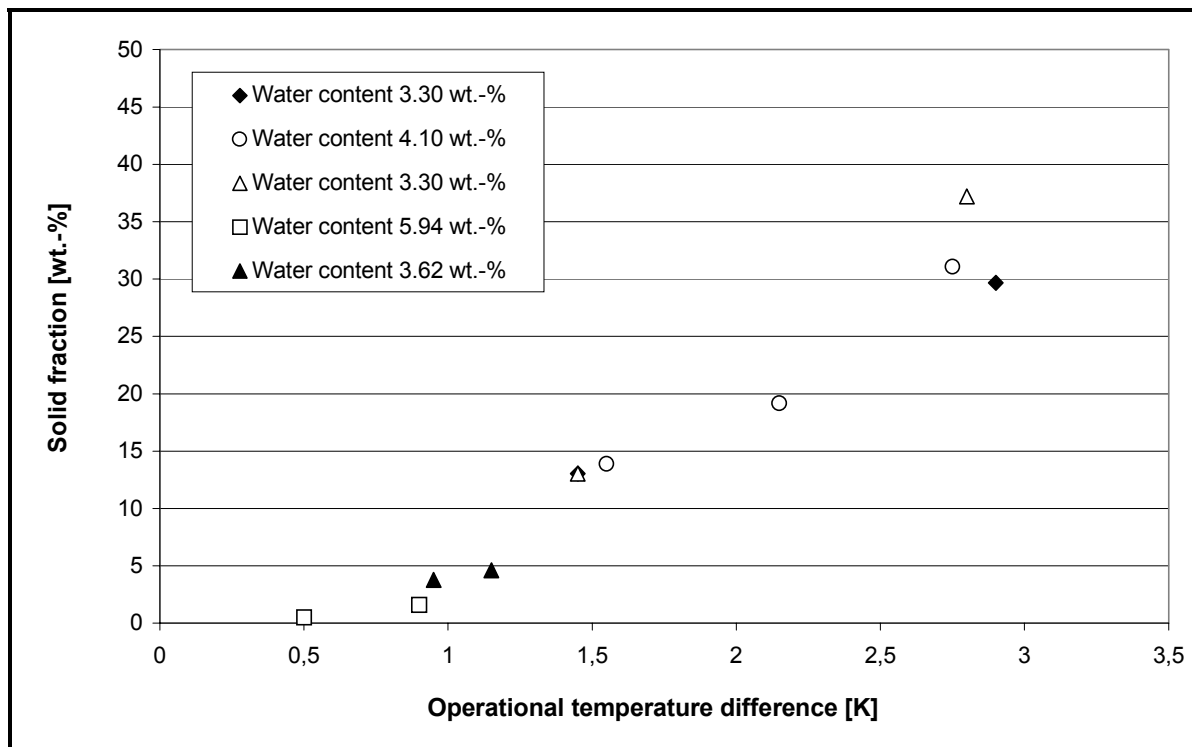


Figure 4.2.3 Solid fractions measured without product out/inflow in the crystallizer loop.

4.2.4 Limiting surface temperature difference for incrustation

The limiting surface temperature difference at which incrustation at the heat exchange surface can no more be avoided can be influenced by two factors in the crystallization process under investigation: the flow velocity and the suspension density. The flow velocity in the inner pipe influences the inner heat transfer coefficient. By increasing flow velocity the inner heat transfer coefficient increases, thus the surface temperature difference (driving force for incrustation) will get smaller. Also the shear stress on the inner wall surface rises by the increasing flow velocity, which increases the removal forces for the crystal growth taking place on the surface.

The maximum allowable bulk and surface temperature differences were determined at conditions at which no incrustation was observed after 15 minutes of operation under crystallizing conditions. Different temperature differences over the heat exchanger wall were obtained by adapting the cooling medium temperature. The cooling medium was cooled to the final temperature in the thermostat before letting it flow through the crystallizer loop. Thereby, the solution in the crystallizer was brought in thermal contact with a much colder liquid. This caused a high driving force for heat transfer and resulted in a fast cooling rate

(crash cooling). The temperature difference, and thus the cooling rate, was controlled by the final temperature level of the cooling liquid. Depending on the cooling liquid temperature it was possible to obtain different values of bulk temperature difference. The bulk temperature difference would not have been adjustable, if the cooling liquid had been gradually cooled to the final temperature in the crystallizer loop. A typical temperature profile from these experiments is presented in Fig. 4.2.4.

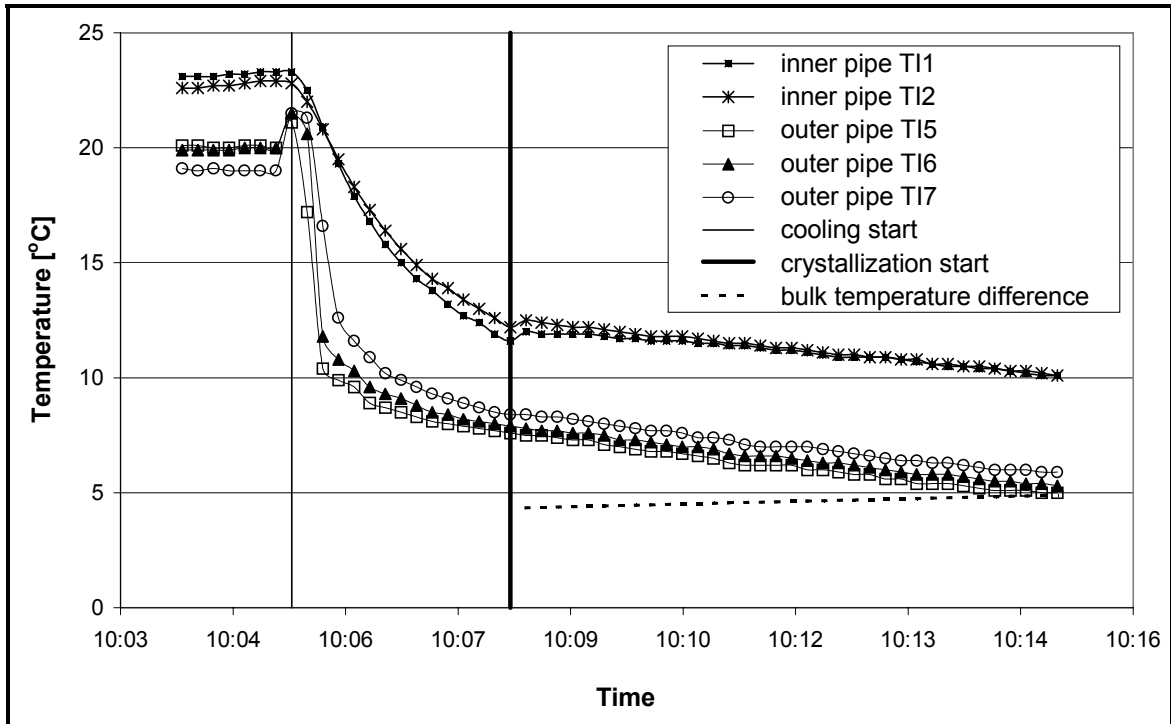


Figure 4.2.4 Temperatures in the crystallizer loop during the measurement of the maximum allowable temperature difference.

The influence of the flow velocity on the maximum allowable temperature difference is presented in Fig. 4.2.5. It can be seen that the process can be influenced positively by increasing the flow rate. No pronounced influence of concentration on the maximum allowable surface temperature difference was found between dmsO concentrations of 94 wt.-% and 98 wt.-%. However, when the dmsO concentration exceeded 98 wt.-%, it was not possible at all to achieve operational conditions at which crystallization did not take place on the heat exchange surface.

It can be seen from Fig. 4.2.5 that the increment of the limiting bulk temperature difference by increasing flow velocity follows a parabolic curve. The curve for the temperature difference on the inner surface shows similar behaviour, though the form of the curve is not so emphasized due to the smaller differences between the temperature differences at the inner surface. It can be seen that the flow velocity starts to influence the temperature differences connotatively first when the flow velocity is 1.5 m/s or higher.

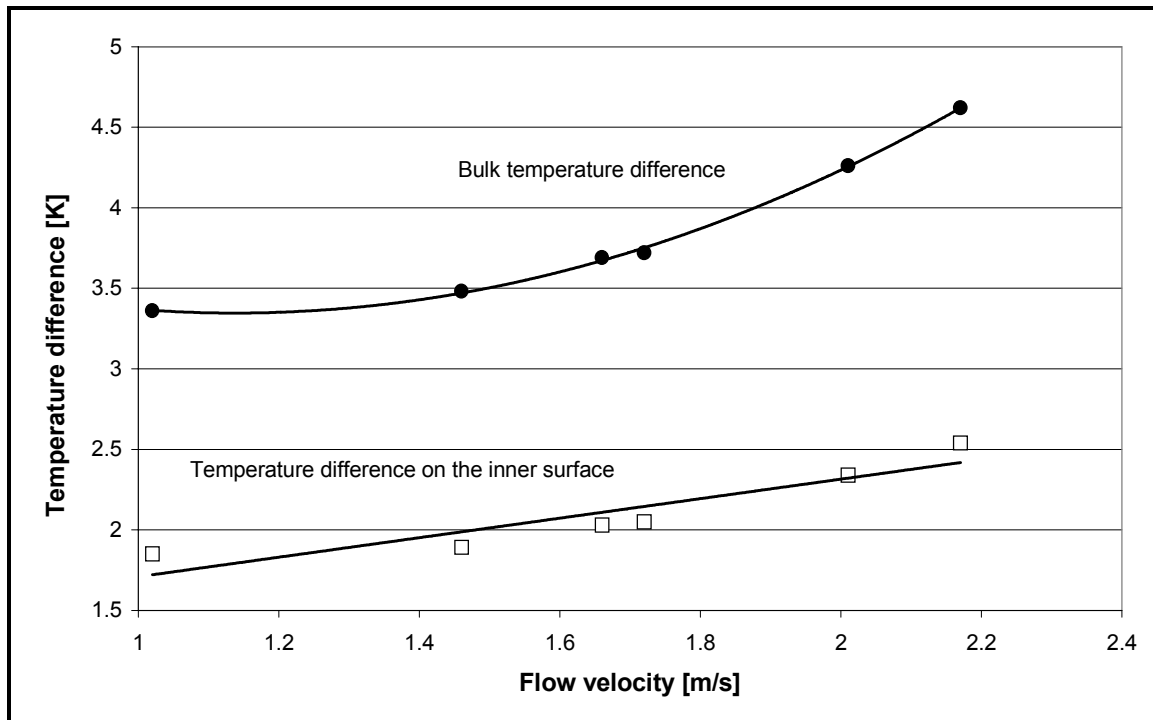


Figure 4.2.5 Limiting temperature difference in a double pipe heat exchanger.

When the process was observed visually it was found that crystallization on the heat exchange surface was taking place continuously. However, the crystalline material was constantly ripped away from the wall by the shear forces created by the flow. The higher the flow velocity the larger the particles that can be removed from the wall. This was proven experimentally by observing the inner pipe wall with a high speed camera equipped with a macro-objective [Täh03]. This means that higher growth rates of the crystallites at higher surface temperature differences can be compensated by the increased shear rate before a stable incrustation will be formed.

The influence of residence time on the process run time is shown in Fig. 4.2.6. In the process under investigation the run time was limited by the fact that in time some incrustation occurred on the heat transfer surface, which led eventually to a blockage. This occurred whatever undercooling was used. The residence times used in the tubular heat exchanger for crystallization were 22 and 40 minutes. The residence times used were limited to relatively low values due to the difficulties in maintaining the small flow rates necessary for the longer residence times. The reason for the difficult control of the circulation flow when the flow rate was very low was the strongly pulsating flow of the main loop, which pushed liquid to the circulation loop.

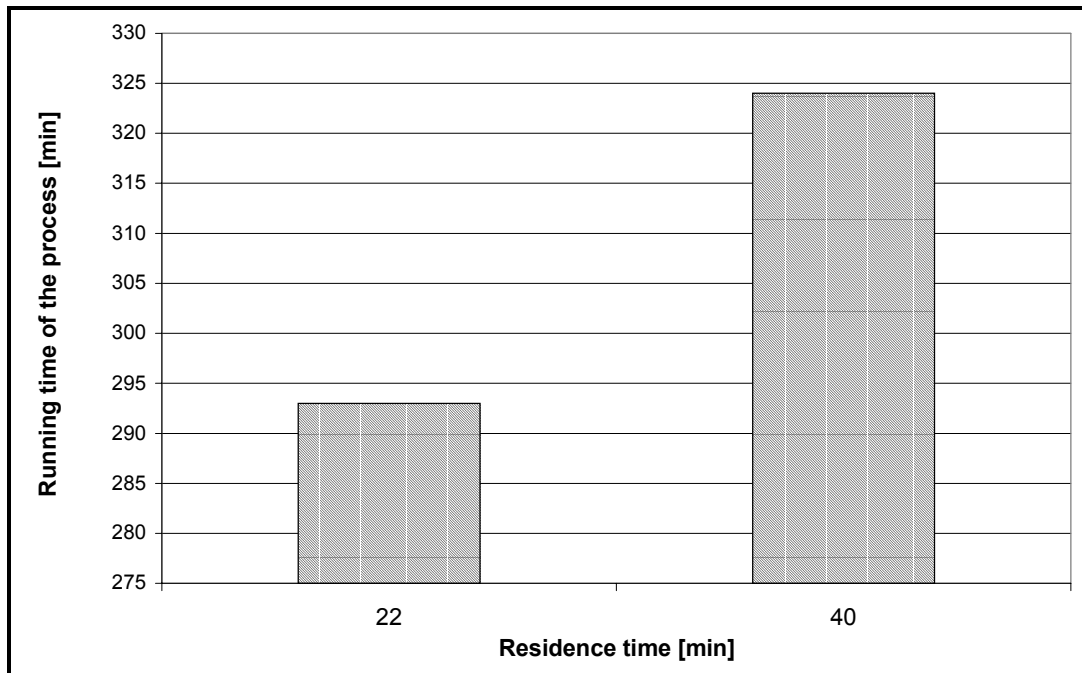


Figure 4.2.6 Influence of residence time on the duration of the process run time.

4.2.5 Heat transfer properties of the double-pipe heat exchanger

The heat transfer coefficients were calculated from the temperatures measured at the inner and outer pipes. The heat transfer properties of the equipment were determined from the measured temperature change in the crystal suspension and in the cooling medium using the Dittus-Boelter correlation [McC93]:

$$Nu = 0.023 Re^{0.8} Pr^{0.33} \quad (4.2.3)$$

The heat flow, the heat flux and the heat transfer coefficients thus obtained are presented in Table 4.2.3. and in Figs. 4.2.7 a) and b).

Table 4.2.3 Heat transfer properties of the experimental equipment.

v [m/s]	$\Delta T(\text{bulk})$ [K]	Re [-]	Nu [-]	h_i [W/m ² K]	U [W/m ² K]	Q [W]	q [W/m ²]
1.02	3.36	7220	82	1095	442	386	1484
1.46	3.48	10340	109	1459	491	445	1710
1.66	3.69	11750	121	1617	508	487	1874
1.72	3.72	12180	125	1664	512	496	1906
2.01	4.26	14230	141	1885	532	589	2265
2.17	4.62	15360	150	2004	541	649	2498

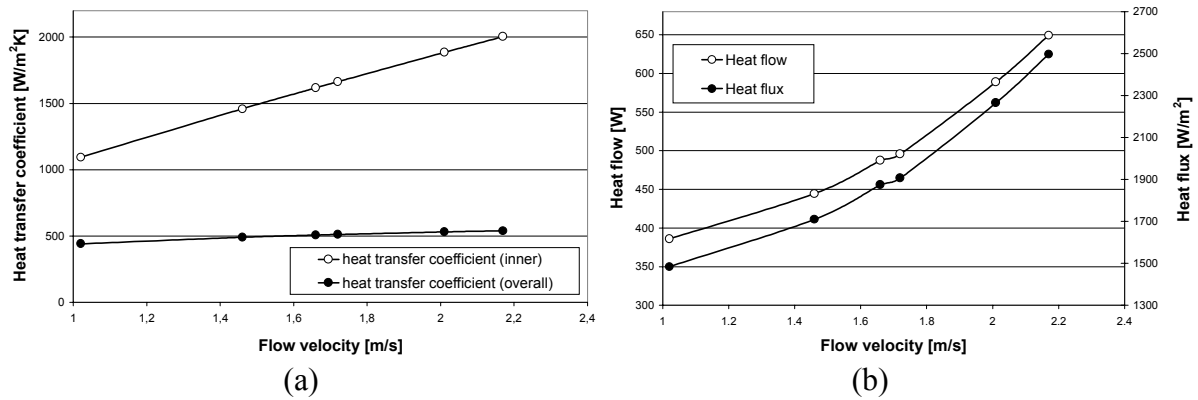


Figure 4.2.7 Heat transfer in the double-pipe heat exchanger used as crystallizer: a) inner and overall heat transfer coefficients, b) heat flow and heat flux.

In addition to the sensible heat of the feed stream and the latent heat of crystallization, heat is also produced into the crystallizer loop by the circulation pump. The heat production from the membrane pump used in the crystallizer loop at the maximum flow velocity of 2.17 m/s was estimated from the temperature rise to be 29 W.

4.2.6 Particle size measurement

The change in the crystal size distributions during the process was measured in-line by a device PSyA provided by MTS GmbH, which is based on a laser beam reflectance measurement. By this method a focused laser beam, which is rotating in a circular track, is pointed to a suspension of particles. The beam reflects from a surface of a particle moving in front of the detector window. The reflected beam is registered by a detector in the sampling probe. A chord length for a particle can be then calculated from the time of reflection and the rotational velocity of the beam. A detailed description of the measurement procedure of the FBRM (Focused Beam Reflectance Measurement) technique has been given recently by Worlitschek [Wor03].

The development of the cumulative size distributions of the dmso crystals is presented in Fig. 4.2.8. The residence time for the experiment presented in Fig. 4.2.8 was 22 minutes and the operational temperature difference used was 2 K. At the beginning of the process a high amount of very small crystals is created by nucleation. After that the crystals start to grow and the nucleation rate settles to a lower value. The number and mass based average crystal sizes at different time points from the start of crystallization for this experiment are given in Table 4.2.4.

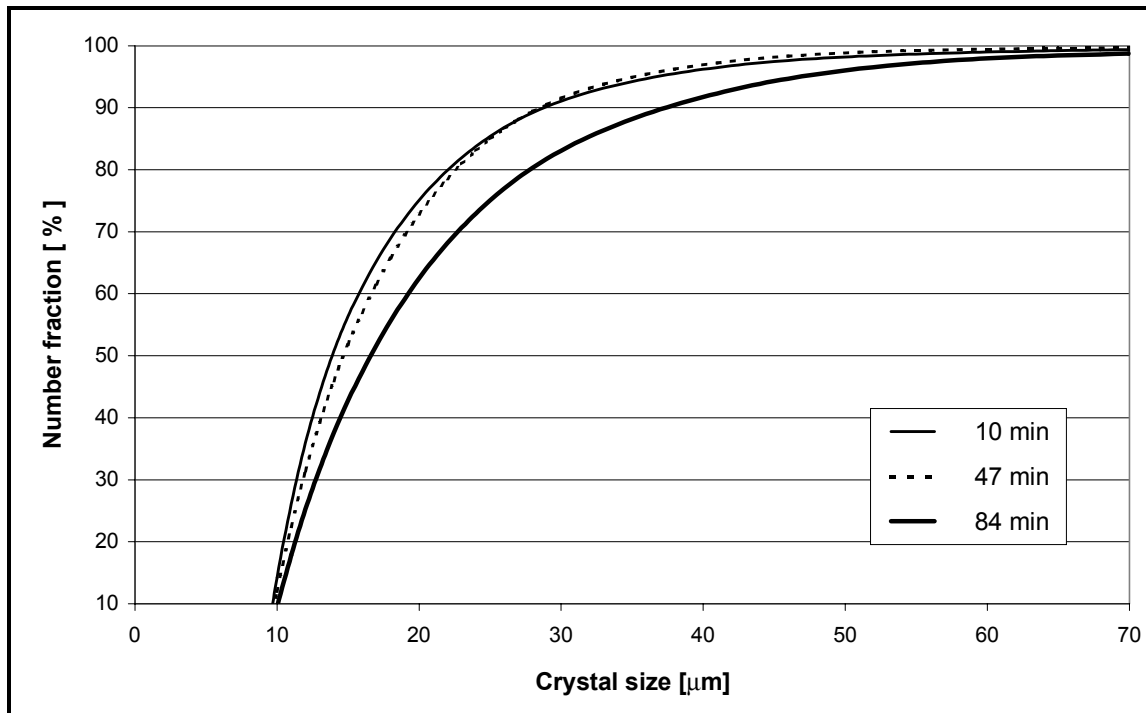


Figure 4.2.8 Cumulative undersize distributions of dmsO crystals crystallized in a double-pipe heat exchanger tube.

Table 4.2.4 Development of the average crystal size from the double-pipe heat exchanger for the system dmsO-water during the crystallization process.

Process time [min]	Average crystal size, number based [μm]	Average crystal size, mass based [μm]
10	10	42
47	12	45
84	17	52

From Table 4.2.4 it can be seen that the crystal size produced in the tubular heat exchanger is quite small compared to crystals in the pilot plant unit (see Table 4.3.2). One reason is the shorter residence times of crystals, but the more important reason is the extremely turbulent flow at pulsating conditions. The high turbulence induces a high nucleation rate and a high number of crystal collisions. From Fig. 4.2.8 it can be seen that the size distributions at 10 and 47 minutes are very close to each other. Significant growth of the crystals can first be seen from the size distribution measured at the time 84 min after the start of crystallization. This can be explained by the undercooling peak at the beginning of the crystallization process.

It must be emphasized that the measured crystal size from the used method is a random segment on the crystal projection, called the chord length. Like with other in-line measuring devices the results are more indicative and show a trend rather than absolute sizes of the crystals. Also, therefore, the mass based average crystal size in Table 4.2.4 is calculated without any consideration of the crystal shape, and can only be used as quantitative information in comparison of crystal size distributions presented in Fig. 4.2.8.

4.3 Experiments with Pilot Plant Equipment

In this chapter the process investigated in the previous chapter is applied to a pilot plant scale in a unit provided by Niro Process Technology. The equipment used in the pilot plant scale is a more robust configuration for suspension melt crystallization. The benefit of this robustness is that the long term operation of the crystallizer can be guaranteed for a wide range of process conditions. In the process presented in Chapter 4.2 the process conditions have to be chosen carefully. For industrial practice, however, a process often has to be able to operate in varying process conditions. In the industrial test unit heat transfer takes place in a scraped surface heat exchanger (SSHE) where high undercoolings can be applied over the heat exchange surface, whereas the loop itself is isolated and not cooled. In the scraped surface crystallizer the heat exchange surface is kept free of crystals by rotating Teflon blades. The undercooling created to the melt in the scraped surface crystallizer is depleted onto the surfaces of the crystals during their way in the loop. This way the crystal suspension is circulated continuously through the SSHE providing conditions for growth of the crystals.

4.3.1 Experimental equipment

The equipment used is a modification of a Niro pilot plant unit presented in literature for example by Lemmer *et al.* [Lem00], where the ripening tank is replaced by a simple loop connecting the input and the output of the SSHE. This simplification serves to reduce the manufacturing and maintenance costs of the crystallizer unit and is aimed to increase the economical competitiveness of the combined melt crystallization and solid-liquid separation unit. The equipment used is presented in Fig. 4.3.1. The following description of the process refers to the numbers presented in Fig. 4.3.1. The solution to be crystallized is pumped from the feed tank (1) to the crystallizer loop (2). The solution is pumped in the loop by the product circulation pump (3) through a scraped surface crystallizer (4). The SSHE cools the process liquid temperature to an operation temperature at which crystal slurry has formed in the crystallizer. The crystal slurry is continuously circulated through the SSHE. A portion of the crystal slurry is pumped with a piston to the wash column (5) for separation. A corresponding amount of fresh feed replaces the slurry, and is further cooled and crystallized in the circulation loop. The crystal suspension from the crystallizer is pushed to the wash column by a piston at a preset time interval. The crystal suspension is filtrated at the bottom of the column resulting in a concentrate and crystals with adhering mother melt. The concentrate can be led back to the crystallizer (concentration of the process liquid) or out of the process. Thereby it is possible to control the suspension density in the crystallizer loop. The crystals with the impure melt rise up in the column and are melted at the top in a heat exchanger (6). One part of the molten crystals is led downwards the column as washing liquid through the wash water pump (7) and part is taken out as product. By this washing action the crystal bed at the upper part of the column becomes gradually cleaner and cleaner. Finally, a pure product is achieved and a sharp wash front forms in the column. Above this wash front the pure wash liquid has replaced the impurities at the crystal surfaces, while below the front the impure

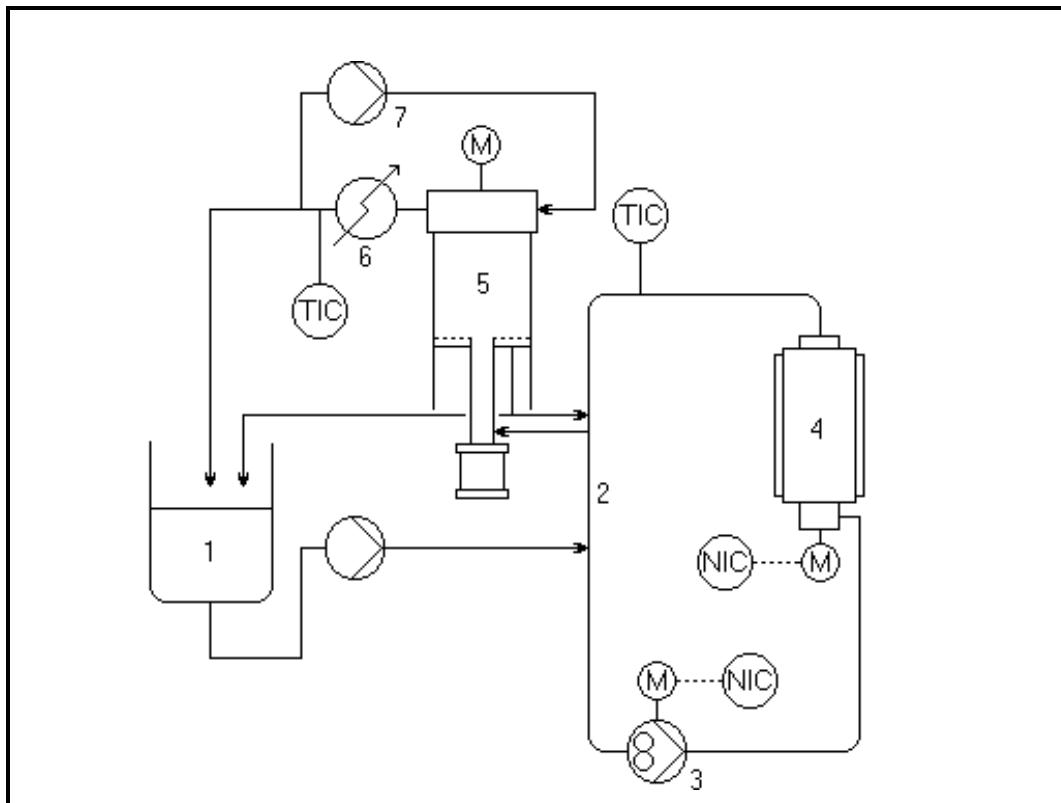


Figure 4.3.1 Pilot plant equipment used in the experiments for melt crystallization. 1) feed tank, 2) crystallizer loop, 3) product circulation pump, 4) SSHE, 5) wash column, 6) heat exchanger, 7) wash water pump.

mother melt still exists with the crystals. Characteristics measures of the used equipment are given in Table 4.3.1.

Table 4.3.1 Characteristics of the pilot plant equipment.

Heat exchange surface	0.26 m ²
Diameter of the circulation loop	100 mm
Flow velocity (crystal suspension)	0.98 – 2.56 m/s
Cooling medium	R22

The main variables investigated during the experiments with the pilot plant unit were the rotational speed of the scraper blades in the SSHE, the concentration of the feed solution, the temperature of the cooling medium in the SSHE (cooling medium R22) and the residence time of the crystals in the crystallizer loop. The product outflow from the crystallizer (thus the residence time) was controlled by the throughput of the wash column. The suspension density in the crystallizer, the average crystal size, the crystal habit and the CSD, as well as the heat transfer coefficient in the SSHE and the loss of cooling capacity through heat production due to pumping and scraping action and due to losses to the environment were taken under investigation. The loss of heat through the loop wall and the heat produced by the circulation pump and the SSHE scraper were measured from the temperature rise of the solution in the loop at different pump and scraper rotational velocities.

Two model systems were investigated with this process: sugar-water system (ice being the crystallizing component) and dmsol-water (dmsol being the crystallizing component), similar to work presented in Chapter 4.2. Thus the equipment was tested both on a special field of melt crystallization being of great importance to the process under investigation – freeze concentration, and on the traditional melt crystallization. The concentrations of sugar and dmsol in the aqueous solution were determined by refractometer analysis.

4.3.2 Suspension density in the crystallizer loop

The suspension density in the crystallizer was measured by taking a sample to a filter as described in Chapter 4.2.3 or by analyzing the concentrations of the crystal suspension in the crystallizer and the concentrate produced by the wash column. The solid fraction can be calculated from the mass balance assuming the crystals contain no impurities with equations 4.2.1 and 4.2.2.

With the cooling medium temperatures used in the experiments the suspension density in the pilot plant unit reaches soon after the formation of crystals a value of approximately 20 wt.-%. The suspension density in the crystallizer is kept constant when the flow of crystals through the wash column equals the crystal production capacity of the heat exchanger. Thus, the suspension density can be controlled by the flow rate through the wash column. When the flow of crystals through the wash column is smaller than the crystal production at the SSHE the suspension density inside the loop rises during the operation. In this aspect the pilot plant unit differs by its function from the function of the tubular heat exchanger. While in the tubular heat exchanger the suspension density reached a stable suspension density level shortly after reaching the corresponding temperature inside the loop, the suspension density in the pilot plant unit developed continuously during the operation. The reason is that in the tubular heat exchanger the temperature difference is small and divided evenly along the circulation loop. On the contrary, in the pilot plant unit the temperature difference at the SSHE is very high, the heat exchange surface compared to the volume of the whole loop, however, smaller. All the crystals in the system are, therefore, created by this surface and pumped further and distributed to the rest of the loop.

Fig. 4.3.2 a) gives an example of the influence of the residence time on the solid fraction of ice crystals in the crystallizer. Fig. 4.3.2 b) shows the influence of the SSHE scraper speed. The influence of the scraper speed on the solid fraction in the crystallizer is caused by the increasing heat transfer coefficient by the increasing scraper speed.

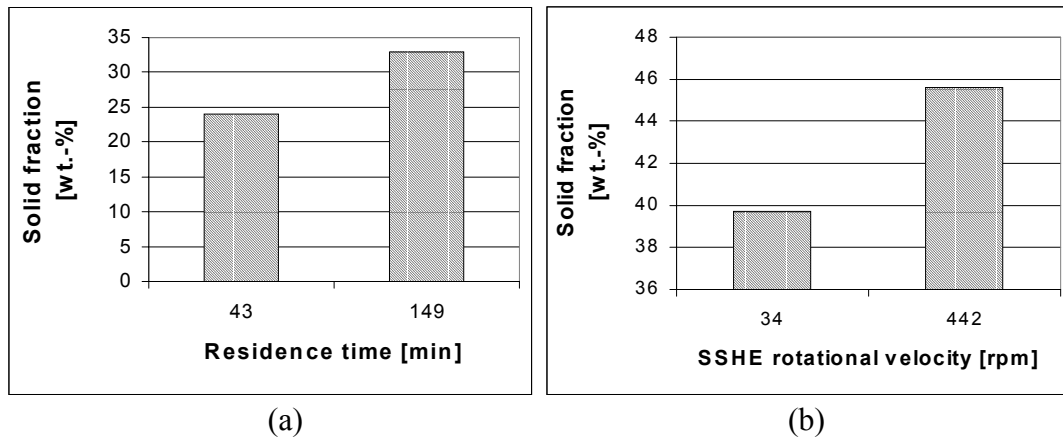


Figure 4.3.2 Influence of the residence time (a) and the SSHE scraper speed (b) on solid fraction in crystallizer.

The solid fraction of ice in the crystallizer at different bulk temperature differences is presented in Fig. 4.3.3. It can be seen that the solid fraction increases linearly with the bulk temperature difference, similarly to Fig. 4.2.3.

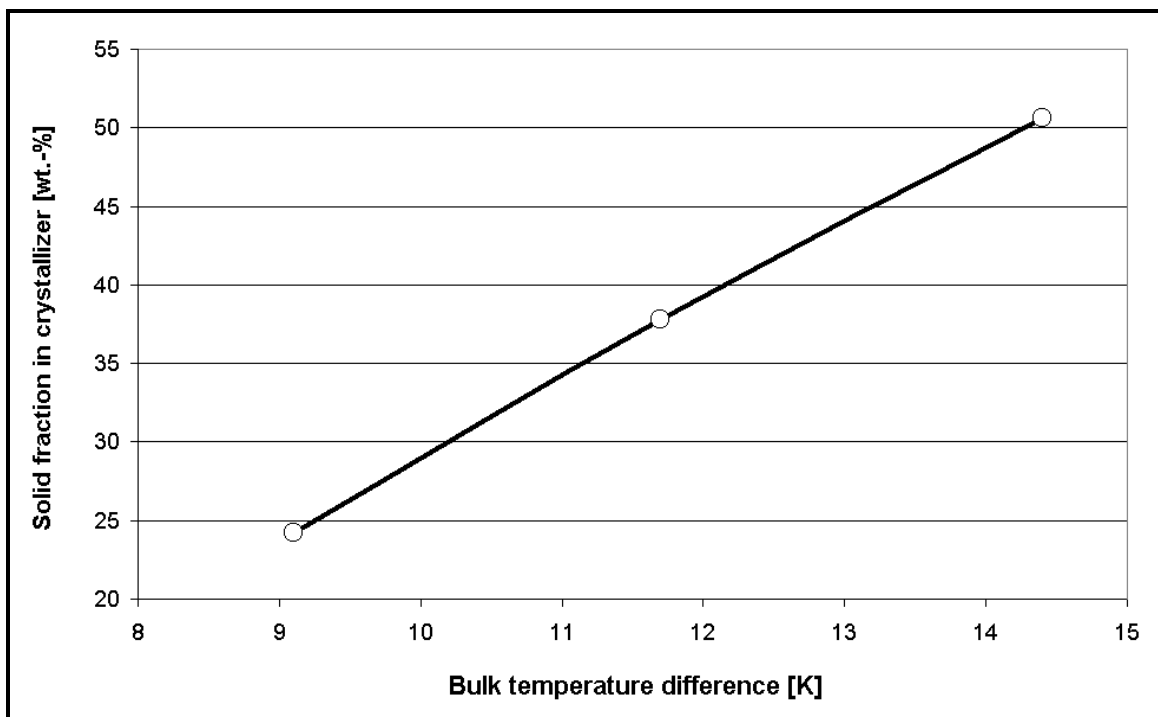


Figure 4.3.3 Suspension density in the crystallizer loop of the pilot plant equipment. SSHE rotational velocity 254 rpm.

The influence of these three variables to the solid fraction in the crystallizer can be compared as follows: A 19% reduction in the undercooling reduces the solid fraction by 25%. However, as high as 92% reduction in the SSHE scraper speed is necessary to decrease the solid fraction 26%. In the case of residence time 70% reduction decreases the solid fraction 27%. Based on these data it is clear that the strongest influence on the suspension density of crystals comes from the undercooling. A change in the scraper speed has only a small influence on the suspension density.

4.3.3 Crystal size and habit

The crystal size and habit were observed from the photomicrographs of samples taken from the loop to an observation chamber under a microscope. The observation chamber was pre-cooled to the crystallizer temperature in order to avoid melting during the sampling. The microscope used was a stereomicroscope Stemi 2000 from Olympus.

A comparison of three different pictures of ice crystals is presented in Fig. 4.3.4. The picture in Fig. 4.3.4 a) shows crystals produced by the traditional Niro process with a growth tank and the picture in Fig. 4.3.4 b) crystals produced in the current work. Fig. 4.3.4 c) shows ice crystals produced by a special type of scraped crystallizer by Vaessen [Vae03] called scraped eutectic crystallizer.

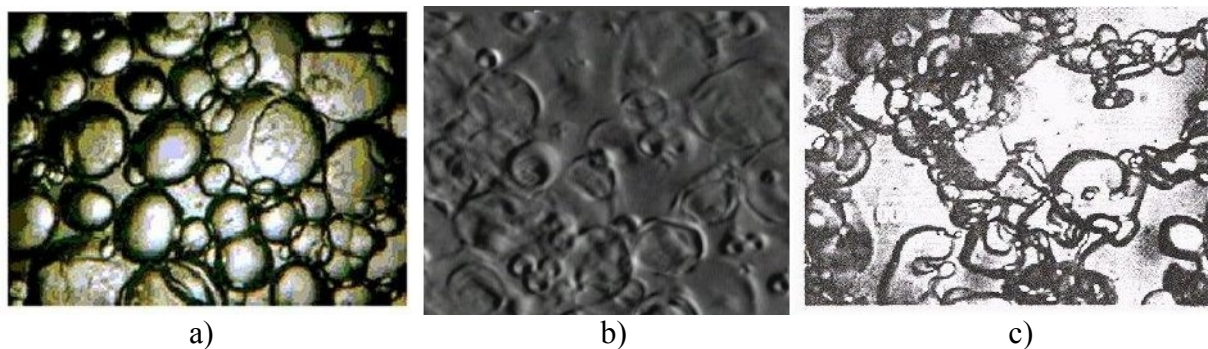


Figure 4.3.4 Crystal habit of ice from three different processes: a) Niro growth tank, b) pilot plant crystallizer used in this work, c) scraped eutectic crystallizer [Vae03].

The cumulative mass distributions for different residence times are presented in Fig. 4.3.5. The average crystal sizes for these experiments are given in Table 4.3.2.

Table 4.3.2 Crystal size distribution characteristics from the pilot plant crystallizer for the system sugar-water. Solution concentration 15 wt.-% sugar, average bulk temperature difference 12 K.

Residence time [min]	Average crystal size [μm]	Maximum size [μm]	Standard deviation [μm]
30	117.1	226.1	46.3
60	149.8	369.3	77.6
90	131.8	297.5	53.7

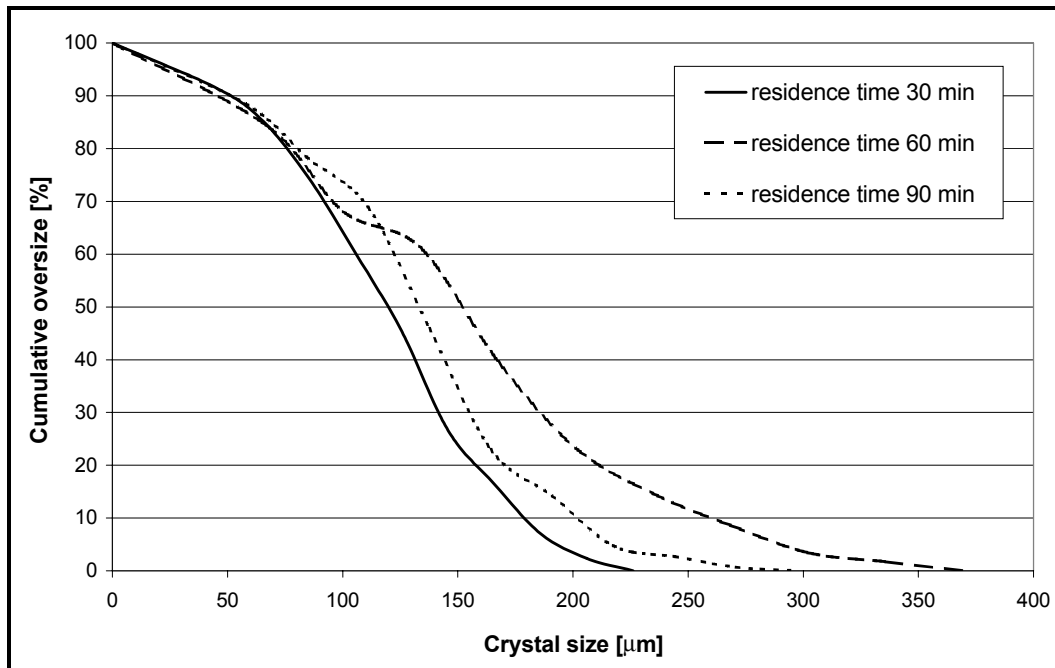


Figure 4.3.5 Cumulative oversize distributions of ice crystals crystallized from sugar-water system at average undercooling of 12 K (refrigerant temperature -14°C).

4.3.4 Scraper speed of SSHE

The scraped surface crystallizer is used where incrustation on the heat exchange surface is considered to be a problem. This may occur especially in crystallization processes where the concentration of the crystallizing component is high (melt crystallization), but also when a large temperature difference is necessary. Both of the above statements are fulfilled in the process with the Niro pilot plant. A large temperature difference is necessary in order to obtain an economical process for the current equipment, because the heat exchange surface to volume ratio is relatively small. In the used equipment this relation is 5.19, while the relation for example for tube and shell heat exchangers is for the inner side 218.18 and for the outer side 81.36 (exchangers from Huels AG available in Fachbereich Ingenieurwissenschaften, Thermische Verfahrenstechnik, surface area 0.48 m^2 , inner volume 2.2 dm^3 , outer volume 5.9 dm^3).

In addition to the heat transfer considerations, which include heat production and enhancement of the heat transfer coefficient, mechanical considerations have often high priority in construction of such equipment. Reducing the scraper speed reduces the installed motor power necessary (cost reduction) and reduces wear in the equipment (maintenance reduction) [Sch04]. Therefore, the necessary minimum scraper speed, and how it is affected by process conditions was investigated.

It was found that when the refrigerant temperature was set to the final value from the beginning on and the scraper speed was under 150 rpm it was difficult to obtain crystals in the crystallizer. The crystals either totally melted away right after their formation, or the suspension density did not grow to the normal level. This suggests that the heat transfer is

hindered. Because the scraper in these cases is not blocked and is functioning, there must form a smooth layer of ice on the heat exchange surface, which hinders heat transfer but does not block the scraper movement. When the refrigerant temperature was reduced slowly at the beginning of the process the chosen final temperature level did not have any influence on the necessary minimum scraper speed. The reason for this behavior is that the undercooling reaches its maximum value at the beginning of the process. The magnitude of the undercooling peak at the beginning is the limiting factor, which determines the limiting scraper speed necessary. This conclusion is further confirmed by the experimental results, which showed that after the formation of suspension the scraper speed could be reduced to the minimum without any malfunction occurring in the crystallization process. The minimum scraper speed applicable in the equipment was 25.2 rpm. However, when the scraper speed is reduced to zero the scraper will be frozen to its place after some time. The blockage of the scraper must be due to the hindered transportation of the suspension from the undercooled surface.

The limiting scraper speed for the sugar-water solution with 15 wt.-% sugar was found to be 150.5 rpm. The measurements were repeated at refrigerant temperatures -13°C and -15°C . There was found to be no difference in the limiting scraper speed with these two cooling medium temperatures.

4.3.5 Reduction in cooling efficiency due to heat production and losses to environment

In addition to cooling the feed to the crystallizer temperature and removing the latent heat released by crystal growth, the heat exchanger must also remove the heat produced by the product circulation pump and the scraper of the SSHE and compensate for the heat losses to the environment. Therefore, the heat balance for the crystallizer from the material balance and the measured temperatures must be supplemented by the heat input from the moving parts and the environment. This extra heat will be called black loss (loss of cooling efficiency), due to the black box nature of the treatment. Although the influence of the rotational velocities of the product circulation pump (PCP) and the scraper of the SSHE have been investigated, the exact contribution from a specific source cannot be determined.

The black losses have been determined by measuring the temperature rise in the crystallizer loop when the cooling is switched off. The heat input can then be calculated from the heat balance and the time taken for the temperature to rise. An example of the temperature rise measurements is shown in Fig. 4.3.8. The process conditions representing the various experiments in Fig. 4.3.8 are given in Table 4.3.3.

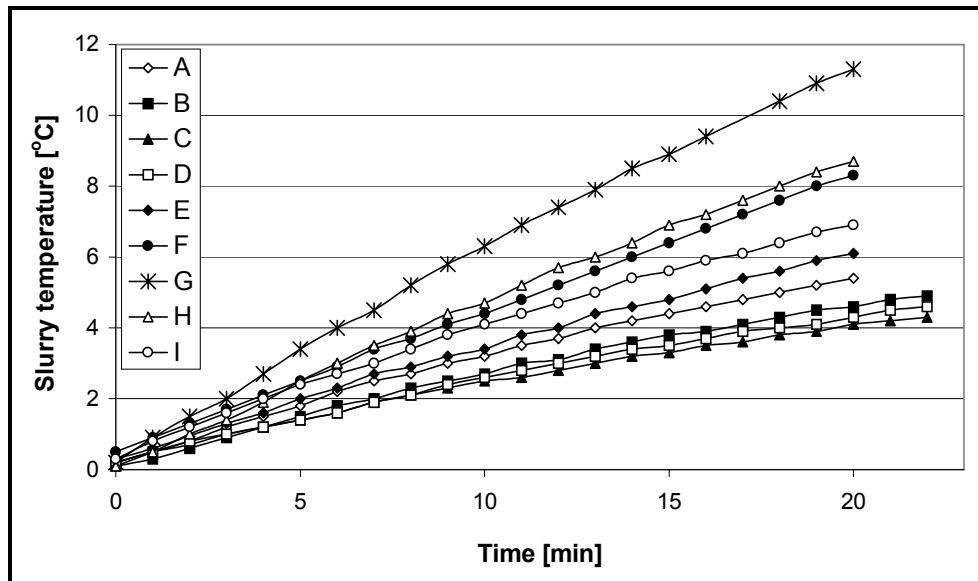


Figure 4.3.8 Temperature rise in the crystallizer by the black loss measurements with sugar-water solution. Solution concentration 15 wt.-% sugar.

Table 4.3.3 Process parameters by the measurement of heat production corresponding to Fig. 4.3.8.

Experiment	A	B	C	D	E	F	G	H	I
SSHE [rpm]	441.6	338.1	251.5	251.5	251.5	251.5	251.5	342.3	442.0
PCP [rpm]	155.9	155.9	155.9	198.3	269.4	320.7	386.1	320.5	262.6

The influence of the rotational velocities of the product circulation pump and the scraper of the SSHE on the heat production are shown in Fig. 4.3.9 and Fig. 4.3.10, respectively. It can be seen from Fig. 4.3.9 and Fig. 4.3.10 that the heat production rises linearly with the increasing SSHE scraper speed (Fig. 4.3.9), whereas the heat production with increasing product circulation pump rotational velocity shows non-linear behaviour (Fig. 4.3.10).

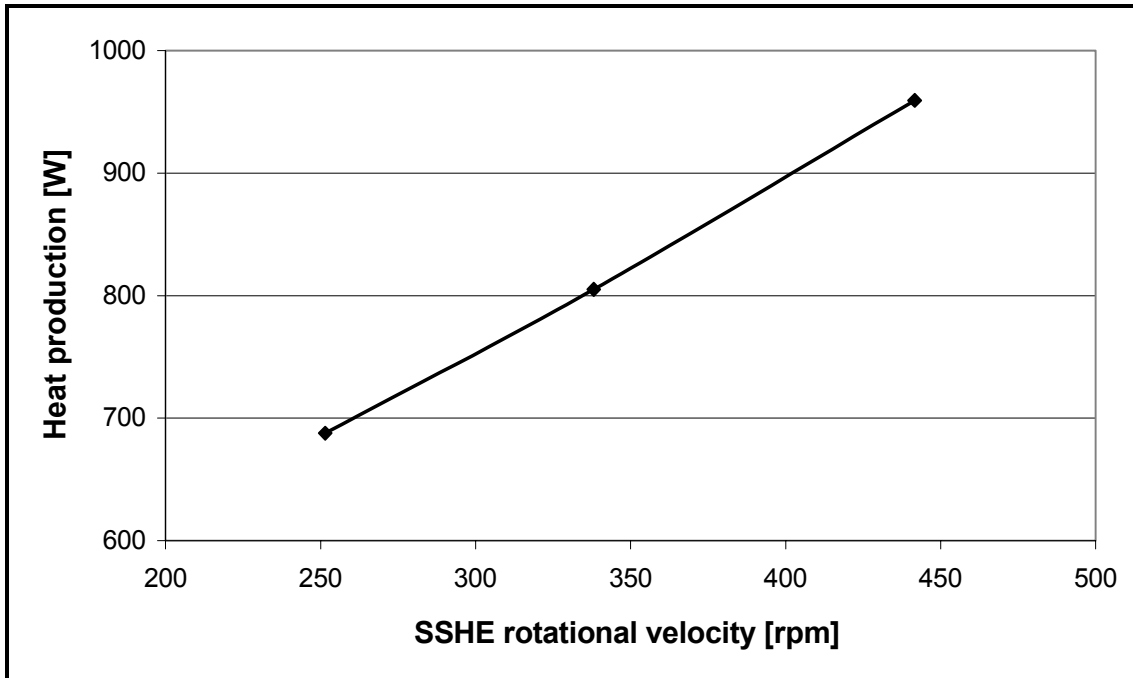


Figure 4.3.9 Heat production in the crystallizer loop at sugar-water solution with concentration of 15 wt.-% sugar. PCP rotational velocity 155.9 rpm.

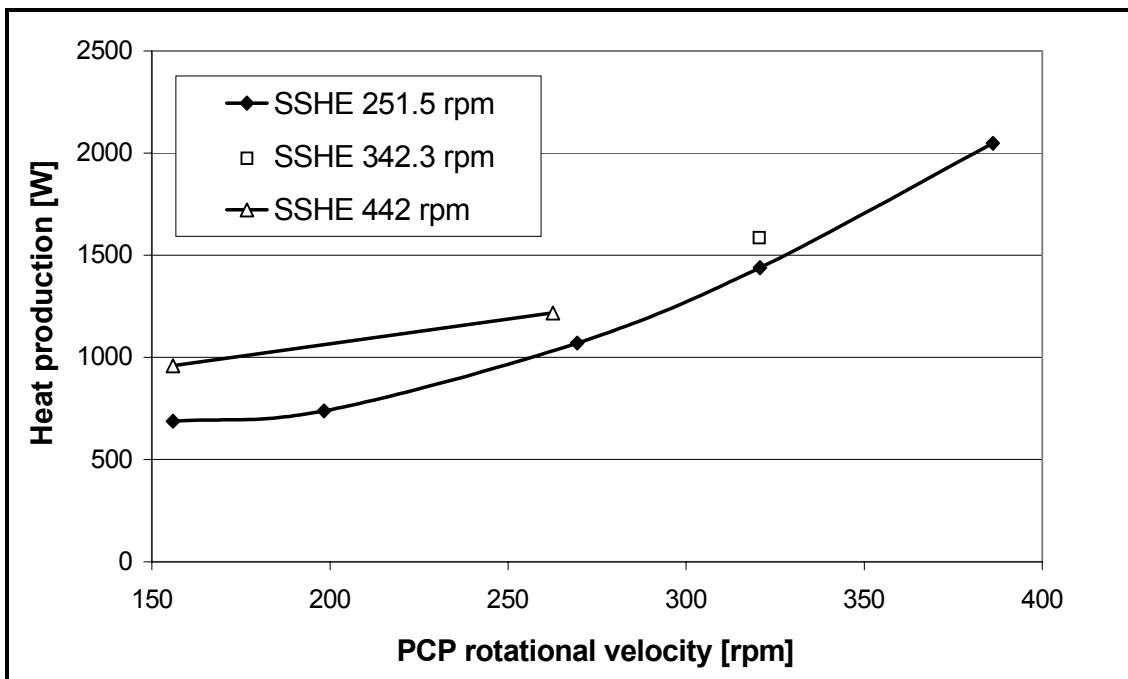


Figure 4.3.10 Heat production in the crystallizer loop at sugar-water solution with concentration of 15 wt.-% sugar.

A comparison of the effect of the SSHE scraper rotational velocity for the two compound systems investigated is presented in Fig. 4.3.11. It can be seen from Fig. 4.3.11 that the heat production for the sugar-water system is much higher than for the dms0-water system.

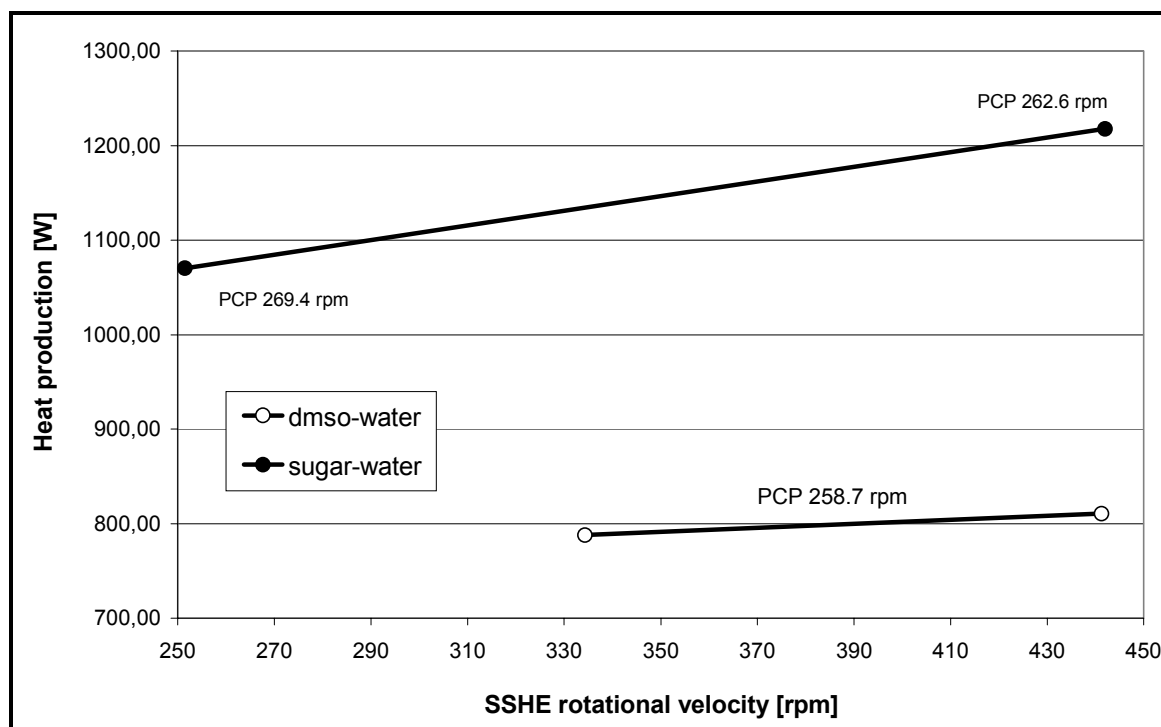


Figure 4.3.11 Comparison of heat production rates in sugar-water (15 wt.-% sugar) and dms0-water (3.0 wt.-% water) systems.

4.4 Particle Characterization from Laboratory Scale Suspension Melt Crystallization

In this chapter the particle form and the size of the crystals produced by laboratory scale suspension melt crystallization are presented. A specially constructed observation chamber equipped with scrapers was used to record the particle properties right after the formation and the removal of the particles at the cooled surface. The qualitative information obtained from the experiments with scrapers is compared with results obtained with crystals grown in suspensions in a stirred crystallizer chamber.

4.4.1 Particle characteristics under scraping action

Four main parameters were investigated in a laboratory scale observation chamber constructed as a scraped surface crystallizer: Temperature difference over the crystallizer wall, rotational speed of the scraper, scraper angle and residence time of crystals in the crystallizer chamber. The purpose was to investigate the crystal size and habit right after crystal formation, which is not possible in a larger scale equipment. A different scraper construction than in Chapter 4.3 was used: In the laboratory scale experiments a crystalline layer was allowed to grow on the heat exchange surface, out of which crystalline material was broken off by the scrapers, while in the industrial scale equipment used in this work the scrapers were used to keep the heat exchange surface crystal free. This way it was possible in the laboratory experiments to study whether and how the scraping influences the crystal form produced.

The construction of the equipment used is shown in Fig. 4.4.1. The scraper blades were set to a fixed distance (3 mm) from the heat exchange surface. The crystals were mixed into the bulk melt and observed through the glass window at the bottom of the chamber. The observation window was kept at a higher temperature in order to avoid crystallization on the window. This kind of construction causes the crystal characteristics to depend stronger on the undercooling at the heat exchange surface, because the crystal size and the shape is influenced both by the structure of the crystal layer on the heat exchange surface and by crystal growth in the suspension. In the case where the surface is kept free of crystals (the equipment in Chapter 4.3), on the other hand, the particle properties are influenced only by crystal growth in suspension.

The experiments were chosen to be carried out with the compound system myristic acid-capric acid. The fatty acid mixture was chosen due to its ease of crystallization as a layer and ease of breaking of crystals from this layer by the scrapers.

The crystals were characterized in terms of crystal size and shape. The characteristic diameter for the crystal size was chosen to be the area equivalent diameter, which is defined as the diameter of a circle possessing the same projection area as the crystal to be characterized. The major axis length used in Chapter 4.3 was not chosen to be the characteris-

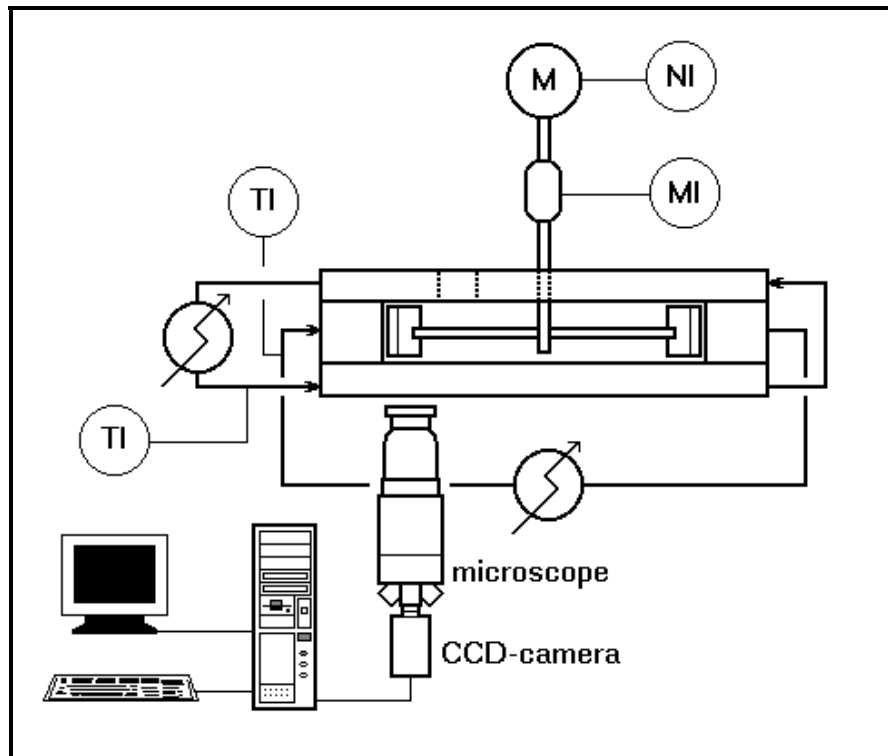


Figure 4.4.1 Experimental equipment for formation of scraped particles.

tic diameter, because the shape of the crystals could differ remarkably, leading to incomparable crystal lengths. The shape of the crystals was characterized by dimensionless form factors; the ones chosen for this work were the relation breadth to length and the circularity. The breadth of a crystal was defined as the maximum distance perpendicular to the major axis length taken as the particle length. The circularity is defined as the relation of the projection area of the particle to the area of a circle possessing the same perimeter as the particle. The circularity is given by the equation

$$\text{Circularity} = \frac{4\pi A_p}{P_p^2} \quad (4.4.1)$$

where P_p is the particle perimeter and A_p the particle projection area. This choice of definition gives the same scale (from 0 to 1) for both the shape factors used [Täh01].

The effect of undercooling on the crystal size of myristic acid is shown in Fig. 4.4.2. It can be seen that the mode of the distribution is changed by increasing undercooling to slightly larger crystal sizes. This size class can be assumed to represent the crystals broken off from the crystal layer by the scrapers. The crystal size distributions in Fig. 4.4.2 thus prove the logical assumption that the layer growth rate is higher at higher undercooling, resulting in larger size of crystal fractures. In addition to this, the crystal size is affected by further growth in the suspension, causing further increment in the average crystal size by increasing undercooling. This can also be seen in the change in the shape of the distribution, as the higher undercoolings make the distribution broader by increasing the fraction of larger crystal

sizes. The modes and average crystal sizes for the distributions presented in Fig. 4.4.2 are given in Table 4.4.1.

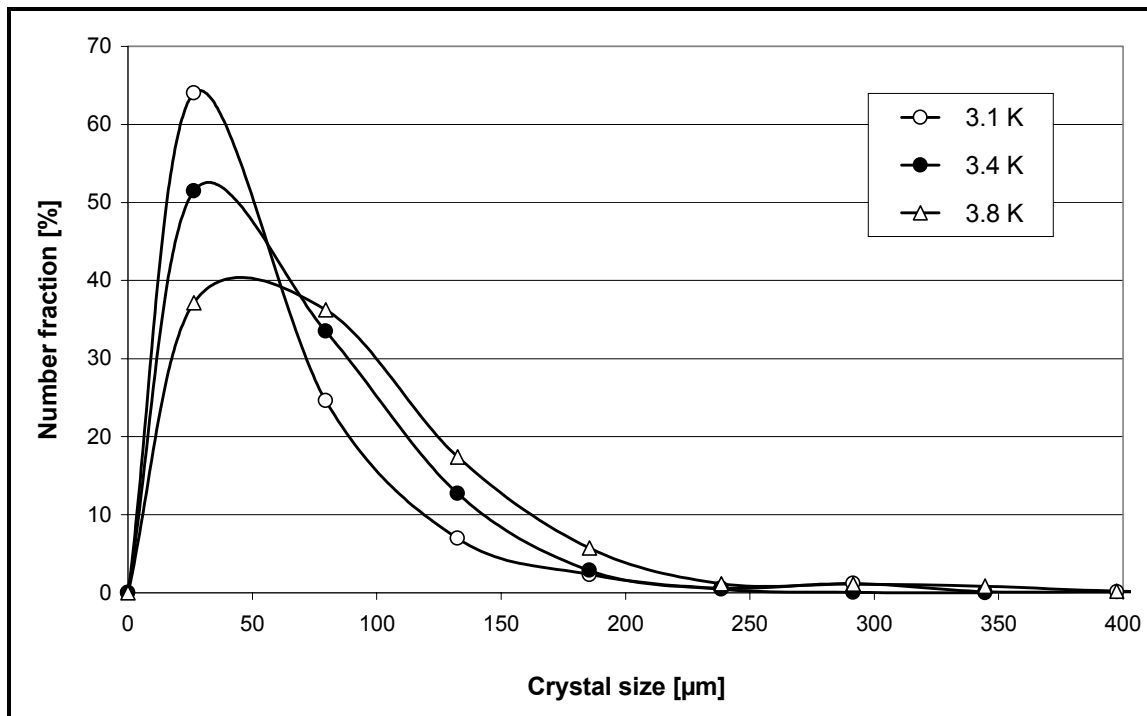


Figure 4.4.2 Crystallization of myristic acid in a scraped surface crystallizer chamber at different undercoolings. Scraper rotational velocity 7.6 rpm.

Table 4.4.1 Average crystal size and mode from distributions presented in Fig. 4.4.2.

Undercooling [K]	Average crystal size [μm]	Mode of distribution [μm]
3.1	44	28
3.4	62	33
3.8	69	44

The effect of the undercooling on the shape of the myristic acid crystals – represented by circularity – is shown in Fig. 4.4.3. It can be seen that increasing undercooling produces crystals that more and more resemble a sphere. This can be explained by growth in the suspension.

Another aspect that follows from the increasing undercooling is the broadening of the circularity distribution. This is caused by the accelerated process of crystal growth in the suspension towards a regular shape and the constant flow of irregular shape crystals broken off from the crystal layer.

The influence of the scraper rotational speed on the obtained crystal size is presented in Fig. 4.4.4 and Fig. 4.4.5. These two figures show that by increasing scraper speed the average crystal size is reduced. This is caused by the shortened period of layer growth between two scraping actions by increasing scraper speed. Thus, the thickness of the removed layer is reduced, which affects directly the size of the produced particles. However, the excess of this

phenomenon can be seen to be strongly influenced by the properties of the compound system. In Fig. 4.4.4 myristic acid was crystallized from its mixture with capric acid. In Fig. 4.4.5 the crystallizing component was capric acid.

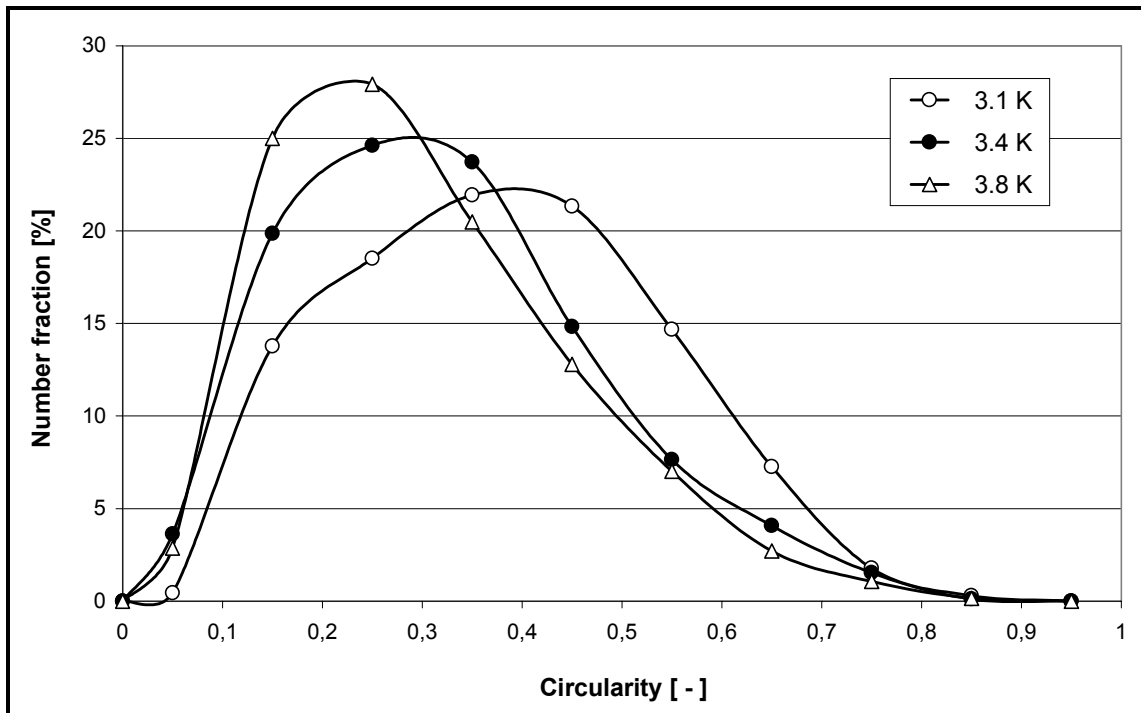


Figure 4.4.3 Crystal form of myristic acid in a scraped surface crystallizer chamber. Scraper rotational velocity 7.6 rpm.

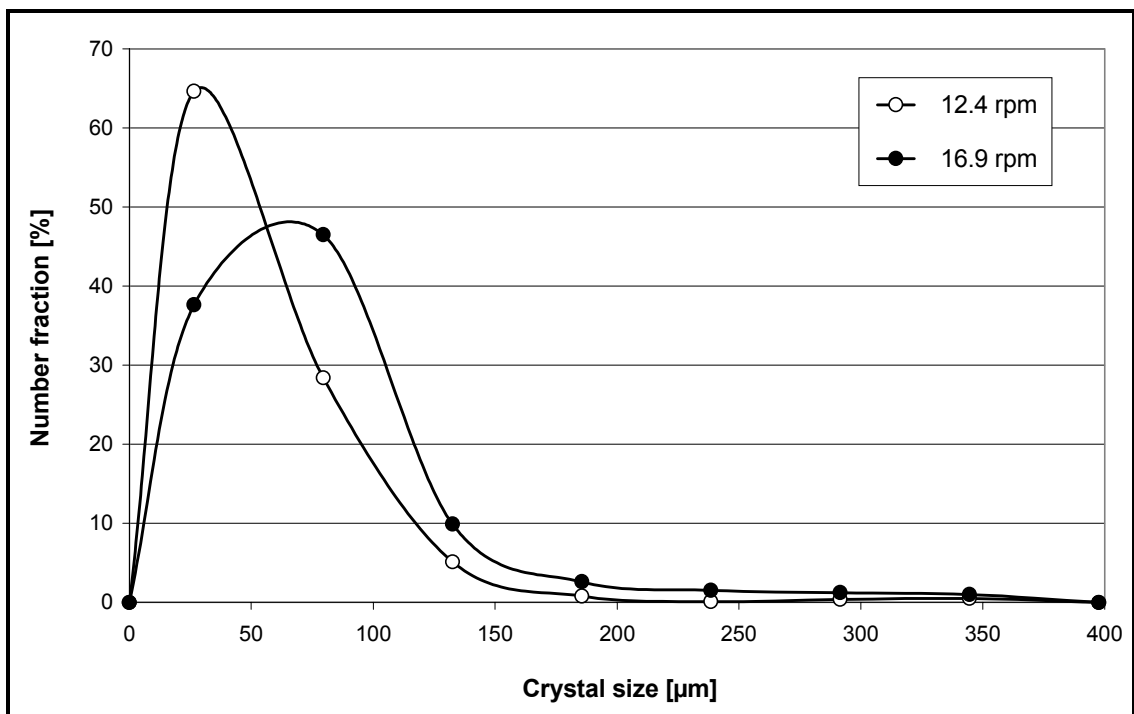


Figure 4.4.4 Crystallization of myristic acid in a scraped surface crystallizer chamber at different scraper rotational velocities. Undercooling 3.4 K.

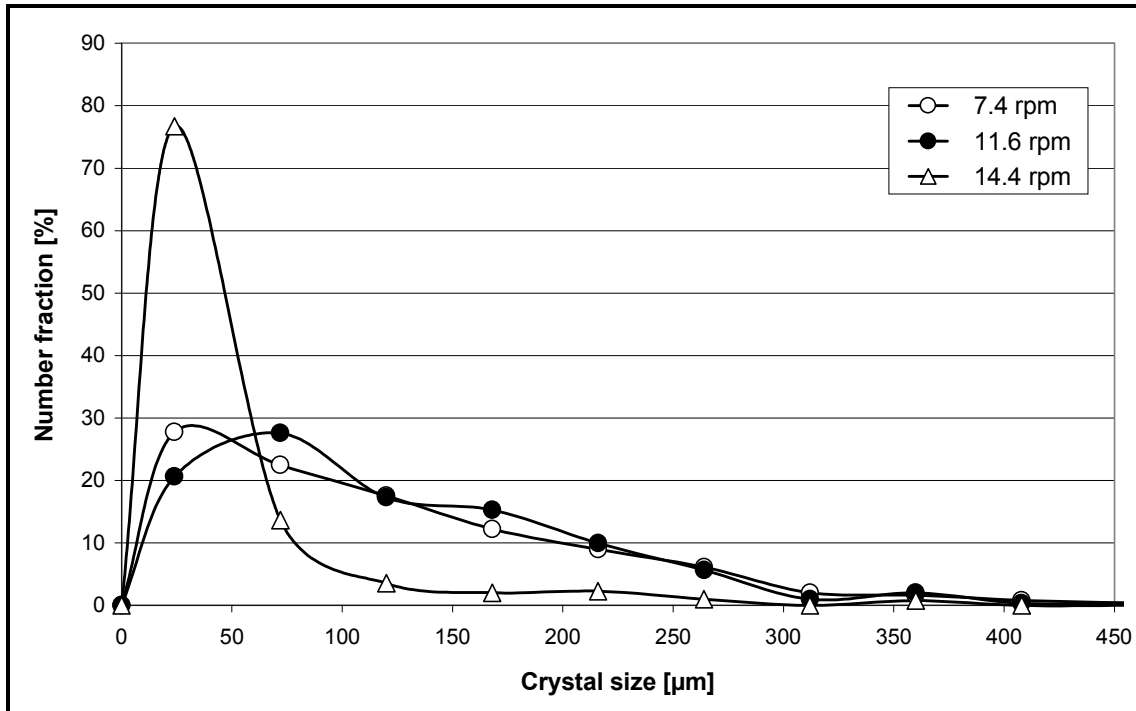


Figure 4.4.5 Crystallization of capric acid in a scraped surface crystallizer chamber at different scraper rotational velocities. Undercooling 5.4 K.

The influence of residence time in the observation chamber on the crystal size distribution of myristic acid is presented in Fig. 4.4.6. The broadening of the crystal size distribution due to simultaneous crystal growth and formation of new crystals is an expected result.

An interesting result is the change in the breadth-length ratio of myristic acid crystals by increasing residence time, presented in Fig. 4.4.7. The result shows that the crystals are

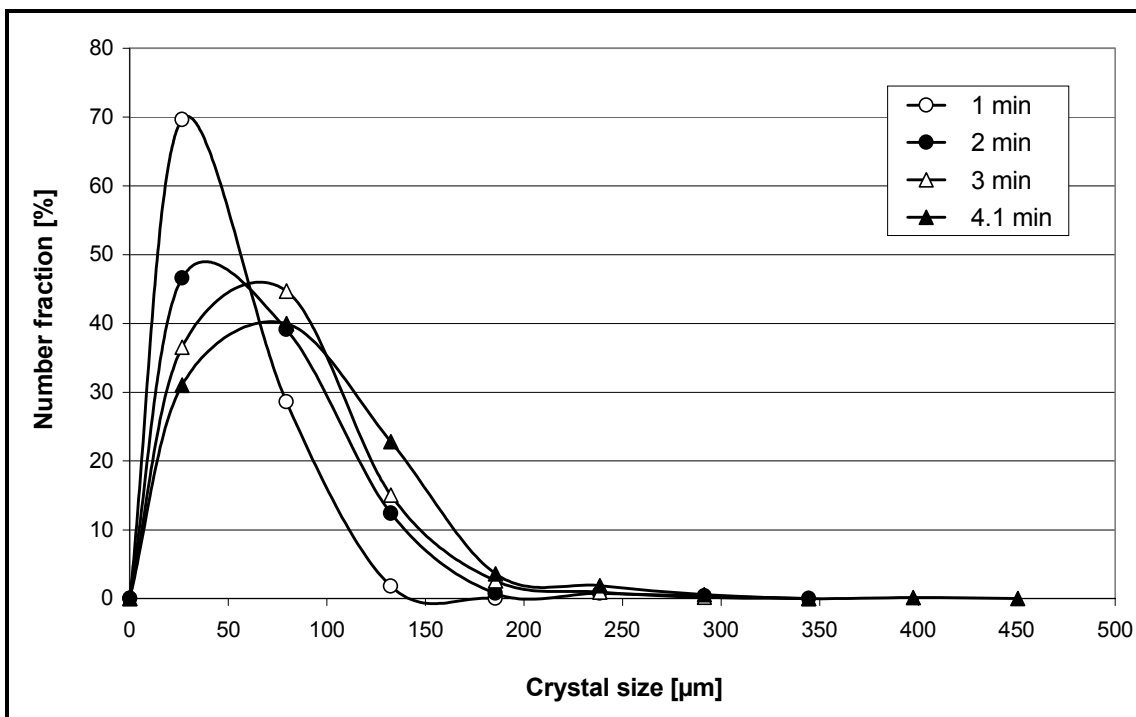


Figure 4.4.6 Development of the size distribution during the crystallization of myristic acid. Scraper rotational velocity 7.6 rpm, undercooling 3.4 K.

prolonged in form when scraped off from the crystal layer. However, in the suspension growth the prolonged shape is even more emphasized, suggesting a needle like growth typical for many organic systems.

The angle of the scraper blades was changed in order to investigate the effect of the direction of the force impacting the crystal layer. The influence of the scraper angle on the crystal size of myristic acid is shown in Fig. 4.4.8. It can be seen that the crystals produced with a smaller inclination of the scraper blades are smaller. The effect of the angle on the crystal form is presented in Fig. 4.4.9. It can be seen that a steeper angle produces more spherical crystals.

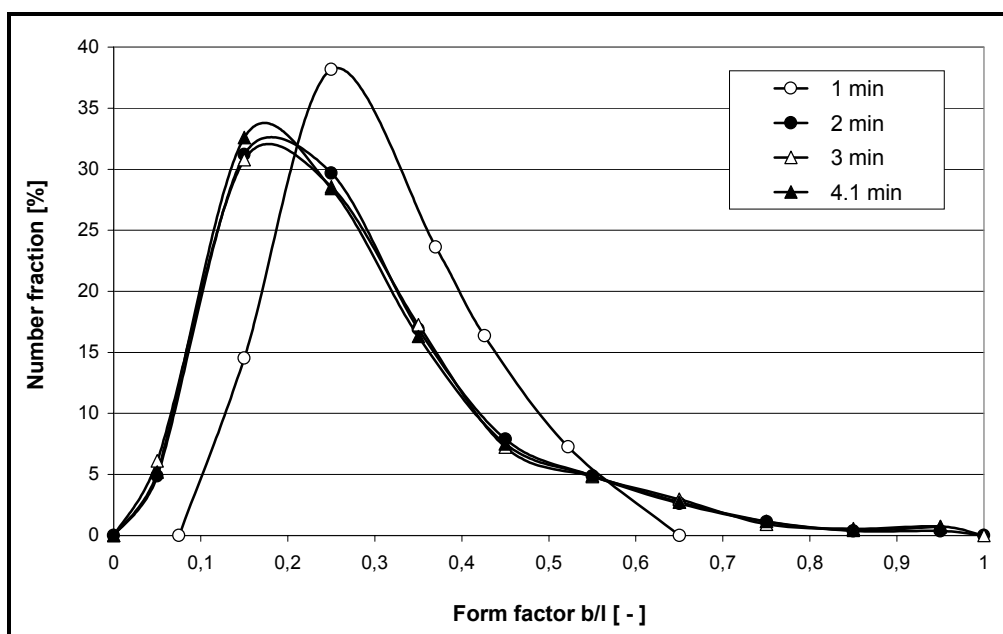


Figure 4.4.7 Development of the crystal form during the crystallization of myristic acid. Scraper rotational velocity 7.6 rpm, undercooling 3.4 K.

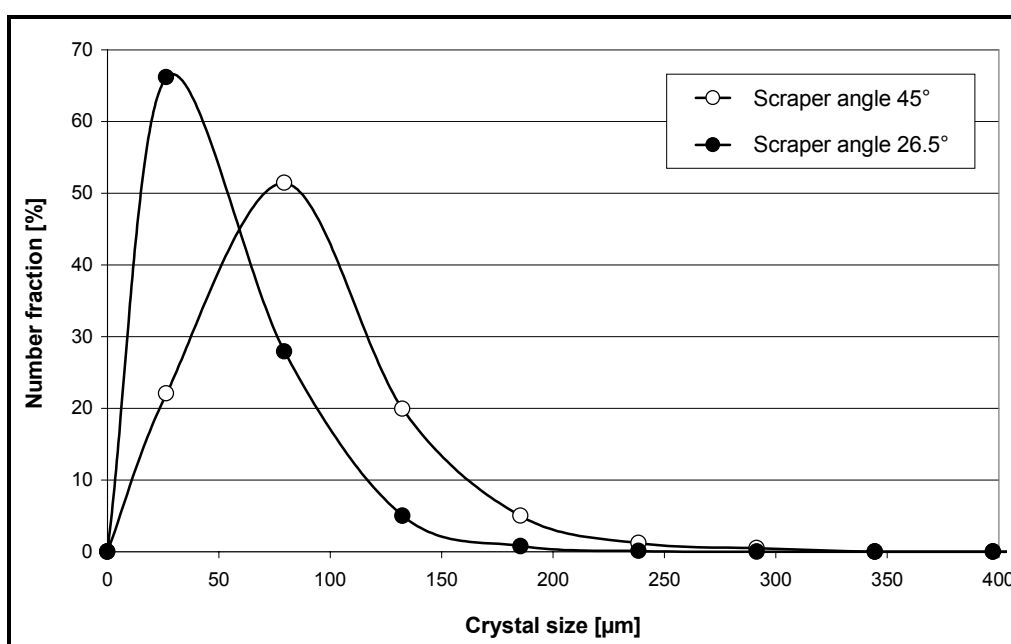


Figure 4.4.8 Crystal size by crystallization of myristic acid at different scraper angles. Scraper rotational velocity 12.4 rpm, undercooling 3.4 K.

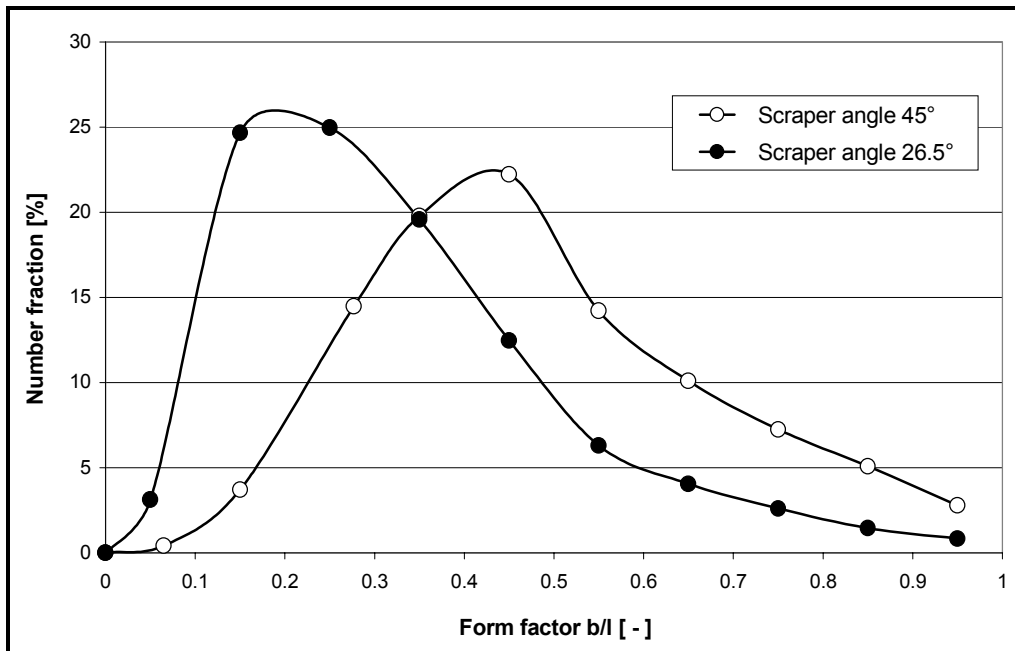


Figure 4.4.9 Crystal form by crystallization of myristic acid at different scraper angles. Scraper rotational velocity 12.4 rpm, undercooling 3.4 K.

4.4.2 Particle characteristics under free growth in a suspension

Suspension melt crystallization without the scraping action was studied using eutectic binary mixtures of p-xylene with its isomers m- and o-xylene. Most of the experiments were carried out with o-xylene as the second component, because of the ease in analytical detection of p- and o-isomers by gas chromatography. The concentration of p-xylene in the experiments was 75 to 95 wt.-%. The melt was crystallized batchwise in a 5 ml observation chamber under a

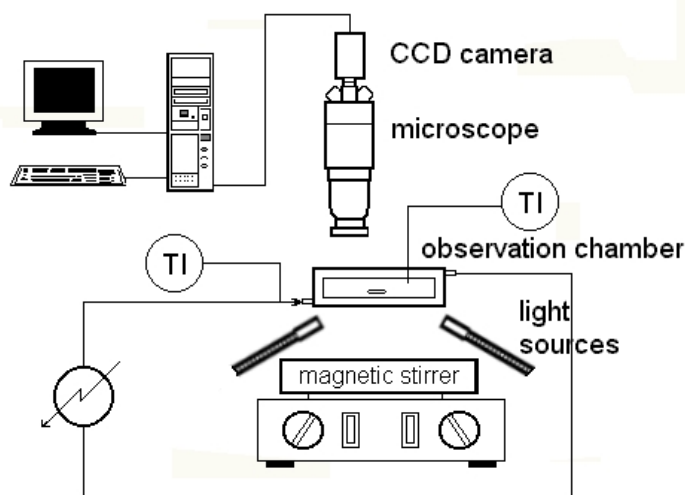


Figure 4.4.10 Experimental equipment for suspension crystallization of p-xylene.

microscope, which allowed desired features to be measured at different time points of crystallization. The undercooling level in the crystallizer was adjusted for the growth period after crystal formation had taken place in a higher undercooling. During the experiments the melt was tenderly mixed with a magnetic stirrer. The experimental setup is shown in Fig. 4.4.10.

The development of the CSD was measured during crystallization using image analysis (Optimas 6.2). From the development of the CSD it could be estimated, whether nucleation or agglomeration took place during the crystallization process. The tendency of the crystals to agglomerate was observed also from the photomicrographs taken for the analysis [Täh02].

The shape of the crystals was characterized by two dimensionless shape factors: the circularity and the aspect ratio. The definitions of the shape factors are the same as in the Chapter 4.4.1.

The amount of melt left in the crystal cake after filtration was measured. This was used as a measure for the efficiency of solid-liquid separation. For these experiments the melt was crystallized in a 50 ml jacketed glass vessel and filtrated in a thermostated glass filter. The concentrations of the xylene components in the crystal cake and in the filtrate were analyzed by gas chromatography.

The temperature in the observation chamber was decreased at a constant rate of 1 °C/min and the metastable zone width was defined at the temperature at which the crystal formation was detected. The crystallization occurred instantaneously, producing a large amount of crystals. The metastable zone width was found not to be affected by the melt composition and was at maximum 0.74 K. The metastable zone widths with m-xylene as the secondary component did not differ from those with o-xylene. The undercooling needed for the initial formation of crystals was found to be insufficiently large for the further process. Resulting excessive nucleation and increase in the suspension density hindered further investigation by image analysis. Therefore, the temperature was raised until the crystals were seen to melt. In 75% melt this occurred at 0.07 K and in 90% melt at 0.11 K overheating. The crystal size distributions of the first crystallite and the partly melted crystals, used as seeds for the growth experiment, are shown in Fig. 4.4.11. That the average size of the melted crystals is only slightly smaller than the size of the first formed crystals has its reason in the fact that the largest crystals had remained in reduced size, while the smaller sizes were totally melted out. The most noticeable change did happen in the suspension density of crystals. The low suspension density thus achieved allowed observation of the crystals during the growth period.

The CSD of crystals after 40 min of growth is also shown in Fig. 4.4.11. It can be seen that after 40 min the larger crystal sizes are clearly emphasized in the crystal population. The reason for this is agglomeration, which was also proven by visual observation. After 40 min undercooling was further increased and the crystals were allowed to grow additional 20 min. The average crystal sizes at different time points of crystallization, as well as the dimensionless shape factors the circularity and the aspect ratio, are given in Fig. 4.4.12. While the amount of crystals in the analysis after 60 min of growth was decisively different to the other CSD definitions, graphical comparison in Fig. 4.4.11 is left out due to the incomparable form of the distribution curves. From Fig. 4.4.12 it can be seen that the circularity changes during the experiment only slightly. The value of circularity for the first crystallite is somewhat higher than the value for the grown crystals. The circularity value increases for the melted seeds because of the rounding that occurs during melting. The aspect ratio decreases during growth to the value of 0.68, which represents the value for the equilibrium shape of the

crystals at this undercooling (0.13 K). The aspect ratio rises to the value of 0.76 after 60 min, because of higher undercooling (0.39 K).

The cumulative size distributions for the seed and the product crystals after 40 min are shown in Fig. 4.4.13. It can be seen that the shape of the size distribution changes during the process because of nucleation. The figure shows that nucleation cannot be avoided even when the undercooling is set to a minimal value under very mild mixing conditions. Although the increase in the number of crystals could not be visually observed, nucleation can be detected from the measured size distribution data.

In order to investigate the effect of the growth process on the crystal shape, experiments were carried out with chosen crystals – marked C1, C2, C3 and C4 – during their growth in static melt conditions. The seed crystals were produced as before and four crystals were taken under observation. The development of the aspect ratio is shown in Fig. 4.4.14. The crystal C2 can be seen to deviate clearly from the other crystals according to the development of its aspect ratio and shape. This can be explained by the crystals orientation to the direction of observation. The crystal lies in a less probable orientation on its second largest face. Therefore, the change in the aspect ratio represents the development of length and thickness, while for the others it represents the development of length and width of the crystals. The change in the crystal habit can also be tracked by observing the growth rates of the a and b directions of the crystal projection. The change in the growth rates for these two directions for the crystal C1 is shown in Fig. 4.4.15. The shape of the crystal is determined by the relation of

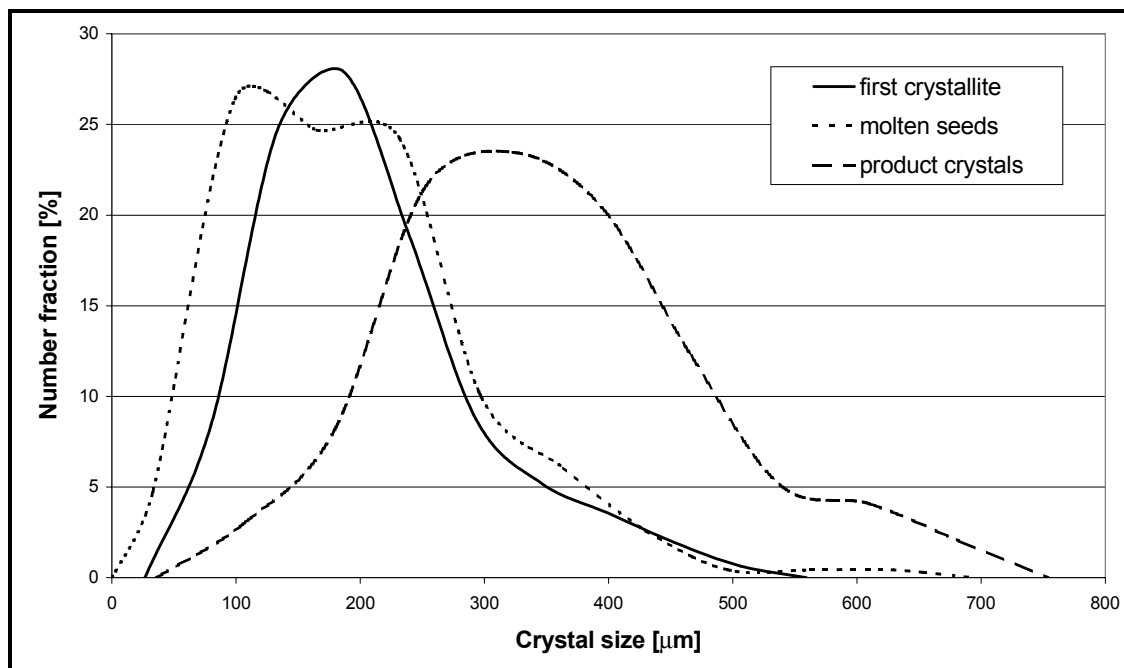


Figure 4.4.11 Size distributions obtained at crystallization of 75% p-xylene.

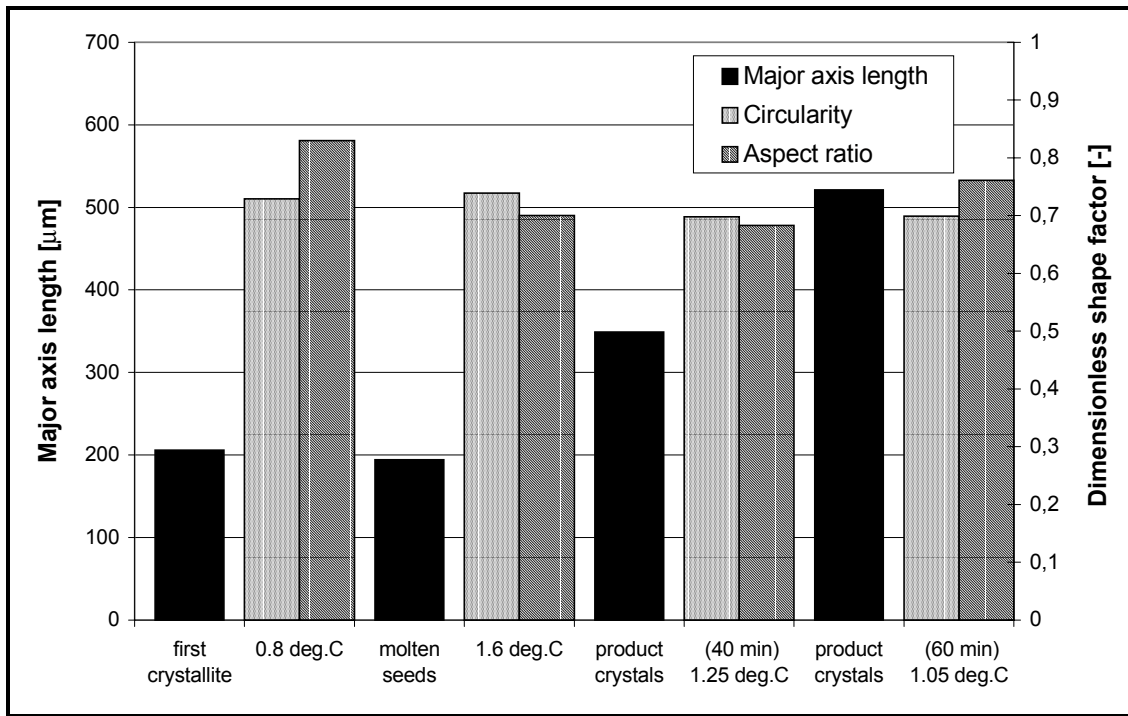


Figure 4.4.12 Comparison of size and shape data for crystallization of 75% p-xylene mixture. The temperatures given refer to the actual crystallization temperatures.

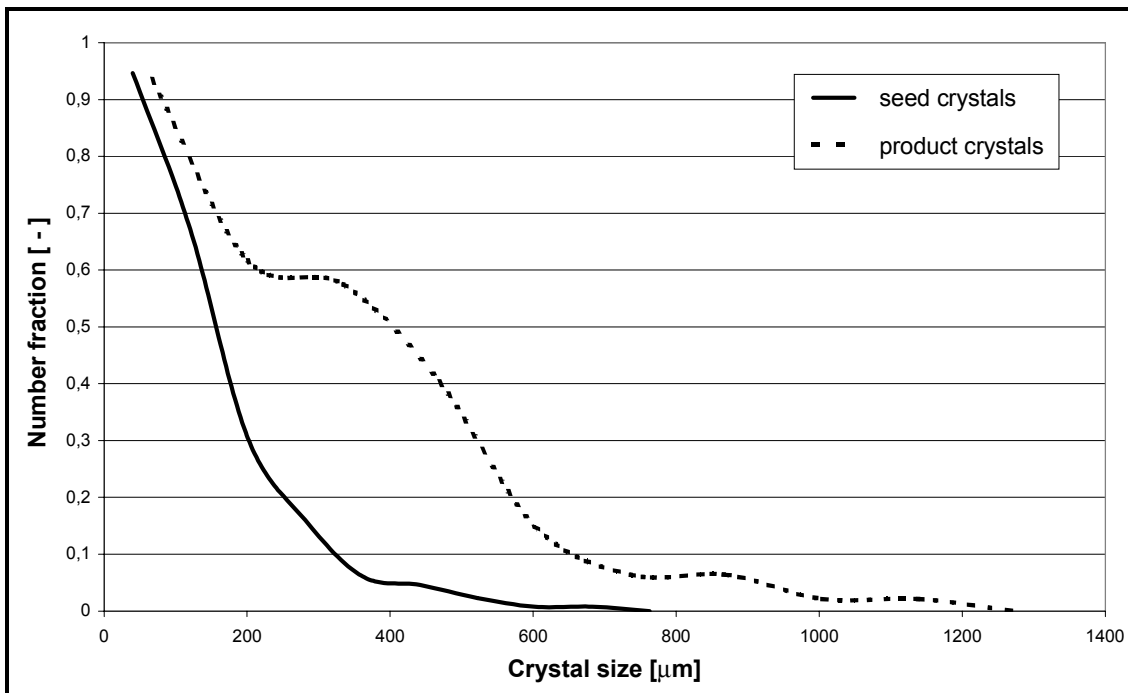


Figure 4.4.13 Cumulative size distribution of seed crystals and product crystals after 40 min of growth in crystallization of 75% mixture of p-xylene.

the individual face growth rates. In Fig. 4.4.15 the relation of the face growth rates, thus the equilibrium shape, changes during the crystallization process. In this case the growth rates approach the same value, at which point the equilibrium shape of the crystal projection represents a square.

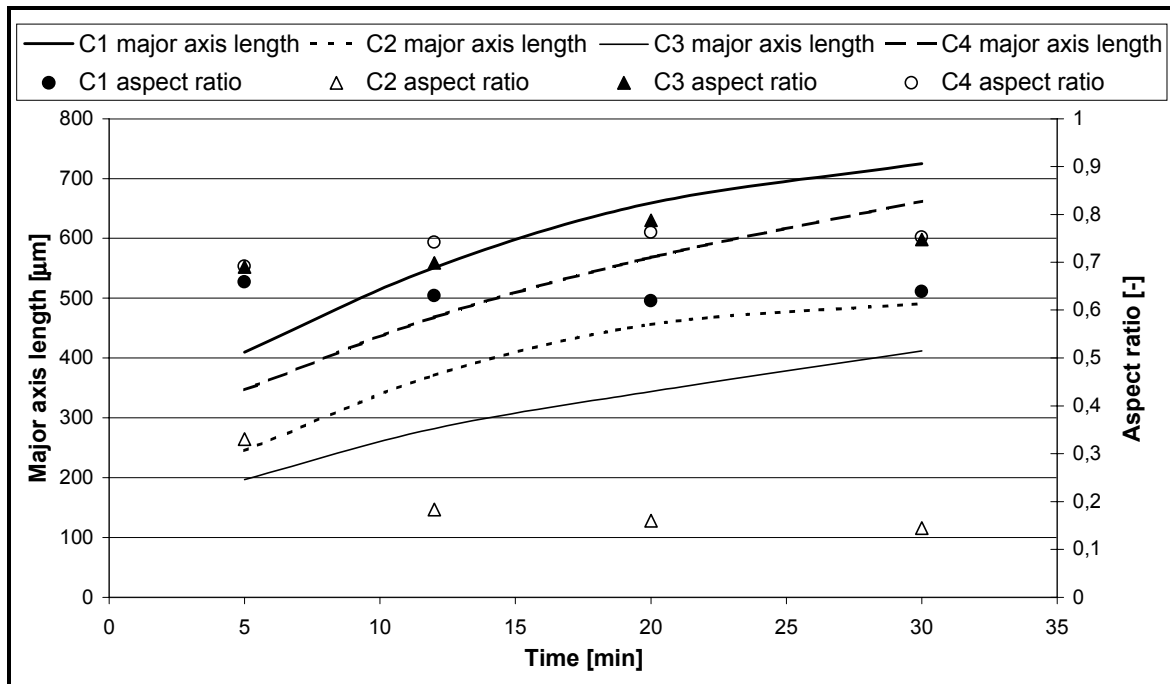


Figure 4.4.14 Crystallization of 75% p-xylene mixture. Undercooling 0.13°C in static melt conditions.

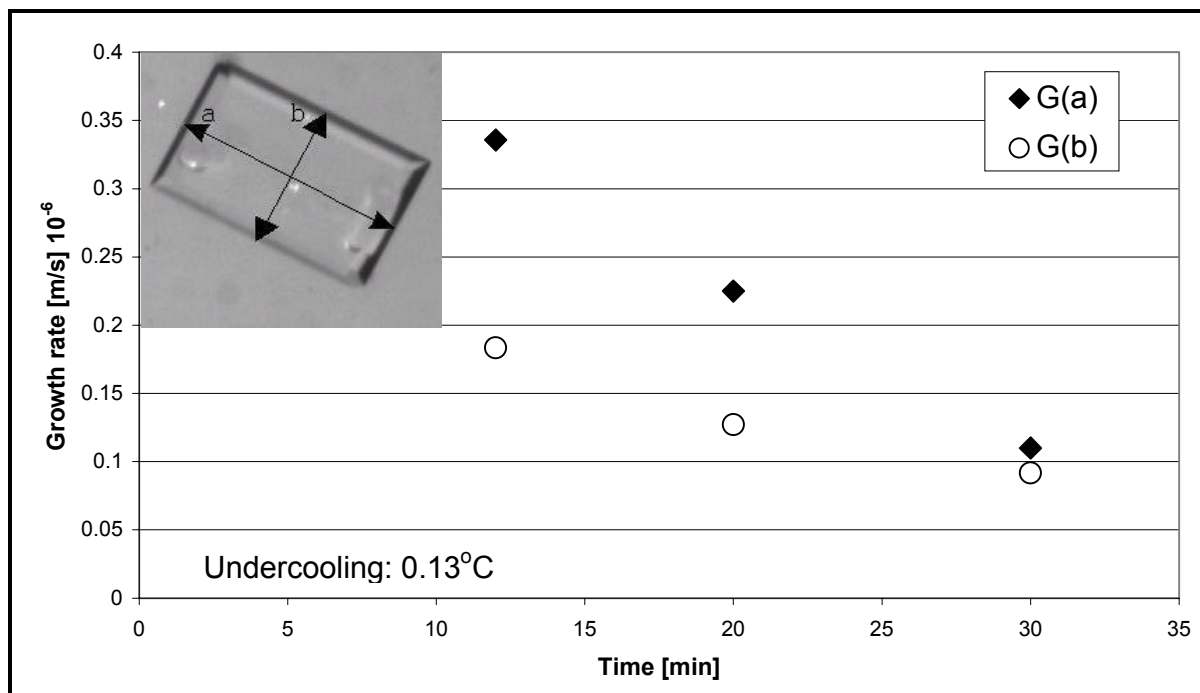


Figure 4.4.15 Growth rates of the main and secondary axis lengths for 75% p-xylene mixture. Undercooling 0.13°C in static melt conditions, crystal C1.

The melt left in the crystal mass after filtration was measured to examine the purification potential of the combined crystallization and solid-liquid separation steps. The amount of melt left in the filter cake was calculated from the mass balance by equations 4.2.1 and 4.2.2.

The achieved purities and rest melt quantities are presented in Table 4.4.2. It was not possible to compare the filtration result using the first-born crystals and the crystals after a growth period reliably. This is because the crystal mass present after the growth period was

much higher than the mass of the firstly born crystals. The average mass of the first crystallite being 2.3% of the initial mass (0.97 g), the one for the grown crystals was 11.7% (5.44 g). Because of the bad filtration results the purities for the experiments with a growth step are also lower than for those without growth.

Table 4.4.2 Concentrations p-xylene and remained rest melt amounts after filtration.

Initial concentration [wt.-%]	75	80	85	90	95
Purity (first crystallite) [wt.-%]	87.3	93.8	95.3	97.4	98.4
Purity (grown crystals) [wt.-%]	86.1	87.6	92.2	93.8	97.9
Amount of rest melt (grown crystals) [wt.-%]	49.8	30.1	30.8	26.3	32.0

4.4.3 Particle characteristics of ice crystals from stirred tank

Crystallization of ice was investigated in order to observe the ice crystal shape in a stirred tank and compare it to the shape of crystal presented in Chapter 4.3. Also the development of the ice crystal shape by continued stirring was examined.

A solution of water and 5 wt.-% of ammonium sulfate was cooled down to its freezing point at -1.6°C . The crystallizer volume in the experiments was 1500 ml and the solution was agitated with a blade mixer at a constant rotational frequency of 700 rpm. A small amount of seed crystals (0.15 g) was added to the solution at the freezing point and the solution was cooled further. At the temperature of -1.85°C crystallization started everywhere in the vessel, while the temperature rose due to the latent heat of crystallization to -1.65°C . At the time of crystallization photomicrographs were taken with an in-line microscope provided by the company MTS and the temperature was let constant.

After 5 minutes new photomicrographs were taken to see the change in the ice crystals. The plate like crystals that first formed had agglomerated into spherical agglomerates. This would suggest that the change in the ice crystals at these conditions would not happen through ripening (as reported by e.g. Lemmer *et al.* [Lem00]), but through agglomeration (as shown e.g. by Kobayashi *et al.* [Kob96]).

The ice crystals before and after agglomeration are shown in Fig. 4.4.16. It can be seen that the crystals formed at the beginning posses similar shape to crystals produced by the pilot plant equipment presented in Chapter 4.3. All the pictures in Fig. 4.4.16 have the same magnification and show the qualitative change in the particle characteristics.

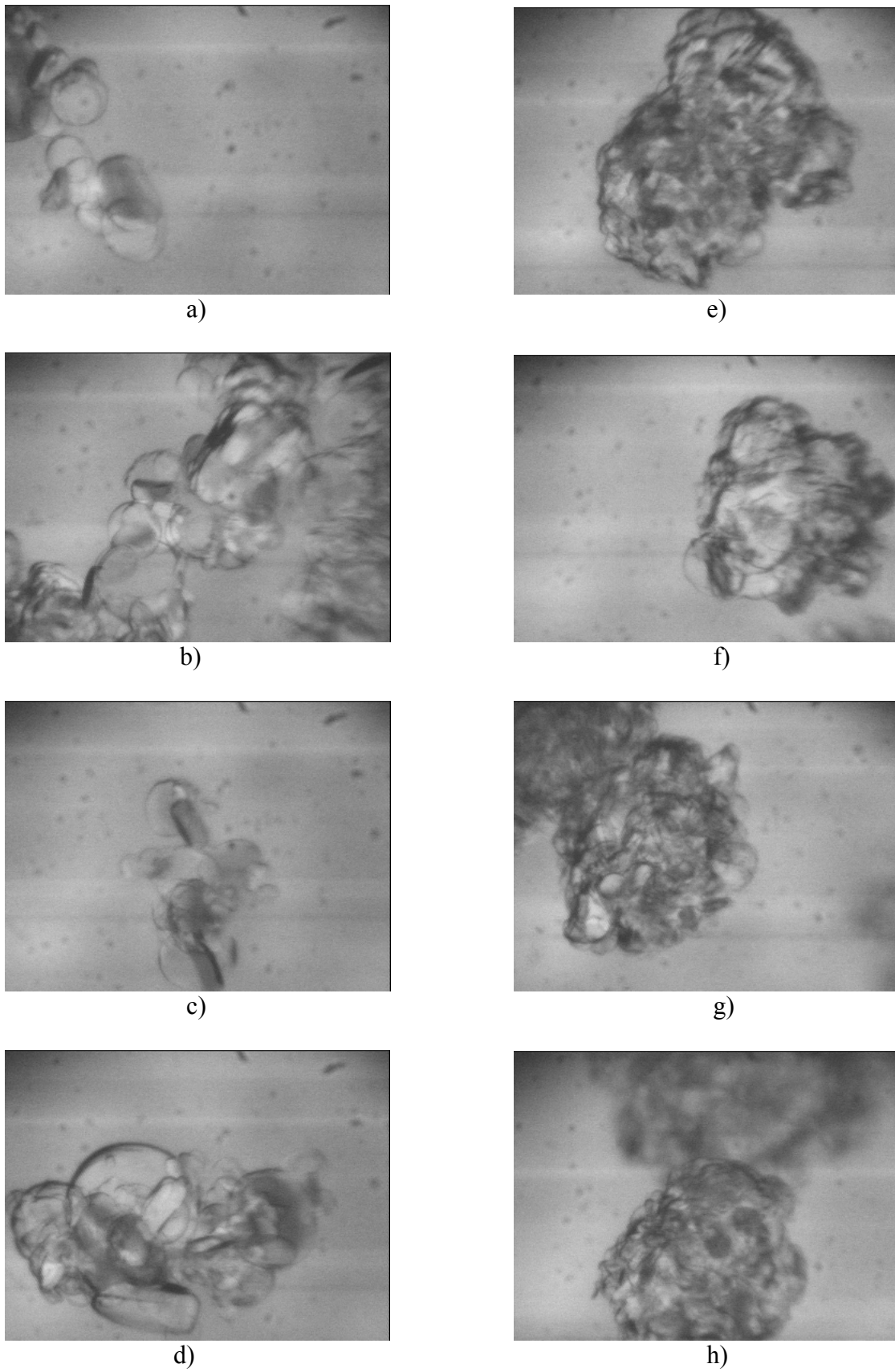


Figure 4.4.16 Ice crystals from ammonium sulfate solution right after their formation (pictures a to d) and agglomerated ice crystals after 5 minutes in the stirred vessel.

4.5 Conditions for Formation of Crystalline Layers

In this chapter experimental work on the influence of the factors, which influence the tendency of crystal formation on cooled surfaces is presented. Results on the influence of undercooling on the induction time of the layer formation and the effect of the concentration of the crystallizing component on the layer texture will be shown. Also observations on the conditions at which the crystallization will take place on a cooled surface and conditions at which the nucleation will start in the liquid phase, thus forming a suspension, are presented.

The experiments have been made in a jacketed vessel. Cooling or heating was provided in the middle by a tube, through which a heat exchange medium was circulated (usually called a cooling finger in cases where the crystallization takes place at the surface of this element). The volume of the vessel was 200 ml and the heat exchange surfaces in these experiments were made of glass. The crystallization took principally place on the walls of the jacketed vessel (not on the cooling finger). The system was equipped with a magnetic stirrer, which allowed the experiments to be carried out in dynamic as well in static conditions. The experimental setup is shown in Fig. 4.5.1.

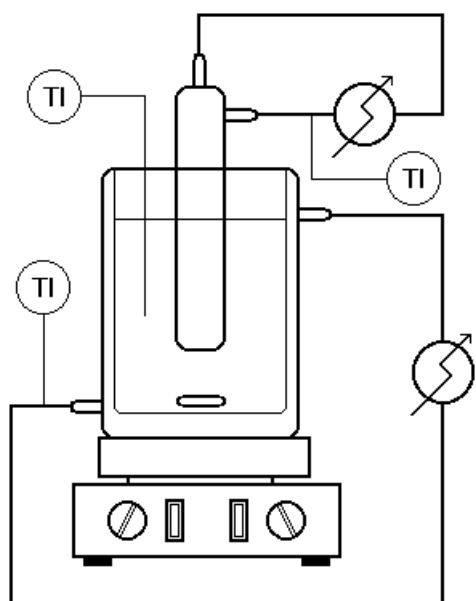


Figure 4.5.1 Experimental equipment for investigation of layer formation.

The experiments were carried out with two chosen fatty acids and their mixtures: Stearic acid and myristic acid. The pure components stearic and myristic acid were investigated in order to investigate the effect of undercooling without the influence of the concentration of the crystallizing component. The effect of concentration on the texture of the forming layer was carried out by crystallizing stearic acid from mixtures of different composition. The chosen compound pair forms an eutectic system. The measured phase diagram is presented in Fig. 4.5.2. The phase diagram was determined using the thaw-melt method and digital scanning calorimetry (DSC). It can be seen from Fig. 4.5.2 that the shape of the liquidus curve for the higher melting component changes its form at concentration of 40 wt.-% of stearic acid. This type of phase diagram is typical for fatty acid mixtures,

and suggests a polymorphic transformation of the crystals at 40 wt.-% of stearic acid. However, all the experiments with mixtures of stearic and myristic acid were carried out with concentrations of 60 wt.-% or more stearic acid, so the possible effect of different polymorphs does not have to be taken into account. A slight change in the form of the liquidus curve can also be seen at the concentration 90 wt.-% stearic acid. This is not a typical form observed at the phase diagrams of fatty acids and can be considered to be due to experimental inaccuracy. The eutectic composition was found to be 25 wt.-% stearic acid while eutectic temperature measured was 49.3°C. Physical properties of the investigated fatty acids are presented in Table 4.5.1.

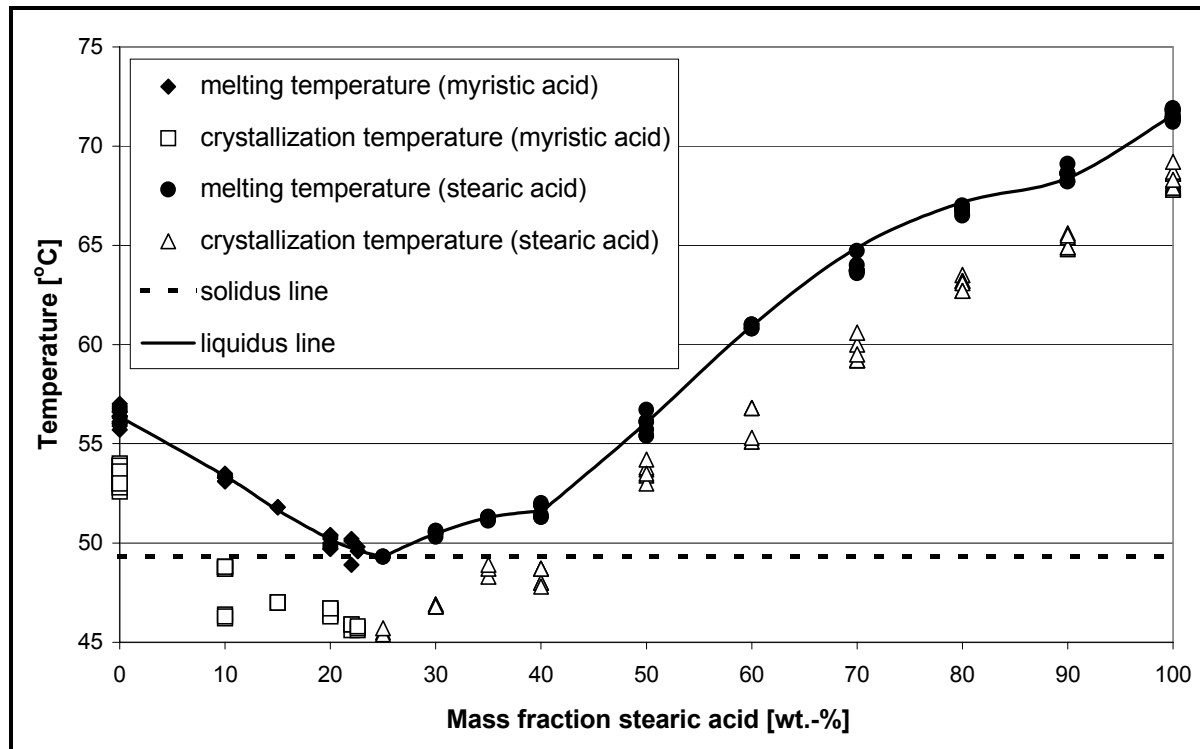


Figure 4.5.2. Phase diagram stearic acid/myristic acid measured by differential scanning calorimetry (DSC).

Table 4.5.1 Physical properties of stearic and myristic acid [Kir85].

	Myristic acid	Stearic acid
Chemical formula	$C_{14}H_{28}O_2$	$C_{18}H_{36}O_2$
Molar weight [g/mol]	228.375	284.483
Melting point [°C]	54.4 (56.4)	69.6 (71.5)
Boiling point [°C]	326.2	376.1
Liquid density (80°C) [kg/m^3]	843.9	838.0(80)
Viscosity (70°C) [mPas]	5.83	9.87
Heat of fusion [kJ/mol]	45.05	62.51

During the growth of the crystal layer the solid-liquid phase boundary can be assumed to be at the melting temperature of the mixture. The actual undercooling at which the crystallization starts to take place is the temperature difference between the equilibrium temperature of the melt and the temperature of the inner wall surface of the jacketed vessel. To determine the undercooling for each experiment the inner wall surface temperature was measured as a function of the temperature set at the thermostat. The resulting calibration line is shown in Fig. 4.5.3. Because the fatty acids are aggressive against plastic materials used in the contact thermometer available for the surface temperature measurement, it was not possible to measure the surface temperature directly in the fatty acid mixtures. Therefore, the surface temperature was measured against air and against water. The surface temperature was measured at static conditions, so the heat transfer at the inner surface is in this case determined by natural convection. The surface temperature for stearic and myristic acid and

their mixtures can be determined by using the measured values for air and water and the characteristic values for natural convection presented in Table 4.5.2. Considering the accuracy of the temperature measurement it is reasonable to give the surface temperature value only with one decimal. With this accuracy the surface temperature for all the fatty acids and their mixtures is 0.3 K higher than the inlet temperature into the outer jacket.

Table 4.5.2 Characteristics of natural convection for the investigated compounds.

	Air	Water	Myristic acid	Stearic acid
Grashof number	$9.88 \cdot 10^5$	$1.71 \cdot 10^{10}$	$4.79 \cdot 10^6$	$1.65 \cdot 10^6$
Prandtl number	0.73	1.18	69.96	118.44
Product GrPr	$7.23 \cdot 10^5$	$2.03 \cdot 10^{10}$	$3.35 \cdot 10^8$	$1.95 \cdot 10^8$
Nusselt number	17.2	222.6	79.8	69.7

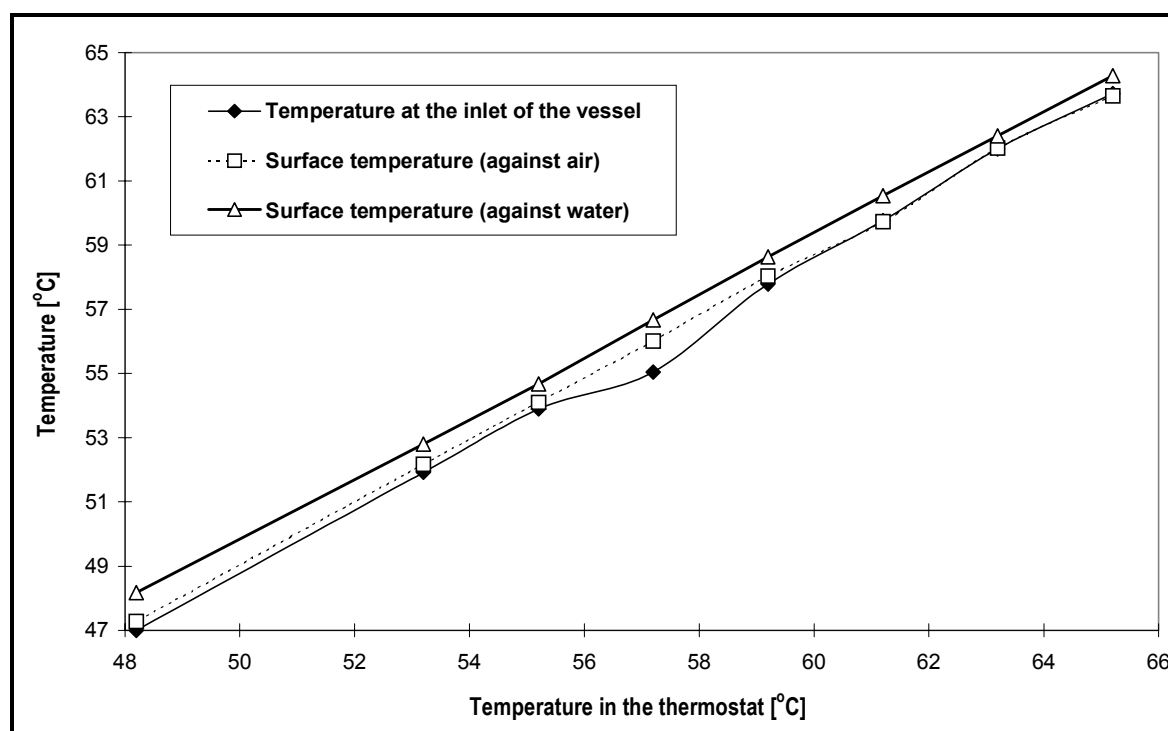


Figure 4.5.3. Surface temperature of the inner wall of the jacketed vessel. Measurement with water at constant water bath temperature of 73 °C.

4.5.1 Growth of pure components

An induction time is needed for the crystallization to start after the introduction of cooling. The induction time is influenced by the degree of undercooling at the wall, the initial temperature of the melt, the agitation intensity and the properties of the mixture, e.g. viscosity and the amount of impurities.

The induction time of crystal formation on the undercooled glass surface in the case of myristic acid is shown in Fig. 4.5.4. When the crystallization is carried out at static conditions the melt adjacent to the surface reaches the crystallization temperature faster as the mixed

melt, which is in better contact with the heated melt inside the vessel. This causes the induction time for the crystallization to be shorter at the static conditions. Interesting is the result that when the temperature of the melt is not kept higher than the equilibrium temperature by extra heat input, at low undercooling on the surface (in this case 4 K) the crystallization does not start on the surface, but in the melt. This is shown by the broken line for the series “mixed melt, no heating” in Fig. 4.5.4.

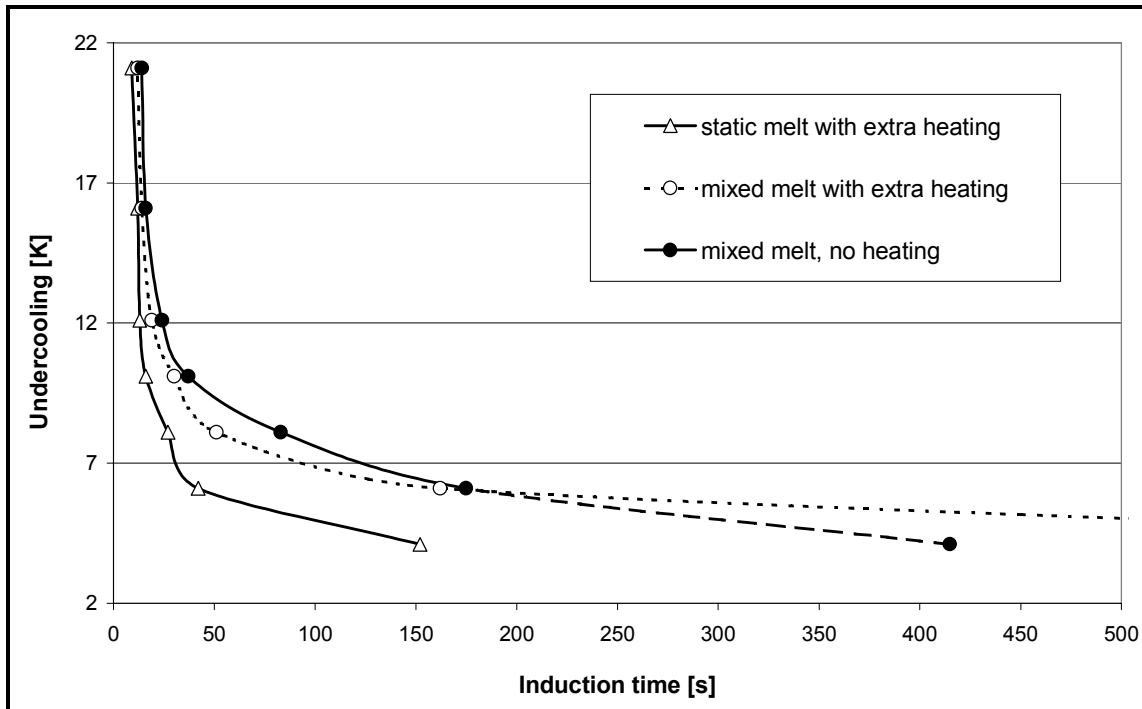


Figure 4.5.4 Crystallization of myristic acid on a glass surface. Induction time for suspension crystallization in mixed melt without heat input is shown by the broken line.

Fig. 4.5.5 shows the time needed for the crystallization to start (induction time) and the time needed for the formation of a complete layer in the case of stearic acid. It can be seen that both of the times start to rise remarkably when the undercooling on the surface is 7 K or less. However, the time needed for the complete layer to form rises much steeper. It can be assumed that the induction time at undercoolings below 7 K is controlled by the formation of nuclei (influence of cooling on the metastable zone width), whereas at undercoolings higher than 7 K the induction time is merely controlled by the growth of the nuclei to a macroscopic size.

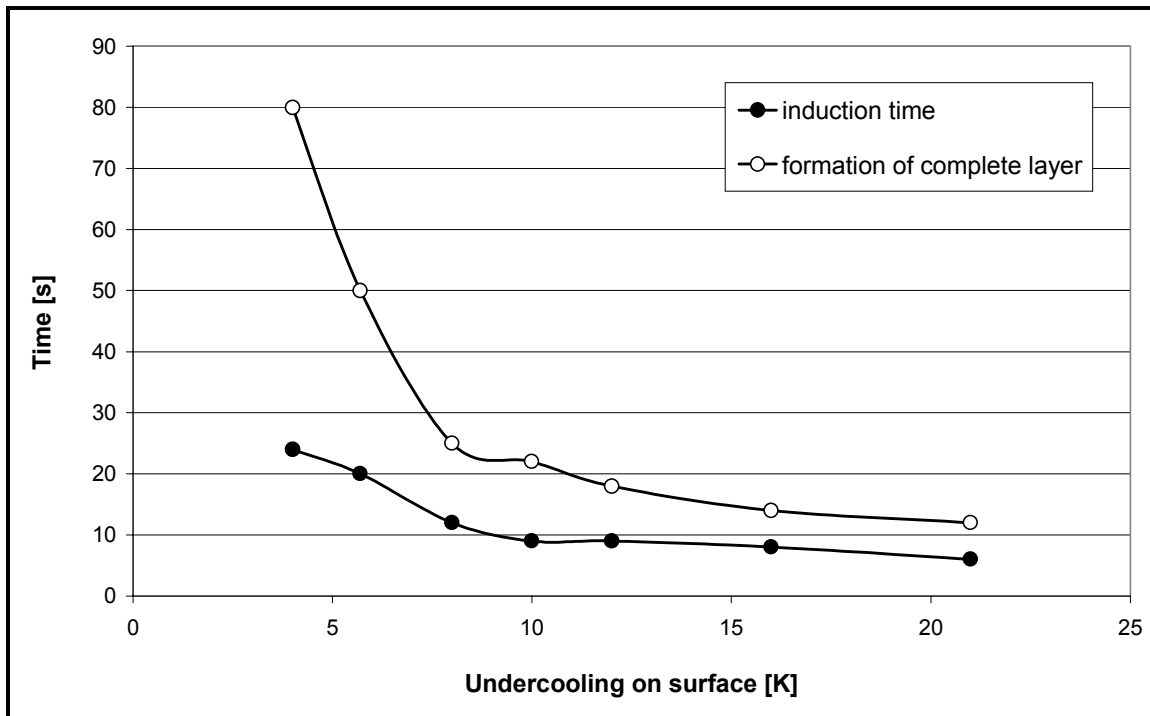


Figure 4.5.5 Crystallization of stearic acid on a glass surface at static conditions.

The dependence of growth rate on the undercooling on the surface at static conditions is presented in Fig. 4.5.6. The data in Fig. 4.5.6 is based on the layer thickness achieved in a constant time of five minutes. The heat resistance of the thicker layers formed at higher undercoolings depress the layer growth rate. Thus the dependence becomes logarithmic, while the dependence in suspension growth is linear.

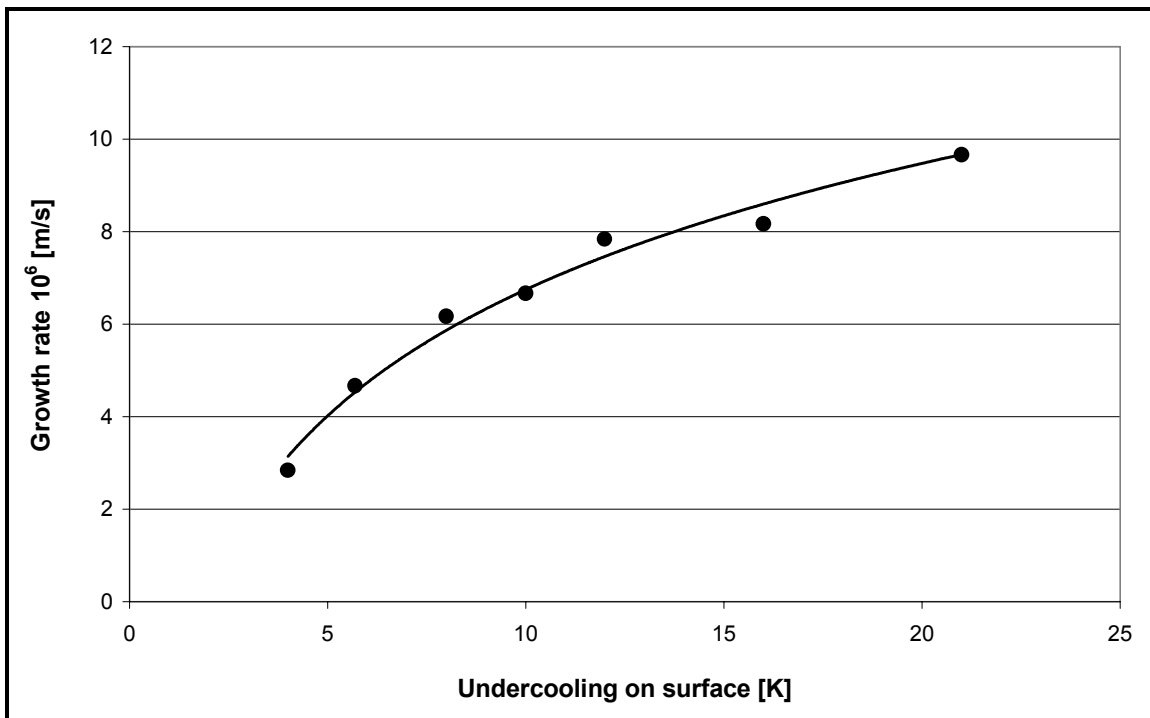


Figure 4.5.6 Crystallization of stearic acid on a glass surface at static conditions.

4.5.2 Crystallization of fatty acid mixtures

The mixtures of fatty acids were crystallized in order to investigate the effect of concentration on the ease of layer formation.

Layer crystallization experiments with equipment presented in Fig. 4.5.1 were made with mixtures of stearic acid and myristic acid. The effect of concentration was investigated by crystallizing stearic acid on the surface of the cooling finger. This way, the formed layer was easier to remove from the vessel for observation. It was found that crystal layers produced from binary mixtures with high amounts of the minor component were very soft compared to the layers produced from the melt of a pure component. The qualitative results over the layer texture are presented in Table 4.5.3. The layers produced with concentrations of 60 and 70 wt.-% stearic acid were very soft. Indeed, it was not possible to remove the crystallite as a solid layer, but the layer fell by touch to a snow like sludge. This has its reason in the increasing amount of inclusions with increasing concentration of the impurity component. Because of high viscosity of the fatty acids and a great similarity in the molecular structure (see Table 4.5.1), the mobility of the molecules out of the phase boundary is restricted. The result is that much of the secondary component present in the melt is also included in the crystal layer. When the stearic acid concentration rises the crystalline layer becomes more and more consolidated. The results are in good agreement with the observations in Chapter 4.2 that incrustations form easier when the concentration of the crystallizing component is high.

Table 4.5.3 Investigation of layer texture of stearic acid.

Concentration of stearic acid [wt.-%]	Observations on layer formation and texture
50	<ul style="list-style-type: none"> • Crystallization starts only after the temperature has been decreased under the eutectic temperature. • Crystallization starts all over in the melt, not only at the wall.
60	<ul style="list-style-type: none"> • Minimum undercooling 9 K ($T = 51.9^{\circ}\text{C}$). Very close to eutectic temperature. • Holes are easily left in the formed crystal layer. • The layer is not compact, but a layer of snow like sludge.
70	<ul style="list-style-type: none"> • Complete crystal layer takes a lot of time to form, even with undercooling of 11 K ($T = 53.1^{\circ}\text{C}$). • The layer is not compact, but a layer of snow like sludge.
80	<ul style="list-style-type: none"> • At undercooling of 5 K the layer forms very slowly. When the undercooling is 7 K a complete layer forms in a relatively short time. • The layer is compact but soft.
90	<ul style="list-style-type: none"> • Crystallization on the cooling finger relatively easy. • The layer is compact but soft.

In order to validate the results experiments with myristic and capric acid were carried out in the equipment presented in Fig. 4.4.1. The torque of the scraper shaft was measured at different concentrations. The result of the torque measurement for crystallization of myristic

acid is shown in Fig. 4.5.7. It can be seen that at the moment when the scrapers start to grind crystalline material out of the layer the torque rises instantly. While the scrapers keep the layer at a constant thickness the growth rate at this point also remain constant. Therefore, also the torque remains constant from this point on, because the amount of crystals to be scraped off remains the same. It can be seen from Fig. 4.5.7 that the torque is higher when the concentration of the crystallizing component is higher. The reason is that the structure of the layer from a melt with a higher concentration of the crystallizing component is harder, as shown in Table 4.5.3.

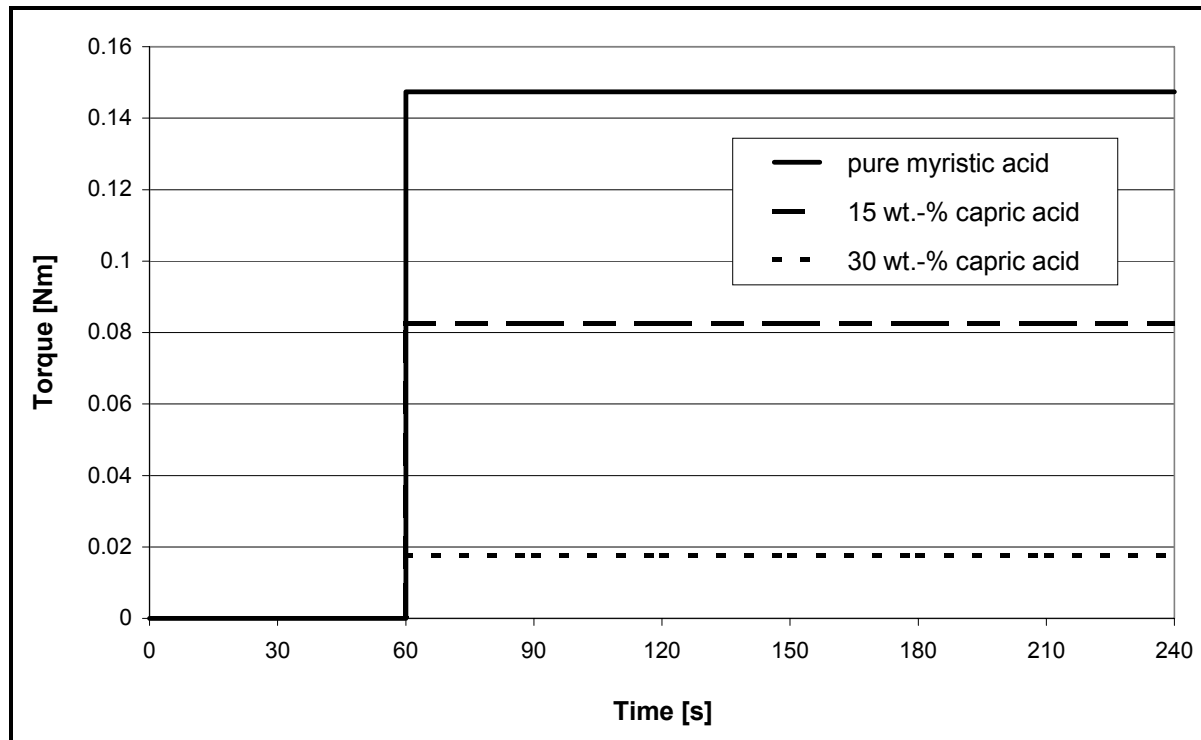


Figure 4.5.7 Torque during breakage of a crystalline myristic acid layer by scrapers.

5. Discussion

5.1 Discussion to Crystallization in the Tubular Heat Exchanger

The results presented in Chapter 4.2 give a first indication that a suspension melt crystallization process can be simplified to a circulation loop through a heat exchanger. However, in melt crystallization this requires careful adjustment of the process conditions, such as undercooling on the heat exchange surface, suspension density in the crystallizer, flow conditions and the concentration of the crystallizing component. Because of the more demanding conditions necessary for the successful operation in melt crystallization, the operation of such a process is somewhat more restricted compared to applications with solution crystallization.

In the tubular heat exchanger it was found that there exists a sharp concentration limit, above which the incrustation could no more be avoided at any applicable flow conditions. For the investigated compound system this limit was at 98 wt.-% of dmsO. Also the crystallization process itself seems to change at this concentration. At concentrations under 98 wt.-% of dmsO, crystals were observed to form all over the heat exchange surface. At higher concentrations, however, large deposits with dendritic growth form at locations apart from each other. Same type of growth has been reported on freezing of water pipes in winter [Loc94]. This limiting concentration depends on the compound system and on the surface material of the heat exchanger and is a limitation to the process of melt crystallization applying circulation through an ordinary heat exchanger.

As mentioned above, the crystals form all over the heat exchange surface, which is the coldest part in the system. The influencing factor by which the crystals are removed by the stream is the shear force on the tube wall. The shear friction created by the flow velocity in the dmsO-water system is shown in Fig. 5.1.1. The shear friction is calculated by the equation:

$$\tau = \frac{f \rho v^2}{2} \quad (5.1)$$

The friction factor, f , is found by iteration from the von Karman equation:

$$\frac{1}{\sqrt{f/2}} = 4.07 \log(\text{Re}\sqrt{f}) - 0.60 \quad (5.2)$$

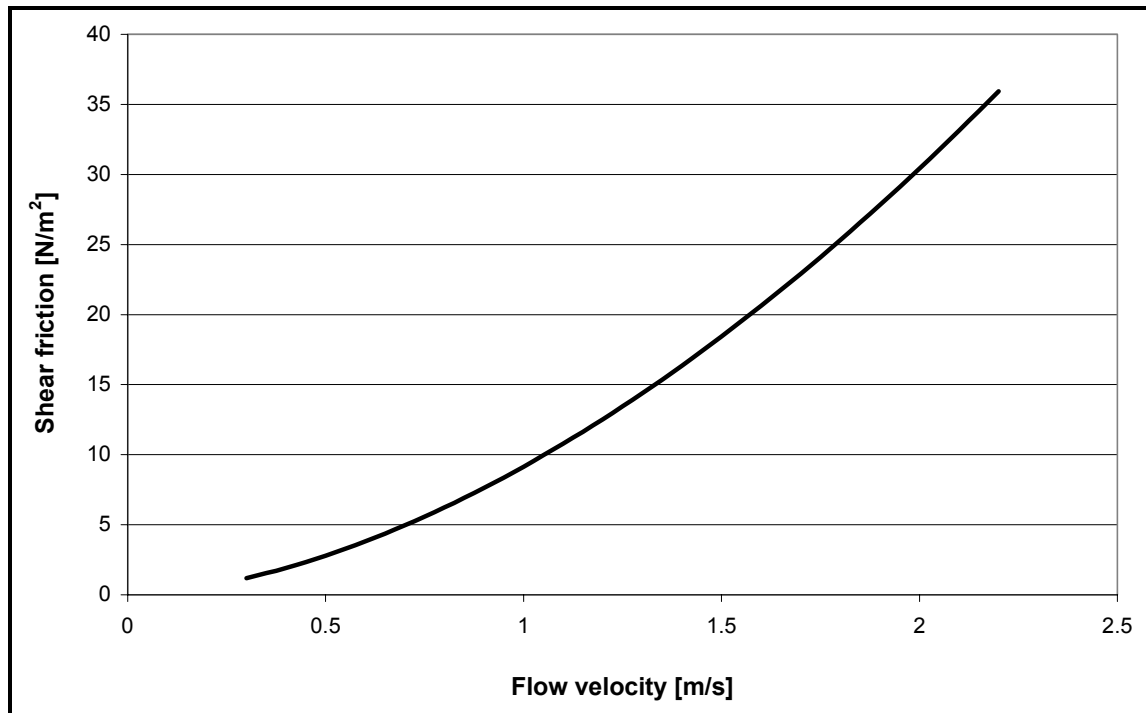


Figure 5.1.1 Shear friction on the tube wall due to the flow of dmso-water mixture.

It can be seen from Fig. 5.1.1 that the shear friction on the tube wall increases by the flow velocity. Comparing with Fig. 4.2.6, the shear friction at which the removal forces start to affect more strongly at the flow velocity of 1.5 m/s is approximately 18 N/m². The precise quantitative estimation of the shear friction is difficult, because the friction forming medium is a suspension, not a clear liquid. The shear friction depends also on the density and on the viscosity of the medium. The difficulty lies in the difficulty of the precise estimation of the suspension viscosity. The suspension viscosity could be estimated for example by the Einstein equation. However, this equation does not take into account the crystal size distribution, which can be very influential.

The solid fraction of crystals in the crystallizer loop at different temperature levels has been presented in Fig. 4.2.3. The crystals present in the stream increase the shear friction on the wall and induce a mechanical impact onto the surface. The higher the suspension density is the larger is also the specific crystal surface area in the crystallizer. This helps the crystalline material to grow on the crystal surfaces, which makes the growth on the heat exchange surface less probable. So, it is beneficial to run the equipment with a high suspension density of crystals. This is furthermore reasonable considering the productivity of the process. However, limitations to the suspension density are set by the conditions at the product output line, where the suspension flow velocity and the tube diameter often abruptly change. At such locations too high suspension densities can lead to blockage or classified product removal. It is interesting to see that with the investigated compound system high solid fractions can be obtained with a relatively small reduction of temperature. This has its cause in the phase diagram. Typical to many eutectic mixtures, the inclination of the liquidus line at high concentration of the crystallizing component is relatively flat. This means that a large change in concentration can be achieved by a relatively small change in the temperature. Near the eutectic point, on the other hand, the concentration would change only slightly, even if the

change in temperature was relatively large. The reason is that near the eutectic point the liquidus line is steeper.

From Fig. 4.2.5 it can be seen that the undisturbed operation of the process can be controlled by the right choice of the flow conditions and the heat flux through the crystallizer wall. The heat flux is governed by the temperature difference between the bulk streams. The bulk temperature difference and the flow conditions determine the temperature of the inner wall surface, which is one of the key parameters responsible for the formation of potential incrustations. It can be seen that the maximum temperature difference changes only slightly at flow velocities from 1 to 1.5 m/s and that the curve is almost parallel to the flow velocity axis. Of course the temperature at these conditions cannot be applied to a static suspension at zero flow velocity. Therefore, there must be a certain minimum flow velocity at which the maximum temperature difference is similar to that at flow velocities 1-1.5 m/s. This minimum flow velocity must be the limit to the total suspension conditions.

It was found that the incrustations leading to blockage always started to form at locations where the force needed to remove the growth sites was the highest (uprising streams) or at locations where particulate settling can be considered a problem (pipe connections with attachment sites for particles). So, it can be concluded that at these locations the adhesive forces on the surface were relatively stronger than the removal forces. The removal forces (shear stress due to the flow) can be increased by increasing the suspension density. The suspension density, on the other hand, can be increased by increasing the operational temperature difference or by increasing the residence time of the crystals. The temperature level in the crystallizer is usually fixed by the product recovery. Therefore, the only possibility to increase the suspension density is to increase the residence time.

The effect of residence time on the run time of the process has been presented in Fig. 4.2.6. There are two reasons for the beneficial influence of the increasing residence time: The increasing suspension density and the lower undercooling in the crystallizer loop. The lower undercooling is a logical result from the fact that the undercooling has more time to deplete onto the crystal surfaces.

The heat exchange in the tubular heat exchanger has been presented in Table 4.2.3 and Fig. 4.2.7. As can be seen from Fig. 4.2.7 a) the inner heat transfer coefficient increases steeply by increasing flow velocity, whereas the overall heat transfer coefficient increases only slightly. The increment in the inner heat transfer coefficient at flow velocities from 1.02 to 2.17 m/s is 83%, and that for the overall heat transfer coefficient 22%. It can be said that the flow velocity in the inner pipe has only a small influence on the overall heat transfer efficiency of the crystallizer. However, the increase in the inner heat transfer coefficient is very important for the whole process. Higher inner heat transfer coefficient means that the heat transfer from the inner surface to the crystal suspension is made more effective. The result is that the temperature difference between the inner heat transfer surface and the crystal suspension decreases, thus the undercooling on the wall decreases. This is beneficial in avoiding incrustations on the heat transfer surface. It follows that larger temperature difference between the bulk streams becomes possible (see Table 4.2.3). This larger temperature difference results in a higher amount of transferred heat and a higher heat flux as can be seen from Fig. 4.2.7 b).

It can be seen from Table 4.2.3 that the heat flux of the crystallization process is relatively high. At high heat flux incrustations tend to form on the heat exchange surfaces. It can be said that the high heat fluxes are the reason for the limitations in the process run time. The heat transfer surface to volume ratio for the investigated process was 144 m^{-1} , while it for jacketed vessels typically used for crystallization purposes is $2\text{-}8 \text{ m}^{-1}$. Despite this comparable large ratio the heat transfer surface was not yet large enough to totally fulfil the demands of the process. For a successful process construction the heat exchange surface should be further extended in order to reduce the heat flux density, which reduces the surface temperature difference.

The shear frictions and heat transfer coefficients discussed above refer to the average flow velocity of the stream. However, the membrane pump used for the circulation of the suspension caused a pulsating flow. The thrusts of the pulse result in repetitive peaks of higher flow velocities, followed by periods of flow velocities much less than the average. The high velocity peaks result in higher shear friction and mechanical impact, and are probably much more efficient in removal of incrustations as would be a steady flow of the same average flow velocity. A centrifugal pump with nearly constant flow was used in the equipment, but it was found inapplicable due to the high heat production. The heat production of the centrifugal pump was 69 W at a flow velocity of 1.45 m/s . This was too much compared to the heat production of the membrane pump, which was 29 W even at the higher average flow velocity of 2.17 m/s .

The crystal size distributions measured in the equipment were shown in Fig. 4.2.8. The relatively high undercooling at the beginning of the process causes the crystal size distributions measured after 10 and 47 minutes to be very near to each other. When the undercooling is at first high a lot of small nuclei are born and the crystal size remains small. After the suspension density in the crystallizer settles to a constant level the undercooling also settles to a lower value. At these conditions the crystal growth process wins on influence over nucleation and the crystal size increases. In the investigated process the increment in the crystal size was observed to happen at the 84 minutes after the formation of the first crystals.

Due to the relatively low allowable heat flux densities relative to competitive processes, industrial applications of the described process will always require large heat exchange surfaces. The large heat exchange surface can be a justified solution when the complex mechanical constructions can be replaced by cheap tube and shell heat exchanger structures.

5.2 Discussion of Pilot Plant Equipment

The crystals produced in the current work and by two alternative freeze concentration processes were shown in Fig. 4.3.4. It can be seen from Fig. 4.3.4 a) and Fig. 4.3.4 b) that the crystals produced in a growth tank have slightly better quality in terms of crystal habit compared to the crystals produced by the modified (simplified) process concept investigated in this work. It can be seen by the comparison of the pictures in Fig. 4.3.4 b) and Fig. 4.3.4 c) that the typical form of ice crystals from freeze concentration processes is a round plate. Special supplementary processes, such as the growth tank, are required to improve the crystal quality. The flat disc shape of the crystals with a spherical projection has already been reported by Huige [Hui72], who estimated the height to diameter ratio of the ice crystals to be 0.26. This might be the reason that some industrial surveys to apply wash column technology to freeze concentration have failed (e.g. [McK72]). However, the Niro wash column used in the pilot plant experiments has no problems to separate the platelet like crystals. Problems are encountered only with very small crystals caused by high undercoolings, which tend to escape through the filter in the wash column. Nevertheless, the crystals in Fig. 4.3.4 b) possess much more homogeneous and more rounded shape than those presented in Fig. 4.3.4 c). This clearly intends that the growth provided in the circulation loop improves the crystal quality in comparison to process where the crystals are just formed in a scraper.

The crystal size and the crystal size distribution depend on the undercooling (the supersaturation), the residence time and on the suspension density in the crystallizer. In this work it was found to depend to lesser extent on the scraper speed. The reason is that the mixing intensity in the crystallizer is in this case not influenced by the scraper, but by the product circulation pump. Unlike in vessel type crystallizers the mixing is through out the crystallizer loop homogeneous and intensive. Therefore, change in the pumping or scraper speed does not cause a significant change in the crystallizing conditions.

The results given in Table 4.3.2 and in Fig. 4.3.5 show that the crystal size at 90 minutes residence time is smaller than at 60 minutes. This is caused by the tendency of the nucleation rate to increase when the suspension density increases. At 90 minutes residence time the suspension density is higher than by 60 minutes residence time. The higher nucleation rate results also in reduction in the crystal growth rate, which explains the missing large crystals with the 90 minutes residence time. The reduction of growth rate is caused by the fact that the undercooling is at a longer residence time lower. If the nucleation rate is high the crystalline material also depletes the undercooling by forming small nuclei instead of increasing the size of the existing large crystals. The large amount of small crystals thus reduces the average crystal size from 149.8 μm at 60 minutes residence time to 131.8 μm at the residence time of 90 minutes. When the nucleation rate is higher the supersaturation is also divided onto a larger number of crystals, thus the maximum crystal size will be reduced. In addition to the increased nucleation rate the crystal breakage in the crystallizer at longer residence time and at larger suspension density is more severe. The crystal breakage occurs predominantly at the largest crystal sizes due to the higher kinetic energy of collisions, which on its part offers an explanation to the missing large crystals at the 90 minutes residence time.

All the distributions presented in Fig. 4.3.5 are somewhat bimodal when presented as number based distributions. There is a larger amount of small crystals, a drop in the number of crystals, and then the main peak. The amount of crystal nuclei produced must be of course enormous compared to the amount of macroscopic crystals. It seems that part of the smaller crystals disappear during their way in the crystallizer loop. This happens probably by melting away in the product circulation pump. The amount of small crystals is thereby reduced, which causes the drop in the distribution curve before the main peak. The smallest crystal taken into the CSD analysis has been the size of 25.4 μm . This is due to the picture quality, which does not allow accurate detection of smaller sizes. With the imaging software used for the analysis (Optimas 6.2) the limiting size in this case would be about 3 microns.

The growth and nucleation rates are estimated using the population balance technique developed by Randolph and Larson [Ran88]. The results of the population balance calculations are presented in Fig. 5.2.1 and Table 5.2.1. In the calculations the shape of the ice crystals is assumed to be the same as described by Huige [Hui72], which results in a volume shape factor of 0.20. In Fig. 5.2.1 the linearization of the data series of the 90 minutes residence time overlaps with that of the 30 minutes residence time and is not shown.

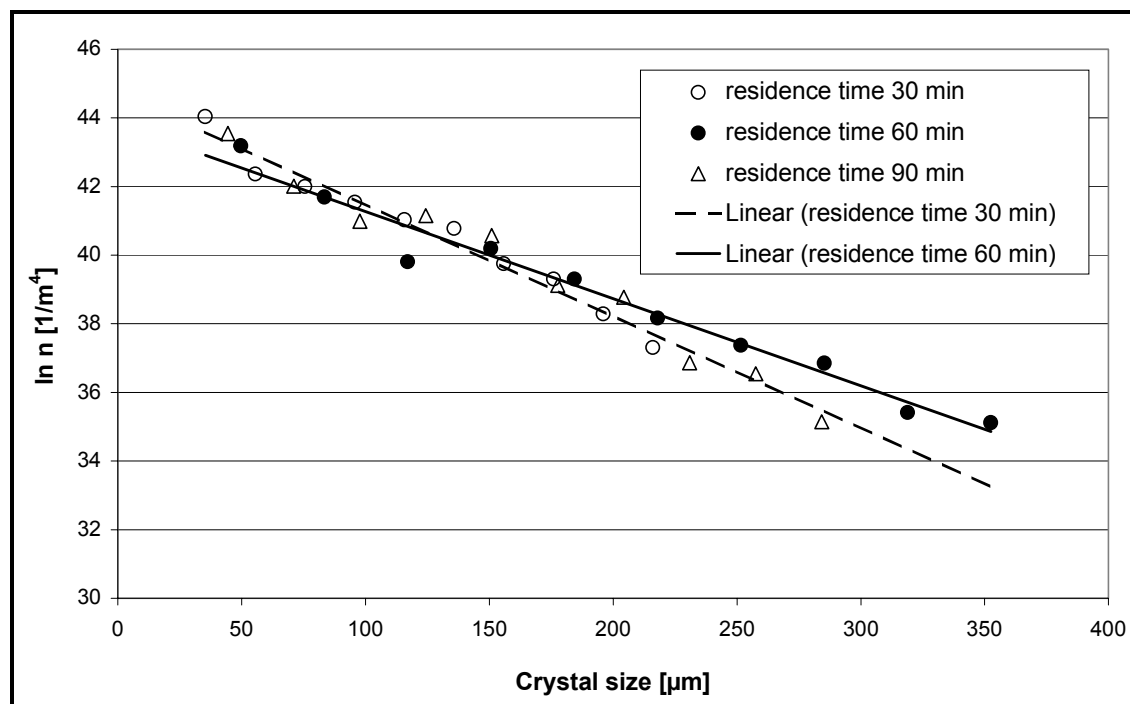


Figure 5.2.1 Population density plot of ice crystals from the pilot plant experiments.

Table 5.2.1 Growth and nucleation rates in the Niro pilot plant.

Residence time [min]	Growth rate $\cdot 10^8$ [m/s]	Nucleation rate $\cdot 10^{-11}$ [1/m ³ s]
30	1.70	4.61
60	1.09	1.17
90	0.57	1.66

The growth rates presented in Table 5.2.1 show that the growth rate for the 90 minutes residence time is much lower than for the shorter residence times. This explains the reduction in the average crystal size by this residence time. However, the size reduction is assumed to occur due to increased breakage in the crystallizer. This assumption makes the MSMPR assumption of the crystallizer invalid. Therefore, also the population balance method for the calculation of the kinetic data is not reliably applicable. In this case the kinetic data presented in Table 5.2.1 for the 90 minutes residence time has to be considered inaccurate. In reality the growth rate must be higher, which results in a higher nucleation rate. This, again, is in good agreement with the former conclusion that the reduction in size at 90 minutes residence time is caused by increased breakage and increased nucleation at a higher suspension density. From the obtained results it can be concluded that for the sugar-water system the optimum residence time is around 60 minutes.

In Table 2.4.1 three heat exchange correlations, those by equations 2.5, 2.15b and 2.18-20, are developed for crystallization conditions for ice. However, it can be seen that the equation 2.5 contains temperatures not measurable in the pilot plant equipment. The correlation was also developed for a different type of an SSHE equipped with rigid knives. On the other hand, the equations 2.18-20 neglect the effect of the SSHE scraper rotational velocity. The reason for this can be found when the process for which the correlation was developed is observed in detail. The correlation developed by de Goede [deG99] has been made for an SSHE, where the scrapers are pressed on the heat exchange surface by springs. In this construction the scrapers rotate relatively slow compared to a votator type SSHE. Also in the process of de Goede there was no votator type rotator shaft, which would have left a narrow gap for the liquid between the votator and the heat exchange surface. Based on this it can be concluded that the equation 2.15b is the correlation to be used in the case of the Niro pilot plant SSHE.

The inner heat transfer coefficients for sugar-water and dmsowater calculated by the correlation 2.15b are shown in Fig. 5.2.2.

From Fig. 5.2.2 it can be seen that at rotational velocities over 100 rpm the heat transfer coefficient shows nearly linear behaviour. It can also be noticed that the correlations predict a zero heat transfer coefficient for zero rotational velocity. This surely does not represent the real heat transfer coefficient at such conditions. However, it can be assumed that the correlation gives reasonable values for the rotational velocity 25 rpm, which is the minimum rotational velocity of the used equipment, and for all the rotational velocities higher than that. The presumption in the use of the chosen correlation is that the axial flow velocity is negligible. If the inner heat transfer coefficient is calculated for the SSHE assuming turbulent axial flow and neglecting the scraper rotation, the heat transfer coefficient for sugar-water will be 1194 W/m²K and that for dmsowater 921 W/m²K. The values above are calculated by the Dittus-Boelter equation for an axial flow velocity of 1.5 m/s. If the axial flow velocity is considered negligible when the heat exchange coefficient from the correlation 2.4.15b (influence of scraper rotational velocity) is ten times higher than the value calculated by the Dittus-Boelter equation, great difference in the investigated compound systems can be noticed. For the sugar-water system the above-mentioned heat transfer coefficient is reached at the scraper rotational velocity of 180.5 rpm. With the dmsowater system, however, a

scraper rotational velocity of 768.3 rpm would be necessary. So, for the dmso- water system the axial flow

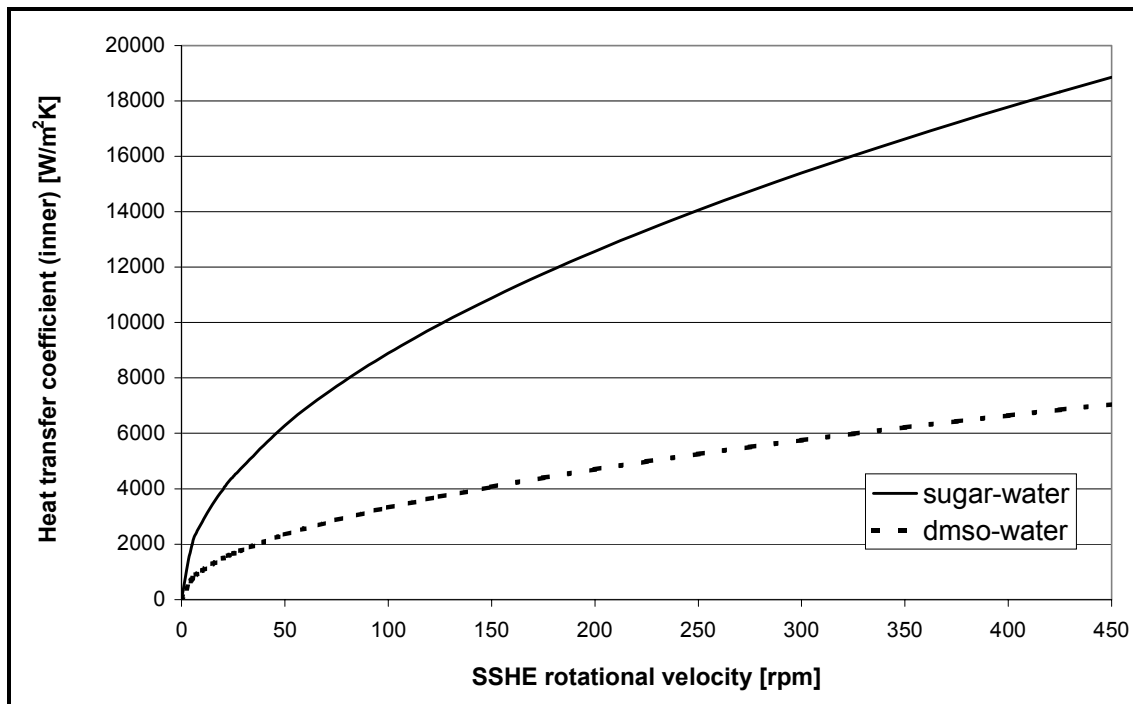


Figure 5.2.2 Inner heat transfer coefficients calculated with correlation 2.15b. Axial flow velocity 1.5 m/s.

velocity has a much greater influence than for the sugar-water system. The different behaviour of the compound systems is due to the relation of the Nusselt numbers of the rotational and axial velocity correlations. For sugar-water this relation is 20.6, clearly emphasizing the rotational velocity influence, whereas it is for dmso-water 10.0. The reason for this is that in the correlation 2.4.15b the Prandtl number is raised to the power of 0.45 and in the Dittus-Boelter correlation to the power of 0.33, whereas the scraper Reynolds number is raised to the powers 0.8 and 0.5, respectively. As a result, when the influence of the Prandtl number on the heat transfer coefficient increases, the increment of the heat exchange coefficient for the compound system with a lower Prandtl number will be relatively smaller.

It can be seen from Fig. 4.3.10 that when the PCP rotational velocity is low (under 200 rpm) an increment in the PCP velocity has a very small influence on the amount of heat produced into the crystallizer. This shows that at low PCP velocities the heat production is mostly due to the SSHE. On the other hand, when the PCP rotational velocity rises (over 300 rpm) heat production values with different SSHE velocities approach each other. This suggests that at these conditions the heat production is mostly due to the PCP.

A fitting of the measured data shown in Fig. 4.3.9 and Fig. 4.3.10 was made, which resulted in the following correlation for the black loss:

$$Q [W] = (1.429 N_{SSHE}) + (0.0217 N_{PCP}^2 - 5.792 N_{PCP} + 996.479) - 304.475 \quad (5.2.1)$$

From Fig. 4.3.11 it can be seen that the heat production with the two compound systems used (sugar-water and dmso-water) differ remarkably. This is caused by the difference in the

physical properties of these two systems. While the viscosity of the sugar-water system at 15 wt.-% of sugar at the used crystallization temperature is 17.3 mPas, the viscosity of dmsu at the corresponding temperature is only 2.5 mPas. This causes the Reynolds numbers for the case of dmsu-water to be higher than for the sugar-water system. This again influences the power number of mixing to be lower in the case of dmsu-water, in which case also the energy dissipation rate is smaller.

Whether there is a maximum net heat flow when the scraper rotational velocity is increased depends on the overall heat transfer coefficient. The inner heat transfer coefficient increases steeper by increasing rotational velocity of the scraper than does the heat production. The steepness of the development of the overall heat exchange coefficient by increasing rotational velocity depends on the outer heat exchange coefficient. The heat transfer coefficient at the outer side does not depend on the axial or radial velocities at the inner side and it can be considered to be constant. Therefore, it suppresses the growth of the overall heat transfer coefficient as the scraper rotational velocity increases. A calculation based on the inner heat transfer coefficient using correlation 2.4.15b and equation 5.2.1 gave the outer heat transfer coefficient. For the investigated range of scraper rotational velocities the maximum net heat transfer was found at the maximum scraper speed of 450 rpm, and was found to be 4350 W/m²K. The outer heat transfer coefficient was estimated by the Dittus-Boelter correlation (Eq. 4.2.3), assuming the flow of the cooling medium was turbulent. Here must be mentioned that exact calculation on the outer side was not possible due to variable operational pressures and temperatures at the outer jacket, and the unknown flow conditions. The net heat transfer based on the calculation above is presented in Fig. 5.2.3.

It can be seen from Fig. 5.2.3 that for all the cooling medium flows presented the net heat flow rises first fast by increasing scraper rotational velocity, reaches its maximum and starts to decrease slowly. Fig. 5.2.3 also shows how the outer side heat transfer coefficient effects the net heat flow. For the outer heat transfer coefficient of 589 W/m²K the net heat flow reaches a maximum of 813 W at 50 rpm and reduces 60% until 450 rpm. For the outer heat transfer coefficient of 2136 W/m²K the heat flow reaches a maximum of 3950 W at 225 rpm, and reduces only 3 % until 450 rpm.

The results over heat exchange coefficients with the results over minimum scraper speed necessary indicate that rotational velocities over 250 rpm are unnecessary. Based on the results obtained in this work the scraper rotational velocity should be chosen to be at the range 150-225 rpm. The development of the temperatures and the undercooling are similar to those presented in Fig. 4.2.3 (Chapter 4.2). When the temperature in refrigerant side of the SSHE is set to the final temperature at the start of the process, the temperature difference to the liquid inside the crystallizer is first high. This temperature difference results in a high driving force for heat transfer, which causes the rate of temperature change inside the crystallizer to be high. At a fast cooling rate the temperature in the crystallizer reaches lower temperature before the kinetics of nucleation result in formation of a suspension than in the case of a low cooling rate [Täh99]. After the formation of a crystal suspension the undercooling can deplete on the crystal surfaces, thus after this point the undercooling in the crystallizer is lower. Therefore, the temperature on the cooling medium side should be decreased slowly to the final operational level in order to apply the minimum scraper rotational velocity.

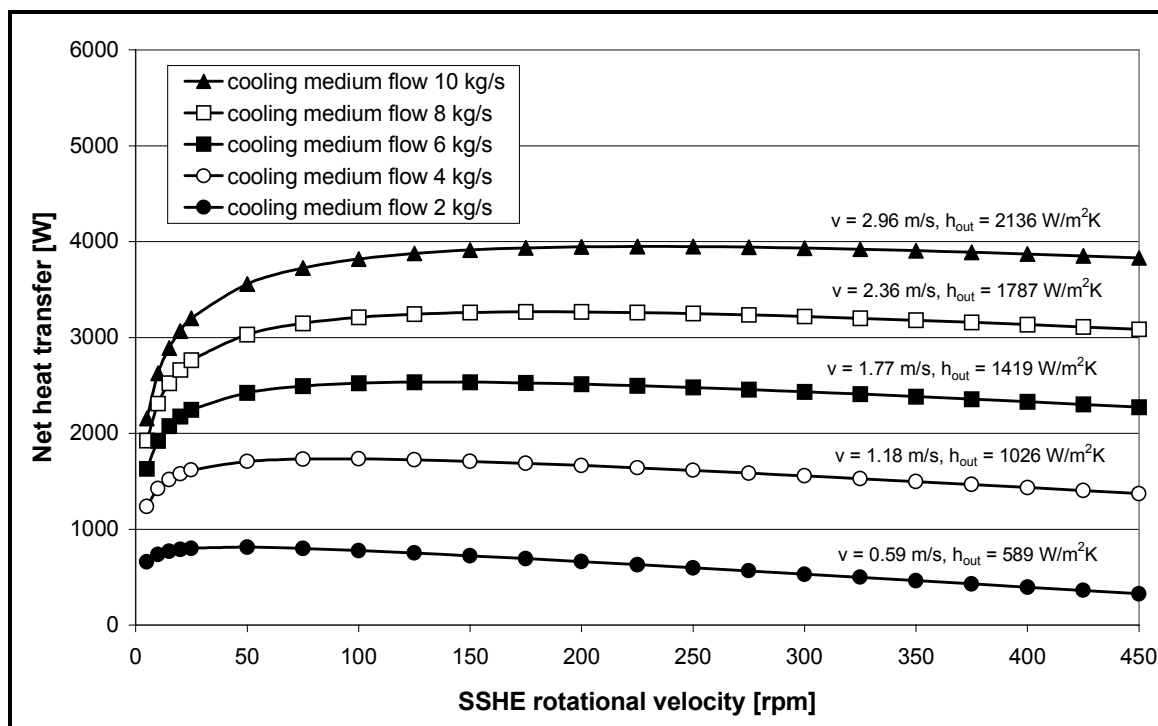


Figure 5.2.3 Net heat transfer at different cooling medium flow rates. Axial flow velocity in the inner pipe 1.5 m/s.

The experiments show that the equipment can be run with high suspension densities up to 40 wt.-% solids (see Fig. 4.3.3). However, when the solid fraction approaches 50 wt.-%, it comes more and more often to blockage in the wash column inlet line. In planning such equipment the suspension density in the crystallizer should, therefore, be designed to be approximately 40 wt.-% solids. This way the productivity per unit volume is maximized and the crystallizer volume can be minimized.

As final conclusions to the experiments with the pilot plant unit, it can be said that the modified construction, where the growth tank is replaced by continuous circulation of the suspension through an SSHE, works very well. The crystal quality from the growth tank can be assumed to be slightly better than that from the process investigated in this work, because of the narrower CSD. However, the shape and habit of the crystals grown in the circulation loop is comparable to that obtained from a growth tank. With the investigated compound system sugar-water the wash column has no difficulties in full separation of the pure crystals and the impure mother liquor. A narrower CSD might be beneficial in cases where the removal of impurities is more difficult, e.g. with multiple impurity components or even higher viscosities. The experiments with the second compound system dmsu-water prove that the process can, in addition to ice crystals, be applied to the purification of chemicals.

5.3 Discussion on Laboratory Scale Suspension Melt Crystallization

The crystal shape and size from melt crystallization are commonly not an important factor considering the product specifications of the final product, since the chemicals produced by melt crystallization are often marketed as liquid. The crystal size and shape are, however, important for the further process steps following suspension melt crystallization, most important of them being the solid-liquid separation.

In the optimization of particle characteristics for the solid-liquid separation the most important task is to minimize the particle surface area. This way the impure liquid attaching on the crystal surfaces will be minimized. The minimization of the particle surface is introduced by increasing the particle size, smoothening the particle surface or changing the particle geometry. In addition to considerations over single particle, even more important is how these characteristics apply to the whole particle population. These are characterized by the particle size distribution and distribution of the particle shape.

The particle characteristics can be influenced by the process conditions in the primary crystallization process. However, the choice of conditions according to the particle characteristics is often restricted, because of other demands on the process (phase behaviour, productivity etc.). Therefore, the particle size and shape are sometimes improved using secondary growth processes, like ripening, agglomeration or growth in additional tanks.

The particle size and shape analysis was made from two-dimensional images. Therefore, considerations over three-dimensional particle form cannot, be made based on the results presented in Chapter 4.4. The particle characteristics analyzed in this work, however, can be compared to each other.

5.3.1 Particle formation in laboratory scale SSHE

The experiments with the laboratory scale SSHE were made using mixtures of myristic and capric acid. Modest undercoolings (3.1-3.8 K for myristic acid and 5.4-5.6 K for capric acid) were used on the heat transfer surface, at which a crystalline layer was formed. The choice of the undercoolings had to be made according to practical considerations over the suspension density in the observation chamber. The suspension density was not allowed to grow too high, otherwise the observation of single crystals through the glass window on the bottom of the chamber would have been impossible. Therefore, a temperature balance between the glass window and the cooled wall had to be found, in order to get suitable amount of crystals to the observation area without melting the crystals before they were photographed. The required undercoolings for the layer growth are relatively small (compare Chapter 4.5) and it can be assumed that the layer growth starts unevenly. However, the scrapers were set at 3 mm distance from the heat exchange surface, which allows the layer growth to smoothen before the scrapers start to remove crystals into the suspension.

The quantitative comparison of the results obtained by crystallization of myristic and capric acid is difficult, because of the different undercoolings applied in the experiments. The

different undercoolings were necessary due to the different growth rates and different tendency of undercooling of the melt.

Two different types of crystal shapes were observed in the crystallizer chamber. Some of the crystals possessed a regular shape. These are the crystals grown in the crystal suspension from nuclei or small crystals scraped from the layer. Usually the fatty acid crystals grown in suspensions are reported to have shapes like needles growing in spherical clusters [Bre99a]. The reason for the regular growth form in this work is the moderate undercoolings on the heat exchange surface and the insulating crystal layer, which result in a small undercooling in the bulk melt. The growth of crystals in the melt and the change in crystal shape presented in Fig. 4.4.7 can be well seen in photographs shown in Fig 5.3.1.

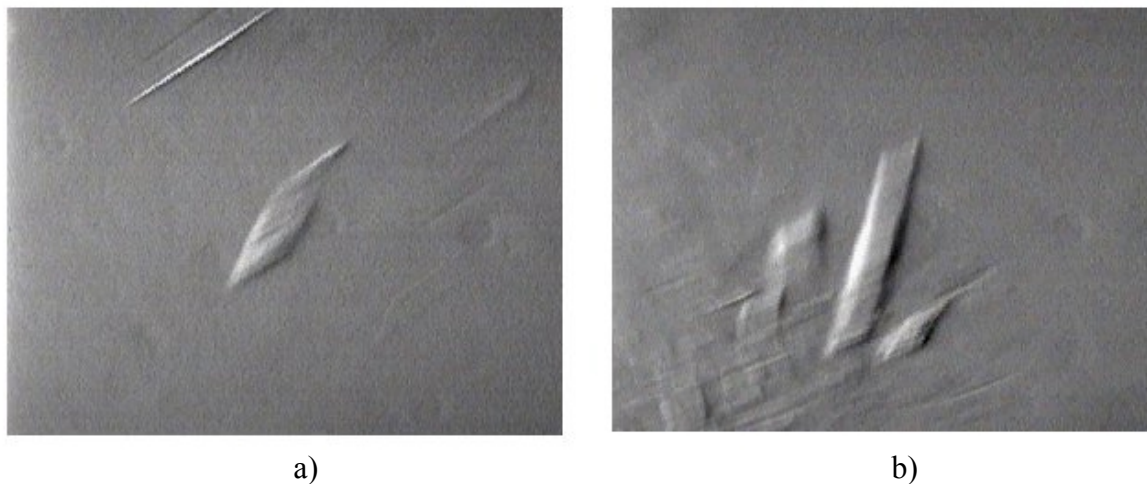


Figure 5.3.1 Crystallization of myristic acid: a) crystal shape 3 minutes after start of crystallization, b) crystal shape after 6 minutes.

It can be seen from Fig. 5.3.1 that the basic form of the crystals is the same, but the crystal after 6 minutes is prolonged in its shape. Both crystals possess a regular shape typical for crystals grown in a suspension.

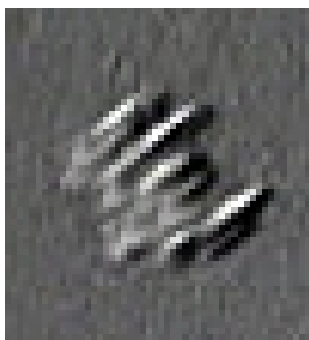


Figure 5.3.2 Crystal broken out of myristic acid layer.

The other type of crystals observed in the experiments is that of an irregular shape. A crystal, which shows typical characteristics for a particle broken off from the crystal layer, is shown in Fig. 5.3.2.

Whereas the crystals broken off from the crystal layer possess a random, irregular shape, the crystals growing in suspension gradually get a more regular shape. The typical forms of crystals in suspension growth usually get shapes with geometrically defined even faces (as shown in Chapter 4.4.2). This means that the perimeter becomes smooth compared to irregular crystals and the shape resembles more that of a sphere. In two dimensional case the projection resembles more the shape of a circle and the circularity approaches unity.

Considering the effect of the scraper rotational velocity on the particle size it was stated in chapter 4.4.1 that the decreasing particle size by increasing rotational velocity has its cause in

the fact that the layer has less time to grow between two scraping actions, and thinner stripes are scratched out of the surface. Another effect can also be considered to cause a similar result: The impact force of the scrapers by higher scraper velocity is larger, breaking the crystal layer easier. At lower rotational velocity the lower impact force proceeds deeper into the crystal layer before a location is found, which is weak enough to be broken. On the contrary, at higher rotational velocity the higher impact breaks the crystal layer already near the surface. This can be considered to be the reason for the result presented in Fig. 4.4.5. At rotational velocities of 7.4 and 11.6 rpm no significant difference can be seen. When the rotational velocity is increased to 14.4 rpm a totally different type of CSD was produced. It can be assumed that the inner structure of the layer is formed from grain boundaries, which break under mechanical stress (breakage at lower mechanical impact). When the intensity of the mechanical impact grows, at certain limiting force the crystal layer is broken close to the surface inside the grain boundaries. Such crystalline structure of layers formed at crystallization of fatty acids has been reported by Brendler and Tiedemann [Bre99b]. This phenomenon depends, of course, on the ductility of the crystal layer. The harder and more ductile the layer, the more the impact force influences the crystal size. If the layer is soft, the layer is rather cut at the point of the scraper. It can be said that the fatty acid layers show tendency to break more according to the latter mechanism. This is indicated by the lack of large number of small particles typical for fracture processes, e.g. comminution.

Because the scrapers are not pressed against the crystal layer on the heat exchange surface, the scrapers can have influence on the deeper layers of the layer only through the crystalline material itself. Therefore, the direction of the tension stress given to the layer also determines the direction of the fracture. When the fracture (preceded by the tension stress) moves in a steeper angle into the crystal layer it will affect the crystalline layer deeper. Thereby, larger particles will be cut off from this layer. This phenomenon for the crystallization of myristic acid can be seen from Fig. 4.4.8. The larger crystal size at steeper angle of the scrapers is due to the deeper impact resulting in crystals with more equal axial dimensions. With a small angle the impact depth remains small resulting in thin stripes.

5.3.2 *Crystal growth in suspension*

The free growth of crystals in a suspension was carried out in a much more lower undercooling than the experiments made in the scraper chamber. The undercoolings used in the crystallization of p-xylene were 0.13-0.68 K during growth and 0.74 K during nucleation. At the formation of crystals at the initial undercooling of 0.74 K a large amount of crystals were formed, and the shape of the crystals was rounded at the corners. Therefore, it is assumed that the source of secondary nucleation in this case was the small nuclei resulting from the abrasion at the crystal corners. This gives an indication that the p-xylene crystals are hard and ductile, which makes the corners break under mechanical impact. In this case nucleation cannot be avoided, no matter how small the undercooling is. This can be seen from Fig. 4.4.13.

Under the controlled growth conditions the crystals grow in a very regular shape. This can be seen from Fig. 4.4.12, where the average aspect ratio and circularity get both values of about 0.7. This can be compared to the form factors from the scraper experiments where the form factors get average values from 0.2 to 0.5. The reason for the regular growth is the low undercooling used during the growth period.

The filtration experiments show that the solid-liquid separation by cake filtration is not very effective method for melt crystallization. The purity of the filtrated crystals is found to depend on the mother liquor concentration, as can be seen from the increasing purity by increasing p-xylene concentration of the melt in Table 4.4.2. Although the specific crystal surface of grown crystals is smaller than the specific surface area of the crystals formed at the beginning of the crystallization process, the filtration result is worse. In addition to the larger mass of crystals, which makes the filtration more difficult, the worse filtration result is caused by the platelet shape of the large crystals blocking the flow of the mother liquor out of the cake.

5.3.3 *Secondary growth of ice crystals*

The experimental results show that ice crystals agglomerate to large spherical particles as presented in Fig. 4.4.14. It suggests an effective method to remarkably increase the size of ice crystals in a short time. However, the problem is that impure liquid is always left entrapped inside the agglomerate. Such entrapped liquid is hard to remove during solid-liquid separation. If the solid-liquid separation is done by filtration, it can be assumed that the removal of the liquid attached onto the surfaces of the large spherical agglomerates is much easier than the removal of the liquid attaching on small crystals. In this case the final purity would probably be higher. On the other hand, if the aim is a very pure product wash column technology is commonly used. In such case the agglomerates are undesirable, and the entrapped liquid can deteriorate the separation affect.

The method of agglomerating ice crystals to form larger particles cannot be applied effectively simultaneously to formation of new crystals. Simultaneous formation of single crystals and agglomerates would necessitate an extra classification procedure, if the agglomerates were to be collected as product. At low undercoolings it is possible to produce agglomerates without formation of new single crystals. The same is true for the ripening processes. Therefore, in continuous processes an extra vessel for the secondary growth phenomena is needed. In batch processes the extra process can be carried out as a secondary process step in the same equipment. Therefore, the improvement of particle characteristics is always combined with additional investment cost, and the benefits of improved particle properties have to be considered from the viewpoint of overall process economy.

5.4 Discussion to Layer Growth Experiments

Formation of crystalline layers on the heat exchange surfaces is applied in certain types of scraper surface crystallizers. The SSHE applications, which include layer growth, are commonly used in crystallization of highly viscous mixtures. In such cases the high rotational velocities required for keeping the heat exchange surfaces clean would result in too high energy inputs by the rotating blades.

For an economical operation of such processes the crystalline layer should form evenly over the whole cooled surface. With short induction time the crystal layer forms all over the cooled surface at approximately the same time. If the time of growth between different areas in the crystal layer differs greatly, there might be gaps left in the crystal layer.

It is clear that higher undercoolings on the heat exchange surface result in shorter induction times for crystal formation. This is presented in Fig. 4.5.4 and Fig. 4.5.5. On the other hand, higher undercooling also results in a faster layer growth rate. The faster growth rates can cause dendritic growth of the layer through surface instability and inclusions trapped inside crystals through kinetic effects. This might effect the final purity of the crystals produced by the SSHE. The purity of the layer itself is actually not important in this case. The purity of the particles broken off from the layer is the decisive factor for the final product purity. The layer can be porous, but if there are no inclusions inside the crystals grown in the layer, the particles formed by the SSHE are usually pure. However, if the particles broken out of the layer are large enough, the porous structure with including impure melt may be carried on to the suspended particles.

The demands on the particle size from such a process can vary remarkably. Sometimes an SSHE is used solemnly for production of small crystals and nuclei for growth in the further process steps. In some applications the crystalline product scraped off from the layer is immediately the crystalline product to be separated by solid-liquid separation. In addition to the other process parameters, this sets different demands on the layer structure. If the particles broken off from the layer are the final product a layer with a hard structure is needed. In this way the particles produced will not be broken or deformed in the suspension so easily. In this case, also the particle shape and size can be better controlled by the process parameters. If particles formed by the SSHE are allowed to be very small, the layer texture is unimportant and the scrapers can be set to break the crystals to a very small size.

As can be seen from Fig. 4.5.4 the induction time for crystal formation in crystallization of myristic acid starts to rise steeply when the undercooling on the surface is reduced below 7 K. For the crystallization of stearic acid, presented in Fig. 4.5.5, the rise in the induction time, and even more clearly in the time needed for the formation of a complete layer, takes place at approximately the same undercooling. It can be assumed that due to the similarity of the investigated substances the crystallization behavior of myristic and stearic acids is very similar. Based on the obtained results the undercooling on the heat exchange surface with myristic and stearic acid should not be lower than 7 K. This can be noticed to be larger than the undercoolings used in the laboratory scale SSHE experiments presented in Chapter 4.4.1. The undercooling in the laboratory scale SSHE was limited to the range 3.1-3.8 K, because of the practical limitations in the suspension density due to the microscopic observation.

The broken line in Fig. 4.5.4 shows the conditions, at which the crystallization in the case of no heat input in the middle starts in a suspension, instead of crystallizing on the cooled surface like in other cases. This suggests that at low undercoolings the nuclei are not attached strongly onto the heat exchange surface, but are able to be transported by convection into the bulk melt. If the bulk melt is undercooled the crystal growth takes preferably place in the melt, because the free surface area of the suspended nuclei is much larger than of those attaching on the heat exchange surface. This causes the undercooling to be released faster on the suspended particles, which abets the growth in the suspension compared to that on the surface. When the suspension density and the particle size increase the mobility of the crystals is hindered and the colder temperature at the vicinity of the heat exchange surface wins on influence. Therefore, an incrustation on the heat exchange surface forms after the crystals have grown to a macroscopic size.

It can be seen from Fig. 4.5.4 that the induction time with heat input in the middle of the mixed melt is shorter than that without heat input. The reason for the effect of extra heating might be the directed temperature gradient in the melt, which increases the mass transfer towards the cooled surface. In the melt with no heat input the temperature of the melt changes by random convective fluctuations. It is possible that without heat input in the middle small crystalline clusters and nuclei are formed earlier on the cooled surface and transported to the bulk melt by convections. This assumption is supported by the result that at low undercooling the crystallization actually starts in the suspension. However, at higher undercoolings the colder temperature on the heat exchange surface produces a higher crystal growth rate, and the crystals on the surface reach faster a stable macroscopic size. Thus, there is a limiting undercooling at these conditions, at which the crystallization starts on the cooled surface. At the experimental conditions presented in Fig. 4.5.4 this limiting undercooling was 6 K.

The qualitative observations over the compactness of the layer given by Table 4.5.3 give an indication over the layer structure. If the crystalline layer is very soft it can be assumed that it consists of a lot of liquid in it. This means that the layer is very porous and the solid material is held together with crystalline bridges, which are easily broken under mechanical impact. In melt crystallization the heat transfer effects usually take place faster than mass transfer. Therefore, by increasing concentration of the secondary component more and more liquid is trapped into the proceeding crystal layer. When the concentration of the crystallizing component is higher the crystallinity increases and the structure of the layer gets harder and less porous. Based on the obtained results it can be said that the concentration of the crystallizing component must be at least 80 wt.-% in order to get a compact crystal layer from the investigated compound system. From Fig. 4.5.7 it can be seen that a myristic acid layer crystallized from a mixture with 30 wt.-% capric acid offers only a very small resistance to the mechanical removal, which means that the layer is very soft. The torque with capric acid concentration of 15 wt.-% is already 4.7 times higher and the torque with the pure myristic acid layer 8.3 times higher.

In the crystallization from a static melt on a cooled finger no detectable purification was observed during the crystallization of stearic acid from its mixture with myristic acid. This is due to the large amount of inclusions left on the porous layer. This makes clear that the macroscopic layer growth rate is different to the production rate of the pure product. The layer

growth rate can be fast, but, however, if the porosity of the layer is high the amount of pure crystals produced will be small. Therefore, it is advantageous to produce as compact layers as possible, even when the layer purity itself is not an important factor.

It can be concluded that the crystal formation on cooled surfaces can be influenced by the process conditions: By undercooling on the cooled surface as well as fluid dynamics and heat input in the bulk melt. The layer structure is strongly influenced by the concentration of the crystallizing component. It can also be concluded that the layer crystallization does not offer an applicable method for the separation of fatty acid mixtures, but further growth in a suspension is necessary in order to produce pure crystals.

5.5 Conclusions and Outlook

5.5.1 Conclusions

In this work it has been shown that a crystallizer construction, where the suspension is continuously circulated in a pipe through a heat exchanger, is suitable for fractionating a melt or an aqueous solution to pure crystals and concentrated mother liquor. This allows a crystallization process without any use of an agitated crystallizer vessel. In this case a compromise is made between the crystal quality and the equipment costs. Applying state of the art techniques for the solid-liquid separation allows this compromise due to the lesser demands put on the crystal size and shape for an efficient separation.

The circulation of the suspension in a pipe makes it possible to deal with crystalline deposits with the aid of flow conditions. The deposit removal forces, resulting mostly from the shear friction at the solid-liquid interface, can be influenced in a pipe flow by the axial flow velocity. With a careful choice of process parameters, crystallization can be carried out using common tubular heat exchangers. By using standard heat exchanger constructions further cost reduction of suspension melt crystallization processes becomes possible.

The use of tubular heat exchangers was investigated in a bench-scale double-pipe heat exchanger. It was found that the maximum temperature difference over the heat exchanger wall applicable in the equipment depended on the axial flow velocity. This dependence followed an exponential curve. A certain minimum flow velocity was found to exist, at which the removal forces start to allow larger temperature differences. In this work the limiting flow velocity was found to be 1.5 m/s. However, the bulk temperature differences applicable in a tubular heat exchanger are small (in this work under 5 K), which makes large heat exchange surfaces necessary in order to obtain sufficient production rates.

Higher temperature driving forces are obtained by applying a scraped surface heat exchanger. Experiments were carried out in pilot-plant equipment on an industrial scale equipped with a combination of scraped surface heat exchanger and circulation loop for crystal growth. It was found that very low scraper rotational velocities (down to 25 rpm) were sufficient to keep the heat exchange surface clean of crystals, when the initial peak of high undercooling at the start of the process was avoided by cooling the process liquid slowly to the crystallization temperature.

The experimental results from a laboratory scale scraped surface crystallizer showed that it is possible to control the size and the shape of the product crystals by adjusting the scraper parameters. However, the effect of the scraping action also depends on the properties of the compound system and can be different for different components.

The results from the experiments with crystals grown freely in a suspension show that not only the size, but also the shape of the crystals has a considerable effect on the efficiency of the solid-liquid separation. The shape of the crystals can be influenced positively by secondary growth mechanisms, which was shown by the example of agglomeration of ice crystals.

The formation of crystalline layers on heat exchanger walls was examined using a cooled glass surface. It was found that the kinetics of layer formation were governed by the

undercooling and the fluid dynamics, whereas the structure, in the case of the compound system investigated (stearic acid-myristic acid), was strongly influenced by the concentration of the crystallizing component. The force necessary for breaking crystalline particles from a layer was found to depend on the layer structure.

This work has shown that melt crystallization can be carried out in a tubular heat exchanger, and that avoiding the use of agitated vessels is possible using a circulating loop. On the other hand, it was also shown that such applications set limitations on the chosen process variables and the final quality of the product crystals. The interdependence of growth of crystalline layers and the characteristics of the particles broken off from such a layer was shown, as well as the influence of the particle detachment process and growth in the suspension on the final particle properties. The knowledge gained from the laboratory scale scraped surface crystallizer provides a basis for adjusting process conditions and equipment construction in processes making use of scrapers suspending crystalline material from grown layers.

5.5.2 Outlook

Future research should concentrate on the further investigation of the use of circulation loops for crystallization, the aim being replacement of large agitated vessels. The use of heat exchangers on the circulation loop must be further examined, in order to assess whether tubular heat exchangers are applicable to wider use within industrial crystallization processes. The installation of standard heat exchangers with large heat exchange surfaces would be necessary to overcome the disadvantage of low temperature driving forces. Incrustations on the heat exchange surface is a constant problem, therefore, combining cycle loops for crystallization with direct cooling methods should be investigated.

There exist various theoretical models for the attachment forces between particles and surfaces based on molecular level interactions. For deposit removal in melt crystallization the forces between crystalline material and a cooled surface should be investigated with respect to the external variables, such as undercooling and fluid dynamics. Combining these to a model together with the removal forces of a flowing stream would give a first indication over the conditions at which growth of a deposit on a surface can be avoided.

In the case of scraping a crystalline layer in order to create crystals for a suspension, the inner structure of the layer, and the conditions by which it is affected, should be attended attention. Understanding that the solid material is not homogeneous, but consists of grain boundaries of various tensile strength, can lead to improved control of the breakage mechanism. This again would lead to improved possibilities for the optimisation of the characteristics of the product particles.

6. Summary

Melt crystallization is a highly selective and energy-efficient method for separation and purification of chemical mixtures. Suspension melt crystallization especially, offers a possibility to produce a highly pure crystalline product in a single separation step. The easiest way of producing the necessary supersaturation in a chemical mixture is by cooling. However, during indirect cooling deposits of the crystallizing material tend to form on the heat exchange surfaces. The suspension of pure crystals also includes the impure liquid from which the crystals were grown. In melt crystallization solid-liquid separation is often more difficult than in solution crystallization, as the crystals and the melt are essentially the same component in thermal equilibrium. These aspects often necessitate complex constructions and techniques, which from their part increase the costs of suspension melt crystallization. In order to overcome this disadvantage the crystallizer configurations and the product characteristics must be optimised.

The aim of this work has been to investigate the possibility of simplifying the crystallizer construction by making use of standard heat exchanger structures. The crystalline deposits on the heat exchange surface have been dealt with by precise selection of the process variables, with special attention given to the flow conditions. The possibility of continuously circulating the crystal suspension through a heat exchanger in order to avoid the use of agitated vessels, has been investigated. The crystal characteristics produced by suspension melt crystallization using various equipment constructions and the formation of crystalline layers on cooled surfaces have been observed. The final aim of the experiments undertaken was to simplify the equipment construction and to obtain better control over the product characteristics for suspension melt crystallization processes.

The experiments applying a standard heat exchanger structure were carried out in a tubular heat exchanger made of glass. A bench-scale laboratory construction consisting of a double-pipe heat exchanger loop was used as a continuous crystallizer, where dimethyl sulfoxide (dms) was crystallized from its mixture with water. The crystals forming on the cold heat exchanger surface were suspended by the shear created by the high flow velocities of the circulating crystal suspension applied in the equipment. The influence of the process conditions on the heat exchange and on the deposit removal was investigated.

The continuous circulation of the crystal suspension through a heat exchanger was further examined in a pilot-plant unit of industrial scale. Compound systems sugar-water (crystallization of ice) and dms-water (crystallization of dms) were used. Heat exchange was carried out in a scraped surface heat exchanger, allowing a wider range of temperature differences over the heat exchange surface. The limiting process conditions, the heat transfer characteristics and the size and shape of the product crystals were investigated.

The results gained from the laboratory and pilot plant crystallizers indicate that circulating the suspension in a continuous loop can provide sufficient conditions for crystal growth. In addition, by careful choice of the operating conditions, common heat exchangers can be applied to suspension melt crystallization.

The product crystals characteristics from suspension melt crystallization were investigated using small-scale laboratory equipment combined with detection through a microscope. Therewith, the development of the size and shape of the crystals during the crystallization process could be observed.

Crystals from a laboratory scraped surface crystallizer were observed right after their detachment from the layer formed on the cooled surface using mixtures of fatty acids. The obtained crystal characteristics were combined with the process conditions and the construction of the scrapers.

Crystals grown freely in a suspension were investigated during crystallization of paraxylene from mixtures of xylene isomers. Characteristics of crystals produced by different crystallization methods (e.g. with or without seed crystals) were compared. Investigations over the effect of the crystal characteristics on the efficiency of solid-liquid separation were carried out.

The secondary growth phenomenon of crystal agglomeration was investigated with ice crystals in an agitated vessel. The ice crystals were found to crystallize as disc shape single crystals, turning to a large spherical form by agglomeration.

The results from laboratory scale scraped surface crystallizer show that the initial crystal size and shape can be influenced by adjusting the scraper function. However, after getting suspended the crystals are strongly affected by the conditions in the melt. The results from the experiments with crystals freely grown in a suspension show that the size and the shape are strongly influenced by the initial conditions. It was found that not only the size, but also the shape of the crystals has a considerable effect on the efficiency of the solid-liquid separation. The shape of crystals can be influenced positively by secondary growth mechanisms, e.g. agglomeration.

The conditions for formation of crystalline layers at cooled surfaces have been investigated using mixtures of fatty acids. The structure of the formed layers has been discussed together with the forces necessary for breaking the layer. The force needed to break a layer is found to depend on the inner structure, which is influenced by the growth conditions.

The results presented in this work will serve for improved understanding of the process of crystal formation and the phenomena at the cooled surfaces during crystallization processes. The improved understanding of these processes gives a basis for the further development of the suspension melt crystallization processes. The results obtained for the deposit removal in the tubular heat exchanger are applicable to removal phenomena in ordinary heat exchangers where problems of deposition by freezing are encountered.

7. Zusammenfassung

Die Kristallisation aus Schmelzen ist ein höchst selektives und energieeffizientes Verfahren der Trennung und Reinigung von Stoffgemischen. Besonders die Schmelzkristallisation aus der Suspension bietet eine Möglichkeit zur Herstellung von hochreinen kristallinen Produkten in nur einer einzigen Trennstufe.

Der einfachste Weg zur Erzeugung der benötigten Übersättigung besteht in der Kühlung des Stoffgemisches. Dabei kann es jedoch zu einer Krustenbildung an den Wärmeübertragungsflächen, durch die kristallisierende Komponenten des Gemisches, kommen. Die Suspension der reinen Kristalle beinhaltet ebenso die verunreinigte Schmelze, aus welcher die Kristalle gezüchtet wurden. Da die Kristalle und die Schmelze die selbe Komponente im thermischen Gleichgewicht sind, ist die fest-flüssig Trennung in der Schmelzkristallisation oft schwieriger als in der Lösungskristallisation. Die zwei genannten Problemkreise erfordern komplexe Anlagenkonstruktionen und aufwendige Trenntechniken. Die daraus folgende Komplexität erhöht somit die Kosten der Schmelzkristallisation aus der Suspension. Um diese Nachteile zu überwinden, müssen die Anlagenauslegung und folglich die Produkteigenschaften optimiert werden.

Das Ziel dieser Arbeit war es nun zu untersuchen, ob durch die Anwendung von standardisierten Wärmetauscherelementen eine Vereinfachung der Kristallisatorkonstruktion möglich ist. Die kristallinen Krusten auf den Wärmetauscherflächen werden durch genaue Einstellung der Prozessbedingungen vermieden. Besondere Aufmerksamkeit muss dabei den Strömungsbedingungen in der Suspension gewidmet werden. Es wurden Möglichkeiten untersucht, die Kristallsuspension in einem Kreislauf kontinuierlich durch den Wärmetauscher zu leiten. Dazu wurden die Kristalleigenschaften gewonnen bei verschiedenen Anlagenauslegungen und die Bildung von Kristallschichten an gekühlten Flächen betrachtet. Das Endziel der durchgeführten Untersuchungen war eine Vereinfachung der Anlagenkonstruktion und eine bessere Kontrolle der Produkteigenschaften bei der Schmelzkristallisation aus der Suspension.

Die experimentellen Arbeiten unter Einsatz von standardisierten Wärmetauscherkomponenten wurde mit einem Wärmetauscherrohr aus Glas durchgeführt. Ein Kreislauf mit einem Doppel-Rohr-Wärmetauscher im Labormaßstab wurde als kontinuierlicher Kristallisator eingesetzt. Als kristallisierende Komponente wurde eine Dimethylsulfoxid (DMSO) - Wasser Mischung ausgewählt. Die Kristalle, die sich an der gekühlten Wärmeübertragungsfläche bildeten, wurden infolge der hohen Strömungsgeschwindigkeiten suspendiert. Es wurde der Einfluss der Prozessbedingungen auf den Wärmeübergang und auf die Entfernung der Verkrustungen untersucht.

Das kontinuierliche Umpumpen der Kristallsuspension durch den Wärmetauscher wurde in einer Pilotanlage im industriellen Maßstab weiter untersucht. Als Modellstoffsysteme wurden Zucker-Wasser (Kristallisation von Eis) und DMSO-Wasser (Kristallisation von DMSO) verwendet. Die Wärmeübertragung wurde in einem Kratzkühler durchgeführt. Dies ermöglichte eine größere Auswahl von Temperaturgradienten über die Wärmeübertragungsfläche. Dabei wurden sowohl die Prozessbedingungen als auch die Wärmeübergangsbedingungen, sowie die Größe und die Gestalt der Produktkristalle untersucht.

Die Ergebnisse, die aus der Labor- und Pilotanlage gewonnen werden konnten, weisen darauf hin, dass hinreichende Voraussetzungen für das Kristallwachstum, durch das Umpumpen der Suspension erreicht werden können. Die Ergebnisse zeigen weiterhin, dass gewöhnliche Wärmetauscher für die Suspensionschmelzkristallisation, bei einer sorgfältigen Wahl der Prozessbedingungen, eingesetzt werden können.

Die Eigenschaften der Produktkristalle aus der Suspensionschmelzkristallisation wurden in Versuchen im Labormaßstab, kombiniert mit mikroskopischen Betrachtung, untersucht. Damit war es möglich, die Entwicklung der Kristallgröße und -gestalt während des Kristallisationsprozesses zu verfolgen.

Kristalle aus dem Laborkratzkühler wurden unmittelbar nach ihrer Abtrennung aus der kristallinen Schicht an der gekühlten Fläche betrachtet. Als Modelstoffsysteme wurden Fettsäuregemische verwendet. Die erzeugten Kristalleigenschaften wurden dann mit den Prozessbedingungen und der Kratzkühlerkonstruktion kombiniert.

Die frei in der Suspension gewachsenen Kristallen wurden bei der Kristallisation von Para-Xylol aus Mischungen mit anderen Xylol-Isomeren untersucht. Dabei wurden die Eigenschaften von Kristallen verglichen, die bei unterschiedlichen Kristallisationsmethoden gewachsen sind (z.B. mit oder ohne Impfkristalle). Untersuchungen über den Einfluß der Kristalleigenschaften auf die Effizienz der fest-flüssig Trennung wurden nachfolgend durchgeführt.

Das sekundäre Kristallwachstum infolge von Agglomeration wurde bei Eiskristallen untersucht. Es konnte nachgewiesen werden, dass die Eiskristalle, die sich als scheibenförmige Einzelkristalle bilden, durch Agglomeration in große kugelhähnliche Körper umwandeln.

Die Ergebnisse zeigen, dass die erste Größe und Gestalt der Kristalle durch die Einstellungen der Kratzerfunktionen beeinflusst werden können. Nach ihrer Suspendierung werden die Kristalle jedoch stark durch die Bedingungen in der Schmelze verändert. Die Auswertung der Ergebnisse aus den Versuchen mit freiem Wachstum der Kristalle in Suspension ergaben ebenso, dass die Größe und die Gestalt stark von den Startbedingungen beeinflusst werden. Es wurde nachgewiesen, dass nicht nur die Größe, sondern auch die Form der Kristalle einen bedeutenden Einfluss auf die Effizienz der fest-flüssig Trennung hat. Die Kristallform kann positiv durch sekundäre Wachstumsmechanismen, z.B. durch Agglomeration, beeinflusst werden.

Die Bedingungen, welche zu kristallinen Schichten an gekühlten Fläche führen, sind untersucht worden. Als schichtbildende Stoffsysteme wurden Fettsäuregemische eingesetzt. Die Struktur der geformten Schichten ist zusammen mit den Kräften, die nötig sind um die Schichten aufzubrechen, diskutiert worden. Es konnte ermittelt werden, dass die Kraft die erforderlich ist, um eine Kristallschicht zu brechen von der inneren Struktur der Schicht abhängt. Die innere Struktur ist ihrerseits durch die Kristallwachstumsbedingungen beeinflussbar.

Die Ergebnisse, die in dieser Arbeit präsentiert wurden, tragen somit zum verbesserten Verständnis des Kristallbildungsprozesses und der Phänomene an gekühlten Flächen während Kristallisation bei. Die verbesserte Kenntnis der untersuchten Prozesse trägt somit zur weiteren Entwicklung der Suspensionschmelzkristallisationsprozesse bei. Die Ergebnisse für die Entfernung von Verkrustungen im Rohrwärmetauscher können auch auf gewöhnliche Wärmetauscher übertragen und somit zur Verkrustungsentfernung eingesetzt werden.

8. List of Symbols

Latin symbols

A_p	particle projection area	[m ²]
a	parameter in Eq. 2.4.17	[-]
B^0	nucleation rate	[m ⁻³ s ⁻¹]
$b1$	parameter in Eq. 2.4.17	[-]
$b2$	parameter in Eq. 2.4.17	[-]
$b3$	parameter in Eq. 2.4.17	[-]
C	parameter in Eq. 2.4.3	[-]
C_R	parameter in Eq. 3.4	[-]
c	concentration	[kgm ⁻³]
c^*	equilibrium concentration	[kgm ⁻³]
c_2	impurity concentration in the liquid phase	[kgm ⁻³]
$c_{2,Prod}$	impurity concentration in the product crystals	[kgm ⁻³]
D_e	equivalent diameter ($D_i - D_v$)	[m]
D_h	hydraulic diameter	[m]
D_i	inner diameter of a heat exchanger, diameter of an inner pipe	[m]
D_{log}	logarithmic pipe diameter	[m]
D_o	diameter of an outer pipe	[m]
D_s	diameter of the scraper system	[m]
D_v	votator diameter	[m]
dW	weight fraction of crystals at size range dL	[-]
e	parameter in Eq. 2.4.3	[-]
F_S	solid fraction	[-]
f	friction factor	[-]
G	crystal growth rate	[ms ⁻¹]
g	acceleration by gravity	[ms ⁻²]
h	heat transfer coefficient	[Wm ⁻² K ⁻¹]
h_f	heat transfer coefficient through a fouling layer	[Wm ⁻² K ⁻¹]
h_i	heat transfer coefficient in an inner pipe	[Wm ⁻² K ⁻¹]
h_o	heat transfer coefficient in an outer pipe	[Wm ⁻² K ⁻¹]
K	parameter in Eq. 3.2.1	[-]
K_P	parameter in Eq. 3.1.1	[sm ⁻²]
k_d	heat conductivity of a deposit layer	[Wm ⁻¹ K ⁻¹]
k_{eff}	effective distribution coefficient	[-]
k_V	volume shape factor	[-]
k_w	heat conductivity of a heat exchanger wall	[Wm ⁻¹ K ⁻¹]
L	crystal length	[m]
l	length of the heat exchanger	[m]
M	molar mass	[gmol ⁻¹]
M_T	suspension density of crystals	[kgm ⁻³]
m	mass	[kg]
m_{FC}	mass of the filter cake	[kg]
m_{RM}	mass of the rest melt in the filter cake	[kg]
m_{tot}	total mass of the filtrate and the filter cake	[kg]
m_T	suspension density of crystals	[kgm ⁻³]
$m_{T,max}$	maximum suspension density of crystals in the heat exchanger	[kgm ⁻³]

\dot{m}_r	removal rate of a deposit	[kg s^{-1}]
N	rotational velocity	[rpm]
\dot{N}	flux of crystallizing species	[$\text{kg m}^{-2} \text{s}^{-1}$]
n	population density, exponent in Eq. 3.2.1	[m^{-4}], [-]
n^0	population density of zero-size crystals	[m^{-4}]
Nu	Nusselt number	[-]
Nu_{th}	theoretical Nusselt number by Eq. 2	[-]
Nu_{tube}	Nusselt number for flow in tubes by the Gnielinsky equation (Eq. 2.4.18)	[-]
P_p	particle perimeter	[m^2]
Pe_{ax}	axial Péclet number	[-]
Pr	Prandtl number	[-]
Pr_w	Prandtl number at the wall temperature	[-]
Q	heat flow	[W]
q	heat flux	[W m^{-2}]
R	gas constant	[$\text{J mol}^{-1} \text{K}^{-1}$]
R_f	fouling resistance	[$\text{m}^2 \text{K W}^{-1}$]
R_f^*	asymptotic maximum fouling resistance	[$\text{m}^2 \text{K W}^{-1}$]
r	particle radius	[m]
Re	Reynolds number based on scraper rotation	[-]
Re_{ax}	axial Reynolds number	[-]
Sc	Schmidt number	[-]
Sh	Sherwood number	[-]
T	temperature	[K]
T_a	temperature at the unfouled side of a heat exchanger wall	[K]
T_b	bulk temperature at the crystallizing side	[K]
T_s	surface temperature at a phase boundary	[K]
t	time	[s]
t_R	residence time	[s]
U	overall heat transfer coefficient	[$\text{W m}^{-2} \text{K}^{-1}$]
v	axial flow velocity	[m s^{-1}]
W_{csl}	work needed to remove a crystal from the surface	[J]
x	thickness of a heat exchanger wall, pipe length (Fig. 3.1.1)	[m]
x_d	deposit thickness	[m]
$x_{2,FC}$	impurity concentration of the filter cake	[-]
$x_{2,filtrate}$	impurity concentration in the filtrate	[-]
Z	number of scrapers	[-]

Greek symbols

ΔH_f	heat of fusion	[Jkg ⁻¹]
γ	interfacial tension	[Jm ⁻²]
$\dot{\gamma}$	shear rate	[Nm ⁻²]
θ	temperature	[K]
θ_c	surface temperature difference (Fig. 3.1.1)	[K]
$\bar{\theta}_{cm}$	average temperature of the cooling medium	[K]
θ_e	equilibrium temperature	[K]
θ_{in}^*	dimensionless temperature at the inlet	[K]
θ_{out}^*	dimensionless temperature at the outlet	[K]
μ	viscosity	[Pas]
μ_w	viscosity at the wall temperature	[Pas]
ζ	parameter defined by Eq. 2.4.19	[-]
ρ	density	[kgm ⁻³]
ρ_f	density of a fouling layer	[kgm ⁻³]
σ_f	shear strength of a deposit layer	[Nm ⁻²]
τ	shear stress	[Nm ⁻²]
τ_y	shear stress at zero shear rate	[Nm ⁻²]

9. References

- [Åla04] Ålander, E. M., Uusi-Penttilä, M. S., Rasmuson, A. C., Agglomeration of Paracetamol During Crystallization in Pure and Mixed Solvents, *Ind. Eng. Chem. Res.*, **43** (2004), 629-637
- [Ara54] Arakawa, K. J., *Fac. Sci., Hokkaido Univ., Japan, Ser. II*, **4** (1954), 311
- [Ark95] Arkenbout, G. F., *Melt Crystallization Technology*, Technomic Publishing Co., Inc., Lancaster (U.S.A.), 1995
- [Arn45] Arnold, P. M., *Continuous Fractional Crystallization Process*, US Patent 2540977, 1945
- [Ban01] Bansal, B., Müller-Steinhagen, H., Xiao, D. C., Comparison of Crystallization Fouling in Plate and Double-Pipe Heat Exchangers, *Heat Transfer Eng.* **22** (2001), 13-25
- [Boh85] Bohnet, M., Fouling von Wärmeübertragungsflächen, *Chem.-Ing. Tech.* **57** (1985) 1, 24-36
- [Boh03] Bohnet, M., Influence of the Transport Properties on the Crystal/Heat Transfer Surface Interfacial on Fouling Behaviour, *Chem. Eng. Tech.* **26** (2003) 10, 1055-1060
- [Bot95] Bott, T. R., *Fouling of Heat Exchangers*, Elsevier Science B.V., Amsterdam, 1995
- [Bra64] Braginski, L. N., Begatschew, V. I., Pawluschenko, I. S., *J. Appl. Chem. USSR* **37** (1964) 9, 1966-1970
- [Bre99a] Breitschuh, B., Drost, M., Windhab, E. J., Process Development for Continuous Crystallization and Separation of Fat Crystal Suspensions, *Chem. Eng. Technol.* **21** (1999) 5, 425-428
- [Bre99b] Brendler, L., Tiedemann, H., Bewertung des Fraktionierungsergebnisses beim mechanischen Schwitzen, *Chem. Ing. Tech.* **71** (1999) 11, 1265-1270
- [Bre80] Brennan, E. D., *Process and Apparatus for Separating and Purifying a Crystalline Metal*, US Patent 4309878, 1980
- [Cha77] Chaffey, C. E., Wagstaff, I., Shear Thinning and Thickening Rheology, II. Volume Fraction and Size of Dispersed Particles, *J. Coll. Int. Sci.* **59** (1977) 1, 63-75
- [Cor01] Cordoba, A. J., Schall, C. A., Solvent Mitigation in a Paraffin Deposit, *Fuel* **80** (2001), 1279-1284
- [Dau89] Daubert, T. E., Danner, R. P., *Physical and Thermodynamic Properties of Pure Chemicals: Data Compilation*, Taylor & Francis, Washington DC, 1989

- [Dav91] David, R., Marchal, P., Klein, J.-P., Villermaux, J., Crystallization and Precipitation Engineering – III. A Discrete Formulation of the Agglomeration Rate of Crystals in a Crystallization Process, *Chem. Eng. Sci.* **46** (1991) 1, 205-213
- [deG88] de Goede, R., Crystallization of Paraxylene with Scraped Surface Heat Exchangers, Ph.D. thesis, Technische Universiteit Delft, 1988
- [deG89] de Goede, R., de Jong, E. J., Scaling Phenomena in Scraped Surface Heat Exchangers, International Symposium on Preparation of Functional Materials and Industrial Crystallization, Osaka, 1989, 28-34
- [deG93] de Goede, R., de Jong, E. J., Heat Transfer Properties of a Scraped-Surface Heat Exchanger in the Turbulent Flow Regime, *Chem. Eng. Sci.* **48** (1993) 8, 1393-1404
- [deM84] de Moet, A. N., Melt Crystallization in the Cooling Disc Crystallizer, in *Industrial Crystallization 84*, Jancic, S. J., de Jong, E. J. (eds.), Elsevier Science Publishers B.V., Amsterdam, 1984, 223-227
- [Din63] Dinglinger, G., Die Wärmeübertragung im Kratzkühler, Ph.D. thesis, Universität Karlsruhe, 1963
- [Eps76] Epstein, M., The Growth and Decay of a Frozen Layer in Forced Flow, *Int. J. Heat Mass Transfer* **19** (1976), 1281-1288
- [Fis97] Fischer, O., A New Process for the Ultra-purification of p-xylene, *Hydrocarbon Engineering* (1997) 3/4, 41-44
- [För99] Förster, M., Augustin, W., Bohnet, M., Influence of the Adhesion Force Crystal/Heat Exchange Surface on Fouling Mitigation, *Chem. Eng. and Processing* **38** (1998), 449-461
- [Gah99] Gahn, C., Mersmann, A., Brittle Fracture in Crystallization Processes, Part A. Attrition and Abrasion of Brittle Solids, *Chem. Eng. Sci.* **54** (1999) 9, 1273-1282
- [Ger91] Gerigk, M. J., Effektive Keimbildung in Zwangsumlauf-Kristallisatoren, Ph.D. thesis, Rheinisch-Westfälische Technische Hochschule Aachen, Aachen, 1991
- [Gho67] Ghosal, J. K., Srimani, B. N., Ghosh, D. N., Study of the Heat Transfer Rate in a Steam Heated Votator, *Indian Chem. Eng.* **9** (2) 1967, 53-58
- [Gni75] Gnielinski, V., Neue Gleichungen für den Wärme- und den Stoffübergang in turbulent durchströmten Kanälen, *Forsch. Ing.-Wes.* **41** (1975) 1, 8-16
- [Gra91] Graham, A. L., Altobelli, S. A., Fukushima, E., Mondy, L. A., Stephens, T. S., NMR Imaging of Shear-Induced Diffusion and Structure in Concentrated Suspensions Undergoing Couette Flow, *Journal of Rheology* **35** (1991) 1, 191-201

- [Haa02] Haasner, T. Beeinflussung der Keimbildung in der Schichtkristallisation durch gezielte Oberflächenmodifikation, Ph.D. thesis, Martin-Luther-Universität Halle-Wittenberg, VDI Verlag, Düsseldorf, 2002
- [Haf88] Hafaiiedh, A., Computer Modelling of the Rheology of Particulate Suspensions, Ph.D. thesis, Alfred University, 1988
- [Hal64] Hallett, J., Experimental Studies of the Crystallization of Supercooled Water, *J. Atm. Sci.* **21** (1964), 671-682
- [Har59] Harriott, P., Heat Transfer in Scraped-Surface Exchangers, *Chem. Eng. Progr. Symp. Ser.* **55** (1959) 29, 137-139
- [Hir85] Hirata, T., Ishihara, M., Freeze-off Conditions of a Pipe Containing a Flow of Water, *Int. J. Heat Mass Transfer* **28** (1985), 331-337
- [Hof74] Hoffman, R. L., Discontinuous and Dilatant Viscosity Behavior in Concentrated Suspensions, II. Theory and Experimental Tests, *J. Coll. Int. Sci.* **33** (1974), 491-505
- [Hou44] Houlton, H. G., Heat Transfer in the Votator Heat Exchanger, *Ind. Eng. Chem.* **36** (1944) 6, 522-528
- [Hug31] Huggins, F. E., *Ind. Eng. Chem.* **23** (1931), 749-753
- [Hui72] Huige, N. J. J., Nucleation and Growth of Ice Crystals from Water and Sugar Solutions in Continuous Stirred Tank Crystallizer, Ph.D. thesis, Technische Hogeschool Eindhoven, 1972
- [Isr85] Israelachvili, J. N., Intermolecular and Surface Forces, Academic Press, Orlando, 1985, 214
- [Jac65] Jackson, K. A., Nucleation from the Melt, *Ind. Eng. Chemistry* **57** (1965) 12, 28-32
- [Kea98] Keary, A. C., Bowen, R. J., Analytical Study of the Effect on Natural Convection on Cryogenic Pipe Freezing, *Int. J. Heat Mass Transfer* **41** (1998) 10, 1129-1138
- [Kir78] Kirk-Othmer Encyclopedia of Chemical Technology, Vol. 24, 3rd ed., Mark, H. F., Othmer, D. F., Overberger, C. G., Seaborg, G. T. (eds.), John Wiley & Johns, New York, 1978, 279
- [Kob96] Kobayashi, A., Shirai, Y., Nakanishi, K., Matsuno, R., A Method for Making Large Agglomerated Ice Crystals for Freeze Concentration, *J. Food Engineering* **27** (1996) 1, 1-16
- [Kön99] König, A., Schreiner, A., Purification by Melt Crystallization of Naphtalene/Biphenyl-Mixtures, in Proceedings of 7th BIWIC, Ulrich, J. (ed.), Halle, 1999, 66-72

- [Kön03] König, A., Phase Diagrams, Chapter 2 in: Melt Crystallization – Fundamentals, Equipment and Applications, Ulrich, J., Glade, H. (eds.), Shaker Verlag, Aachen, 2003, 7-40
- [Kon71] Konviser, I. A., *Cholod. Techn.* **48** (1971) 1, 16-20
- [Kul65] Kulatschinski, A., *Molochn. Prom.* **26** (1965) 2, 11-15
- [Lat59] Latinen, G. A., Discussion of the Paper “Correlation of Scraped Film Heat Transfer in the Votator”, *Chem. Eng. Sci.* **9** (1959) 4, 263-266
- [Lem00] Lemmer, S., Klomp, R., Ruemekorf, R., Jansen, H., Scholz, R., Abwasser-vorkonzentrierung nach dem Niro Freeze Concentration Process, *Chem.-Ing. Tech.* **72** (2000) 10, 1229-1233
- [Lin66] Lindemayer, C. S., Chalmers, B., Morphology of Ice Dendrites, *J. Chem. Phys.* **45** (1966), 2804-2806
- [Lin04] Linnikov, O. D., Spontaneous Crystallization of Potassium Chloride from Aqueous and Aqueous-Ethanol Solutions, Part 2: Mechanism of Aggregation and Coalescence of Crystals, *Cryst. Res. Technol.* **39** (2004) 6, 529-539
- [Liu99] Liu, W., Garside, J., Crystallization of Sunflower Oil on a Scraped Metal Surface, 14th International Symposium on Industrial Crystallization, Cambridge, 1999
- [Loc94] Lock, G. S. H., *Latent Heat Transfer*, Oxford Univ. Press, Oxford, 1994
- [Lon98] Long, P. X., Hsieh, J. S., Hart, P. W., Fresh Water Usage Reduction Through Freeze Concentration of Mill Effluent Using Gas Hydrate, *AIChE Symposium Series* **319** (1998) 94, 151-158
- [Lou96] Louhi-Kultanen, M., *Concentration and Purification by Crystallization*, Acta Polytechnica Scandinavica, Chemical Technology Series No. 241, Helsinki, 1996
- [Mac76] Macintosh, D. L., White, E. T., The Formation of Inclusions in Sugar Crystals, *AIChE Symposium Series* **72** (1976) 153, 11-20
- [Mat91] Matsuoka, M., Developments in Melt Crystallization, in *Advances in Industrial Crystallization*, Garside, J., Davey, R. J., Jones, A. G. (eds.), Butterworth-Heinemann, Oxford, 1991, 229-244
- [McC93] McCabe, W. L., Smith, J. C., Harriott, P., *Unit Operations of Chemical Engineering*, 5th ed., McGraw-Hill Book Co., Singapore, 1993, 341
- [McK72] McKetta, J. J., *Encyclopedia of Chemical Technology*, 2nd ed., Wiley-Interscience, New York, 1972
- [Mer95] Mersmann, A., *Crystallization Technology Handbook*, Marcel Dekker, Inc., New York, 1995

- [Mid69] Middleton, G. J., Kontinuierlich arbeitender Fraktionier-Kristallisator, CAV 1969, Juli
- [Miy97] Miyashita, H., Yoshida, M., Yamane, T., Nishimura, T., Heat Transfer Correlation in High Prandtl (High Schmidt) Number Fluid in Votator Type Scraped Surface Heat Exchanger, Chem. Eng. Japan **30** (1997) 3, 545-549
- [Mon94] Mondy, L. A., Brenner, H., Altobelli, S. A., Abbott, J. R., Graham, A. L., Shear-Induced Particle Migration in Suspensions of Rods, Journal of Rheology **38** (1994) 2, 444-452
- [Mol74] Molinari, J. G. D., Dodgson, V., Theory and Practise Related to the Brodie Purifier, The Chemical Engineer (1974) 7-8, 460-464
- [Mor96] Mori, H., Nakamura, M., Toyama, S., Crystallization Fouling of Calcium Sulfate Dihydrate on Heat-Transfer Surface, J. Chem. Eng. Japan **29** (1996) 1, 166-173
- [Mor86] Morita, M., Nakamura, K., Takegami, T., Industrial Continuous Melt Crystallization, Proceedings of World Congress 3 of Chemical Engineering, Tokyo, 1986, 1072-1075
- [Mul01] Mullin, J. W., Crystallization, 4th ed., Butterworth-Heinemann, Oxford, 2001, 347
- [Nik65] Nikonov, I. V., Pistschew. Technol. **5** (1965), 148-150
- [Nik67] Nikolajew, L. K., Pistschew. Techn. **4** (1967), 146-147
- [Nir98] Niro Process Technology B.V., Applications of Crystallization Technology (company brochure), 1998
- [Nir00] Niro Process Technology B.V., Crystallization and Separation (company brochure), 2000
- [Özo92] Özoguz, M. Y., Zur Schichtkristallisation als Schmelzkristallisationsverfahren, Ph.D. thesis, Universität Bremen, VDI-Verlag, Düsseldorf, 1992
- [Pat01] Patience, D. B., Mohameed, H. A., Rawlings, J. B., Crystallization of Para-Xylene in Scraped Surface Crystallizers, AIChE Journal **47** (2001) 11, 2441-2451
- [Pen69] Penney, W. R., Bell, K. J., Heat Transfer in a Thermal Processor Agitated with a Fixed Clearance Thin, Flat Blade, Chem. Eng. Progr. Symp. **65** (1969) 92, 1-11
- [Pet64] Petukhov, B. S., Roizen, L. I., Generalized Relationships for Heat Transfer in a Turbulent Flow of Gas in Tubes of Annular Section, High Temperature **2** (1964), 65-68

- [Ran88] Randolph, A. D., Larson, M. A., Theory of Particulate Processes, 2nd ed., Academic Press, Inc., San Diego, 1988, 83-87
- [Rib97] Ribeiro, F. S., Souza Mendes, P. R., Braga, S. L., Obstruction of Pipelines Due to Paraffin Deposition During the Flow of Crude Oils, *Int. J. Heat Mass Transfer* **40** (1997) 18, 4319-4328
- [Rit85] Rittner, S., Steiner, R., Die Schmelzkristallisation von organischen Stoffen und ihre großtechnische Anwendung, *Chem.-Ing. Tech.* **57** (1985) 2, 91-102
- [Rou98] Rousseau, R. W., Contact Nucleation in Industrial Crystallizers: An Overview, in *International Symposium on Industrial Crystallization*, Tokyo, 1998, 72-81
- [Roy90] Roy, K. A., Freeze Crystallization Leaves Contaminants Out in the Cold, *Hazmat World*, Dez. 1990, 56-61
- [Sch50] Schmidt, J., Verfahren und Vorrichtung zur kontinuierlichen Gewinnung von Konzentraten aus Lösungen, Deutsche Patent 900209, 1950
- [Sch02] Scholz, R., Ruemekorf, R., Verdoes, D., Nienoord, M., Wash Columns – State of the Art and Further Developments, in *Proceedings of 15th International Symposium on Industrial Crystallization*, Chianese, A. (ed.), AIDIC Servizi S.r.l., Sorrento, 2002, 1425-1430
- [Sch03a] Scholz, R., Ruemekorf, R., Separate Organics by Suspension Crystallization, Chapter 8 in: *Melt Crystallization – Fundamentals, Equipment and Applications*, Ulrich, J., Glade, H. (eds.), Shaker Verlag, Aachen, 2003, 191-212
- [Sch03b] Scholz, R., private communication, 2003.
- [Sch04] Schreurs, B., private communication, 2004.
- [Sch00] Schuldei, S., Zur Schmelzkristallisation in Apparaten der Lösungskristallisation, Ph.D. thesis, Universität Bremen, Shaker Verlag, Aachen, 2000
- [Shi98] Shirai, Y., Ice Crystallization for Freeze Wastewater Treatment, in *International Symposium on Industrial Crystallization*, Tokyo, 1998, 740-745
- [Ske58] Skelland, A. H. P., Correlation of Scraped-Film Heat Transfer in the Votator, *Chem. Eng. Sci.* **7** (1958) 3, 166-175
- [Ske62] Skelland, A. H. P., Oliver, D. R., Tooke, S., Heat Transfer in a Water Cooled Scraped Surface Heat Exchanger, *Brit. Chem. Eng.* **7** (1962) 5, 346-353
- [Söh96] Söhnel, O., Bravi, M., Chianese, A., Mazzarotta, B., Growth Kinetics of Sodium Perborate from Batch Crystallization, *J. Crystal Growth* **160** (1996), 355-360

- [Son04] Sonnenberg, J.-P., Schmidt, E., Numerische Bestimmung von Haftkräften Submikroner Partikeln, in Produktgestaltung in der Partikeltechnologie, Band 2, Teipel, U. (ed.), DWS Werbeagentur und Verlag GmbH, Karlsruhe, 2004, 49-58
- [Syk66] Sykora, S., Navratil, B., Heat Transfer on Scraped Walls, Collect. Czechoslov. Chem. Commun. **31** (1966) 8, 3299-3308
- [Syk68] Sykora, S., Navratil, B., Karasek, O., Heat Transfer on Scraped Walls in the Laminar and Transitional Regions, Collect. Czechoslov. Chem. Commun. **33** (1968) 2, 518-528
- [Tab91] Tabor, D., Gases, Liquid and Solids and Other States of Matter, 3rd ed., Cambridge University Press, Cambridge, 1991
- [Täh99] Tähti, T., Louhi-Kultanen, M., Palosaari, S., On-line Measurement of Crystal Size Distribution During Batch Crystallization, in Proceeding of 14th International Symposium on Industrial Crystallization, Cambridge, 1999
- [Täh01] Tähti, T., Brendler, L., Ulrich, J., Characterization of Solid Phase after its Mechanical Separation in Scraped Surface Crystallizer, PARTEC 2001, Nürnberg, 2001
- [Täh02] Tähti, T., Brendler, L., Ulrich, J., Control of Undercooling in Crystallization of p-Xylene Mixtures, in Proceeding of 15th International Symposium on Industrial Crystallization, Chianese, A. (ed.), Sorrent, 2002, 1239-1244
- [Täh03] Tähti, T., Möhring, D., Verschuur, R.-J., Scholz, R., Ulrich, J., Simplifying Suspension Melt Crystallizers, in Proceedings of 10th BIWIC, Coquerel, G. (ed.), Rouen, 2003, 51-58
- [Tak84] Takegami, K., Nakamura, N., Morita, M., Industrial Molten Fractional Crystallization, in Industrial Crystallization 84, Jancic, S. J., de Jong, E. J. (eds.), Elsevier Science Publishers B.V., Amsterdam, 1984, 143-146
- [Tro67] Trommelen, A. M., Heat Transfer in a Scraped-Surface Heat Exchanger, Trans. Inst. Chem. Eng. **45** (1967) 5, 176-178
- [Uhl66] Uhl, V. W., Gray, J. B., Mixing. Theory and Practice, 2nd ed., Academic Press, New York, 1966
- [Ulr81] Ulrich, J., Zur Kristallkeimbildung durch mechanischen Abtrieb, Ph.D. thesis, Rheinisch-Westfälische Technische Hochschule Aachen, Aachen, 1981
- [Ulr02] Ulrich, J., Bülau, H. C., Melt Crystallization, in Handbook of Industrial Crystallization, 2nd ed., Myerson, A. S. (ed.), Butterworth-Heinemann, Woburn, 2002, 161-179
- [Ulr03] Ulrich, J., Glade, H. (eds.), Melt Crystallization – Fundamentals, Equipment and Applications, Shaker Verlag, Aachen, 2003

- [Vae03] Vaessen, R. J. C., Development of Scraped Eutectic Crystallizers, Ph.D. thesis, Technische Universiteit Delft, 2003
- [Ven99] Vendel, M., Rasmuson, A. C., Mechanisms of Initiation of Incrustation, *J. AIChE* **43** (1997) 5, 1300-1308
- [Ver03a] Verdoes, D., Nienoord, M., Suspension-Based Melt Crystallization: Principles, Equipment, Applications, Course on: Theory and Application of Melt Crystallization, Halle, 2003
- [Ver03b] Verdoes, D., Nienoord, M., Suspension-Based Melt Crystallization: Principles, Equipment, Applications, Chapter 5 in: Melt Crystallization – Fundamentals, Equipment and Applications, Ulrich, J., Glade, H. (eds.), Shaker Verlag, Aachen, 2003, 93-128
- [Wag77] Wagstaff, I., Chaffey, C. E., Shear Thinning and Thickening Rheology, I. Concentrated Acrylic Dispersions, *J. Coll. Int. Sci.* **59** (1977) 1, 53-62
- [Wei97] Weigand, B., Braun, J., Neumann, S. O., Rinck, K. J., Freezing in forced convection flows inside ducts: A review, *Heat and Mass Transfer* **32** (1997), 341-351
- [Wei72] Weisser, H., Untersuchungen zum Wärmeübergang im Kratzkühler, Ph.D. thesis, Universität Karlsruhe, 1972
- [Wen82] Wenzlau, H., Ay, P., Gramlich, K., Zur Modellierung des Wärme- und Stofftransportes in Kratzkühlerkristallisatoren, *Chem. Techn.* **34** (1982) 4, 179-182
- [Win90] Wintermantel, K., Wellinghoff, G., Melt Crystallization - Theoretical Presumption and Technical Limits, in Proceedings of the 11th Symposium on Industrial Crystallization, Mersmann, A. (ed.), Garmisch-Partenkirchen, 1990, 703-708
- [Wöh91] Wöhlk, W., Hofmann, G., Schmelzkristallisation. Zum Beispiel Bisphenol A-Phenol, *Chemische Industrie* **6** (1991), 62-70
- [Woo01] Wood, W. M. L., A Bad (Crystal) Habit - and How it Was Overcome, *Pow. Tech.* **121** (2001), 53-59
- [Wor03] Worlitschek, J., Choice of the Focal Point Position Using Lasentec FBRM, *Part. Part. Syst. Charact.* **20** (2003) 1, 12-17
- [Yan02] Yang, Q., Liu, Y., Gu, A., Ding, J., Shen, J., Investigation of Induction Period and Morphology of CaCO₃ Fouling on Heated Surface, *Chem. Eng. Sci.* **57** (2002) 6, 921-932

Curriculum Vitae

Personal data

Family name: Tähti
First name: Tero
Date/place of birth: 18.08.1972 in Hämeenlinna, Finland
Nationality: Finnish
Marital status: married

Education

Aug. 1988 – May 1991: Gymnasium Hämeenlinnan yhteiskoulun lukio, Finland
Aug. 1991 – Feb. 1999: Lappeenranta University of Technology, Finland
Feb. 1999 – Oct. 1999: Research scientist at Lappeenranta University of Technology, Chemical Engineering department, Finland
Oct. 1999 – Aug. 2004: Research scientist at Martin-Luther-Universität Halle-Wittenberg, Fachbereich Ingenieurwissenschaften, Institut für Verfahrenstechnik/TVT